

https://dspace.org/

Evaluation of processes for landfill gas utilization

Pillay, Odelia

2014-09-05
http://hdl.handle.net/10539/15417

Downloaded from a DSpace repository. https://dspace.org/

EVALUATION OF PROCESSES FOR LANDFILL GAS UTILIZATION

Odelia Pillay

A dissertation submitted to the University of the Witwatersrand, Faculty of Engineering and the Built Environment, in fulfilment of the requirements for the part time degree of Masters of Science in Chemical Engineering.

Johannesburg, 2014

Declaration

I declare that this dissertation is my own unaided work under the supervision of my Supervisor Dr. S Kauchali. It is in submission to the Degree of Masters of Science in Chemical Engineering to the University of the Witwatersrand, Johannesburg. This dissertation has not been submitted before for any degree or examination to any other University.

_____

(Signature of Candidate)

_____ day of _____, _____

(day) *(month)* *(year)*

Abstract

Through many studies and investigations over the years, landfills have evolved into efficiently operated bioreactors to produce methane (CH_4) which can be used and converted into useful fuels as the concern of global warming increases. The processes outlined within this dissertation are a development of a graphical technique that allows various technologies to be developed with syngas production as an intermediate step and considers mass balance to determine the stoichiometric region for syngas production. Energy balances were used to limit the stoichiometric region to autothermal operation, carbon boundaries identified further restrictions on the stoichiometric region and contours of Higher Heating Values (HHV) identified regions to obtain high calorific value syngas.

A comparison of different processes suggests that despite electricity generation being simpler, the process emits the highest amount of carbon dioxide (CO_2) emissions (2.50 CO_2/ mol landfill gas (LFG)) with fuel processes (synfuel (CH_2) and Dimethyl Ether (DME)) yielding lower CO_2 emissions with a high of 1.10 CO_2/ mol LFG. The production of chemicals or syngas through zero CO_2 emission processes, produces zero or very little CO_2 as compared to the other processes and do not require energy intensive steps in order for the process to go to completion.

This dissertation develops a systematic graphical technique that enables the study of possible conversion processes and flow sheets utilising LFG. Furthermore, from this analysis it is shown that there are more possibilities of LFG usage for chemicals and fuel production in addition to traditional electricity generation.

In memory of my loving mother

Karnegie (Kay) Pillay

Acknowledgements

I wish to thank the following persons for their contribution to my work:

- Dr. Shehzaad Kauchali for his continued assistance, guidance, inspiration and insight into gasification and reforming throughout this research as well as interpretation of results and continued support of this work
- WSP Environmental for provision of funds and allocating study leave when necessary
- My Dad, Steven Pillay for his encouragement and support throughout the research period
- My family for their continued support and motivation

Contents

DECLARATION ..... **I**

ABSTRACT ..... **II**

ACKNOWLEDGEMENTS ..... **IV**

LIST OF FIGURES ..... **VII**

LIST OF TABLES ..... **IX**

NOMENCLATURE ..... **X**

1 INTRODUCTION AND BACKGROUND **1**

1.1 THE SUSTAINABILITY OF LANDFILL GAS 2

1.2 USES OF LANDFILL GAS 4

1.3 PROBLEM STATEMENT AND RESEARCH MOTIVATION 7

2 LITERATURE REVIEW **9**

2.1 LANDFILLS 9

2.2 GAS COMPOSITION 10

2.3 LANDFILL GAS EXTRACTION PROCESS 14

2.3.1 Gas Wells *14*

2.3.2 Leachate *19*

2.4 GAS CLEANING 20

2.4.1 Primary Cleaning *20*

2.4.2 Secondary Cleaning *21*

2.5 ELECTRICITY 26

2.5.1 Electricity generation *26*

2.5.2 Solid Oxide Fuel Cells *29*

2.6 ELECTRO-CATALYTIC REDUCTION OF CO_2 31

2.7 SYNFUELS PRODUCTION 34

2.8 DME PRODUCTION 35

3 METHODOLOGY AND CLEAN DEVELOPMENT MECHANISM PROJECTS **38**

3.1 METHODOLOGY 38

3.2 CLEAN DEVELOPMENT MECHANISM PROJECTS 39

4 THEORY **41**

4.1 HISTORY OF BOND EQUIVALENT DIAGRAMS 41

4.2 BOND EQUIVALENT DIAGRAMS 42

4.3 REPRESENTING SPECIES ON THE CHO DIAGRAM 44

4.4 STOICHIOMETRIC REGION OF OPERATION FOR LFG 45
4.4.1 Reforming Reactions using the CHO Diagram *46*
4.5 GRAPHICAL REPRESENTATION OF REACTIONS 49

5 ENERGY BALANCE CONSIDERATIONS 53

5.1 AUTO-THERMAL OPERATIONS 53
5.2 IDEALISED STOICHIOMETRIC REGION (CALORIFIC VALUES) 56
5.3 CARBON BOUNDARY 59

6 RESULTS 63

6.1 ELECTRICITY GENERATION USING AN INTERNAL COMBUSTION ENGINE 63
6.1.1 Basic Flow diagrams *63*
6.2 ELECTRICITY GENERATION USING SOFC'S 66
6.2.1 Basic Flow Diagrams *67*
6.2.2 Electricity generation depicted on CHO diagram *69*
6.3 ELECTRO-CATALYTIC REDUCTION OF CO_2 74
6.3.1 Basic Flow Diagram *74*
6.3.2 Methane generation depicted on the CHO diagram *77*
6.4 SYNFUEL PRODUCTION 81
6.4.1 Basic Flow Diagram *81*
6.4.2 CH_2 generation depicted on the CHO diagram *84*
6.5 DME PRODUCTION 88
6.5.1 Basic Flow Diagram *89*
6.5.2 DME generation depicted on the CHO diagram *91*
6.6 CO_2 EMISSION FREE PROCESSES 95
6.6.1 Basic Flow Diagram *96*
6.6.2 Chemical Generation depicted on the CHO diagram *99*

7 CONCLUSIONS 103

REFERENCES 110

APPENDIX A – REPRESENTATION OF CHO DIAGRAMS 118

APPENDIX B – DETERMINATION OF THE THERMALLY BALANCED LINE 122

APPENDIX C – CALCULATING CALORIFIC VALUES 128

List of Figures

Figure 1.1: Schematic layout of Landfill gas to Electricity Project (Interwaste Environmental Solutions, 2010)....2
Figure 1.2: Emissions Evolution Curve for Coastal Park (Theeboom and Nontangane, 2010)....3
Figure 2.1: Landfill gas production over the course of time (Koch, 2001)....11
Figure 2.2: Changes in Typical LFG composition after Waste disposal (Berger and Mann, 2001)13
Figure 2.3: Vertical LFG extraction wells (U.S. EPA LMOP, n.d) 16
Figure 2.4: LFG Collection system with horizontal Trenches (U.S. EPA LMOP, n.d)....16
Figure 2.5: The area of influence and spacing of vertical gas wells (Swanepoel, 2009)....17
Figure 2.6: The area of influence and spacing of horizontal gas wells (Swanepoel, 2009)....18
Figure 2.7: LFG Extraction site plan (U.S. EPA LMOP, n.d)....19
Figure 2.8: Removal of H_2S for CO_2, methane and electricity production (Malik et al., 1987)....23
Figure 2.9: One third of all landfill sites have a severe siloxane problem (Xebec Adsorption Inc., 2007)....25
Figure 2.10: Silica build up on heads and scrapped pistons of Caterpillar and Jenbacher engines (Xebec Adsorption Inc., 2007) 25
Figure 2.11: The flow of LFG from extraction to electricity generation (Swanepoel, 2009) 26
Figure 2.12: Practical SOFC with three phase boundary to facilitate charge transfer (Kee et al., 2004)....30
Figure 2.13: Simplified scheme of a photo-electro-catalytic device for CO_2 reduction to fuels using solar energy (Centi and Perathoner, 2009 32
Figure 2.14: Product yield from Nitrogen-doped nanotubes (Centi and Perathoner, 2009) 33
Figure 2.15: Process flow diagram of 100 t/day DME synthesis plant (Yotaro et al., 2006)....36
Figure 3.1: Flow chart of the Methodology....38
Figure 4.1: CHO Diagram....43
Figure 4.2: The Star of Gasification....45
Figure 4.3: Graphical representation of LFG reactions using Feed 1....50
Figure 4.4: Graphical representation of LFG reactions using Feed 2....51
Figure 4.5: Graphical representation of LFG reactions using Feed 3....52
Figure 5.1: Indicating the TBL - Feed 1....54
Figure 5.2: Indicating the TBL - Feed 2....55
Figure 5.3: Close up Representation of HHV – Feed 1....57
Figure 5.4: Close up Representation of HHV – Feed 2....58
Figure 5.5: Thermally balanced line, carbon boundaries and calorific value contours for Feed 1..60
Figure 5.6: Thermally balanced line, carbon boundaries and calorific value contours for Feed 2..61
Figure 6.1: Electricity generation using an Internal Combustion Engine.....64
Figure 6.2: Electricity generation using an Internal Combustion Engine represented on the TBL – Feed 1. 65
Figure 6.3: Electricity generation using an Internal Combustion Engine represented on the TBL – Feed 2 66
Figure 6.4: Electricity generations using SOFC's and dry reforming – Feed 1 67
Figure 6.5: Electricity generations using SOFC's and Feed 2 69
Figure 6.6: Electricity production using Feed 1....70
Figure 6.7: Electricity production using Feed 2....72
Figure 6.8: Electro-catalytic reduction of CO_2 using H_2O to produce methane....75
Figure 6.9: Electro-catalytic reduction of CO_2 using H_2 to produce methane 76

Figure 6.10: Production of methane using the Sabatier reaction 77
Figure 6.11: Methane generation using Feed 1 78
Figure 6.12: Methane generation using Feed 2 80
Figure 6.13: CH_2 production using Feed 1 82
Figure 6.14: CH_2 production using Feed 2 with a H_2O recycle stream 83
Figure 6.15: CH_2 production using Feed 2 – no recycle stream 84
Figure 6.16: CH_2 production using Feed 1 85
Figure 6.17: CH_2 production using Feed 2 with a H_2O recycle stream 87
Figure 6.18: CH_2 production using Feed 2 – CO_2 elimination 88
Figure 6.19: DME production using Feed 1 with a CO_2 recycle stream 89
Figure 6.20: DME production using Feed 1 without a CO_2 recycle stream 90
Figure 6.21: DME production using Feed 2 91
Figure 6.22: DME production using Feed 1 with a CO_2 recycle stream 92
Figure 6.23: DME production using Feed 1 without a CO_2 recycle stream 94
Figure 6.24: DME production using Feed 2 95
Figure 6.25: Production of chemicals with zero emissions – Feed 1 96
Figure 6.26: Production of synfuels with zero emissions – Feed 2 98
Figure 6.27: Production of synfuels with zero emissions – Feed 2 (r_2) 99
Figure 6.28: CHO diagram for Feed 1 – representing locus of chemicals 100
Figure 6.29: CHO diagram for Feed 2 – representing locus of syngas 102
Figure A1: CHO Diagram 119
Figure A2: Representing mixtures 121
Figure C1: Representing Calorific Value Contours on the CHO Diagram for Feed 1 133
Figure C2: Representing Calorific Value Contours on the CHO Diagram for Feed 2 135

List of Tables

Table 1.1: Advantages and Disadvantages of Medium pipeline gas (U.S. EPA LMOP, n.d).....5
Table 1.2: Advantages and Disadvantages of High pipeline gas (U.S. EPA LMOP, n.d).....6
Table 2.1: Comparison between Vertical and Horizontal gas wells (Swanepoel, 2009).....15
Table 2.2: Comparison of electricity production technologies (U.S. EPA LMOP, n.d).....27
Table 2.3: Typical Costs associated with electricity production technologies (U.S. EPA LMOP, n.d).....28
Table 5.1: Equations representing the Thermally Balanced Line for Feed 2.....55
Table 5.2: Endothermic reactions for Feed 3.....56
Table 6.1: Formation of zero emission locus.....97
Table 7.1: Summary of Results 107
Table A1: Molar Masses 120
Table B1: Enthalpies of Formation.....123
Table B2: Balanced Reactions.....125
Table B3: Enthalpy Ratios 125
Table B4: Balanced Reactions – Point A 125
Table B5: Balanced Reactions – Point B 126
Table B6: Balanced Reactions – Point C 126
Table B7: Equations representing the Thermally Balanced Line for Feed 2 127
Table B8: Endothermic reactions for Feed 3 127
Table C1: Percentage of Products.....129
Table C2: HHV for reactions according to Li et al, 2004.....129
Table C3: Calculating α 130
Table C4: Calculating β 131
Table C5: Calculating α and β for Feed 1 131
Table C6: BE percentages for Calorific Values for Feed 1 132
Table C7: Calculating α and β for Feed 2 134
Table C8: BE percentages for Calorific Values for Feed 2 134

Nomenclature

C&D	Construction and Demolition
CH_2	Synfuel
CH_4	Methane
CHO	Carbon-Hydrogen-Oxygen
CNG	Compressed Natural Gas
Co	Cobalt
CO_2	Carbon dioxide
Cu	Copper
DME	Dimethyl Ether
GHG	Green House Gas
H:H	High hazardous landfill
H:h	Low hazardous landfill
HHV	High Heating Value
H_2	Hydrogen
H_2O	Water
H_2S	Hydrogen sulphide
HC	Hydrocarbons
K	Kelvin
kW	Kilowatts

LFG	Landfill Gas
LNG	Liquid Natural Gas
MFC	Microbial fuel cell
MJ/m^3	Mega Joules per meter cubed
MSW	Municipal solid waste
Ni	Nickel
NOx	Nitrogen oxide compounds
TiO_2	Titanium oxide

1 Introduction and Background

Landfills are one of the largest human caused sources of methane, resulting in increased amounts of greenhouse gases. The use of landfills began by burying municipal refuse directly or after on-site burning and very little attention was given to the hazards associated with the generation of methane and toxic leachates as wastes decomposed. Gases produced by landfills are known as landfill gas (LFG) and is a by-product of the decomposition of waste in anaerobic conditions. These gases contain approximately 50 percent methane (CH_4) and 50 percent carbon dioxide (CO_2) with traces of other organic and inorganic compounds (Strachan et al., 2005). If these gases are extracted and cleaned in the correct manner, it can be used as renewable energy and thus reduce carbon emissions to the environment (Themelis and Ulloa, 2006).

In this dissertation, it is shown that landfill gas can be utilized as other fuel sources other than electricity. By utilizing the CHO diagram, various systems were analysed to assess the following:

- Environmental impacts associated with each process;
- Energy requirement as in adiabatic, endothermic and exothermic reactions;
- Carbon deposition through carbon boundaries;
- Calorific values; and
- The stoichiometric region which is the most desirable region to operate a process.

A few processes are analysed to determine which would be the most feasible option to convert LFG into useful products. Certain processes may become complex, and their design difficult to analyse. Mass balances and Carbon – Hydrogen – Oxygen (CHO) diagrams are used to limit the overall changes and product distribution as the product distributions are restricted to a confined exothermic region (Kauchali, 2012). Operation outside the desired region would result in energy intensive processes and may not make the process feasible.

1.1 The Sustainability of Landfill Gas

Through many studies and investigations over the years, landfills have evolved into efficiently operated bioreactors to produce CH_4 which can be used and converted into useful fuels. Most landfill gas projects involve the production of electricity through combustion of the gas. Current technologies allow for a 25 to 35 % conversion of energy to electricity. The rest of the energy is lost as heat which could be recovered and reused in the system.

In South Africa, it is estimated that up to 6% of the country's renewable energy target could be met using technologies such as converting LFG into electricity (Interwaste Environmental Solutions, 2010). Interwaste Environmental Solutions is closely associated with projects concerning waste to maximise the benefits of landfill gas utilisation in Gauteng as can be seen in Figure 1.1 below. Some of these projects which include flaring and power generation are already in full operation.

Ener-G Systems in South Africa is currently working on a project on the Marie Louise Landfill site situated in Dobsonville, Roodepoort to the North West of Johannesburg. They intend on converting the gas into electricity. The site is approximately 450m long and 500m wide and is predicted to provide enough gas to generate up to 6 MW of electricity (WSP, 2009). Ener-G Systems propose to install a 2 MW plant to monitor the gas yield from the site in order to determine the gas reserves. Once the reserves have been determined, the size of the energy generating plant will be increased to maximise electricity generation.

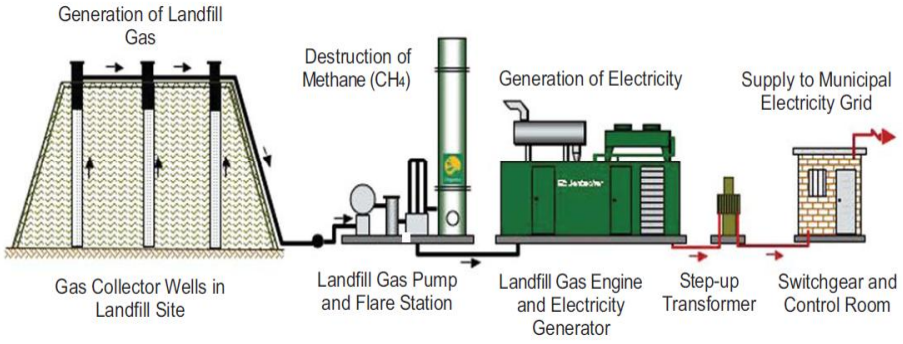


Figure 1.1: Schematic layout of Landfill gas to Electricity Project (Interwaste Environmental Solutions, 2010)

Landfill gas results from site surveys from the Coastal Park landfill site in Cape Town was made available and analysed by WSP and was used to predict the date of closure for the landfill. Figure 1.2 depicts the resulting landfill gas that will be generated over the next 112 years at the Coastal Park landfill site (Theeboom and Nontangane, 2010).

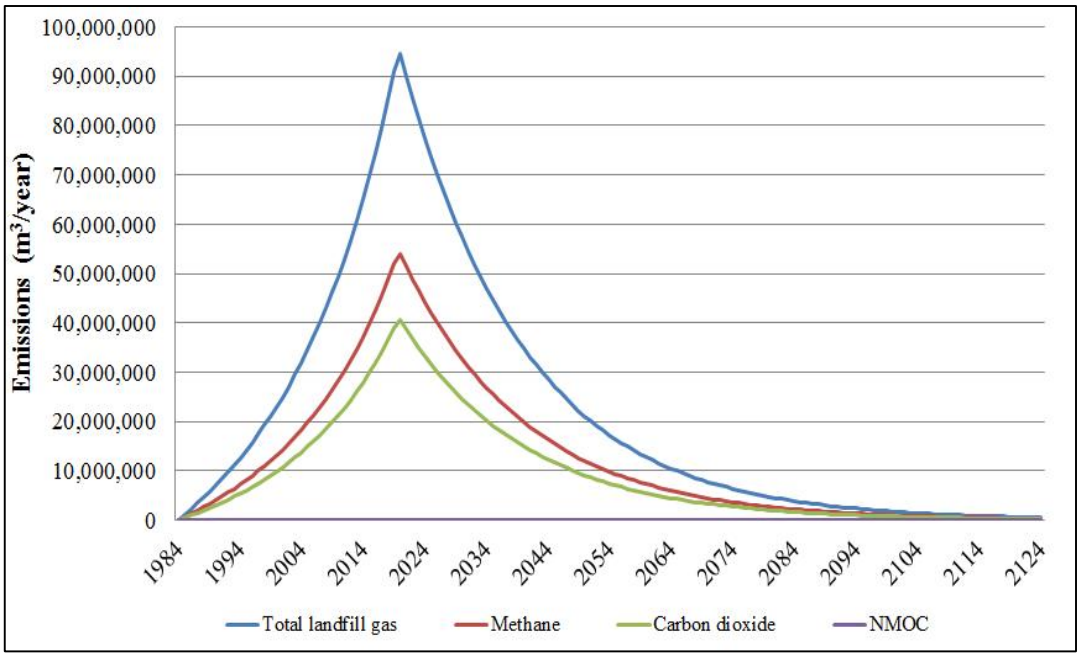


Figure 1.2: Emissions Evolution Curve for Coastal Park (Theeboom and Nontangane, 2010)

CH_4 and CO_2 generation has been occurring since 1994 and should peak in 2024. The best period for LFG utilization would be between 2004 and 2054. That would equate to 50 years of a renewable energy source.

Through the utilisation of LFG energy, environmental and economic benefits to energy users and the community are achieved. According to U.S. EPA LMOP, n.d, landfill gas Projects assist with:

- The reduction of emissions of GHG's that contribute to climate change;
- Offsets the use of non-renewable resources, such as coal, oil and natural gas;
- Improves local air quality;
- Provides income for Landfills;
- Provides energy cost savings for users of LFG energy; and

- Creates jobs and economic benefits for communities and businesses.

If different processes of converting the LFG into useful products are analysed, one can produce a useful source of energy on a large scale by decreasing the carbon emissions considerably. Though the benefits of LFG products are many, there is still a lot of controversy around this matter. These include the effect of moderating oil prices, sustainable energy production, continuous methane production from the wells and lifespan of the landfill to name a few.

1.2 Uses of Landfill Gas

The use of landfill gas as an energy source is a new concept to many, and research on LFG applications is still being investigated (U.S. EPA LMOP, n.d and Swanepoel, 2009). It can be thought of as a renewable resource, unlike petroleum and is produced from waste. Successful applications of LFG are electricity generation and direct use in boilers, kilns and furnaces as suggested in Pilarczyk et al., 1987, Malik et al., 1987, Bove and Lunghi, 2005 and Themelis and Ulloa, 2006. Another alternative use is the production of fuels (U.S. EPA LMOP, n.d and Stearns et al 1984); however this is not widely used and is still under investigation. More complicated processes are required for diesel and fuels; however fuels are required to burn when used in vehicles, hence producing emissions such as SO_2, NO_x and CO_2. The gas can also be converted into pipeline quality gas (compressed natural gas - CNG) and liquid natural gas (LNG). This process of converting the gas into high quality pipeline gas is highly expensive. The advantages and disadvantages of direct pipeline gas can be seen in Table 1.1 and 1.2 below.

Table 1.1: Advantages and Disadvantages of Medium pipeline gas (U.S. EPA LMOP, n.d)

Use	Technology	Advantages	Disadvantages
Medium Pipeline gas	• Boiler • Dryer • Process Heater	• Maximum amount of recovered gas flow utilised • Cost effective • Limited cleaning to remove condensate and particulate matter • Gas can be blended with other fuels	• Quality of gas needs to be improved or equipment to be retrofitted • All recovered gas must be used or it is lost • Costs increase with length of pipeline, hence consumer of energy must be nearby
	• Infrared Heater	• Limited cleaning to remove condensate and particulate matter • Relatively inexpensive • Easy installation • Small amounts of gas required • Can be coupled with another energy projects	• LFG utilization is limited to seasonal changes
	• Greenhouse	• Can mix different technologies	• LFG utilization is limited to seasonal changes
	• Artisan	• Small amounts of	• Can be expensive,

Use	Technology	Advantages	Disadvantages
	studio	gas required • Can be coupled with a commercial project	hence project economics may be limited without outside funding sources
	• Leachate evaporation	• Good option for landfills where leachate disposal is expensive	• Capital costs are high

The CO_2 separated can either be flared if in small quantities or can be processed into high purity liquid CO_2, used for coal beds and for oil and gas enhancements. The carbon dioxide can also be used for waste water treatment, dry cleaning or for the production of dry ice.

Table 1.2: Advantages and Disadvantages of High pipeline gas (U.S. EPA LMOP, n.d)

Use	Technology	Advantages	Disadvantages
High Pipeline Gas	• Pipeline quality gas	• Can be sold into a natural gas pipeline	• Potentially expensive gas processing required • Tight management of well-field operation needed to limit oxygen and nitrogen intrusion into LFG can increase costs
	• CNG • LNG	• Alternative fuels for vehicles at the landfill or refuse hauling trucks	• Potentially expensive gas processing required • Tight management of well-field operation

Use	Technology	Advantages	Disadvantages
		• Supply to general commercial market	needed to limit oxygen and nitrogen intrusion into LFG can increase costs

Different applications require different processes and hence these processes require different energy inputs and give of different energy outputs. Thus, by analysing energy balances around each process shown, one can find the optimum process of converting LFG into useful products.

1.3 Problem statement and research motivation

The need for alternative energy sources comes from the depletion of coal reserves, gas and crude oil within the next 150 years. Furthermore, the depletion of the ozone layer and the current environmental issues are forcing people to recycle and re-use wherever possible. The conversion of LFGs into useful products is quickly becoming popular with global warming and today's need for carbon credits. Companies around the world are looking to "Go Green" by reusing and recycling. It has also been argued that by converting LFG into fuel, the use and production of CO_2 is of great advantage in the prevention of climate change than other petroleum fuels. This is because the carbon used and produced during LFG Fuel production is part of a "free carbon cycle" whereas the emissions released from crude oil are part of a "locked carbon cycle" (Robson, 2004). The total greenhouse gases will also be reduced considerably by the combustion of the recovered methane contained in the landfill gas. Thus by implementing the use of landfills and other such alternatives to produce power is a great benefit to the up keeping of the environment (Hongguang, 2006).

Processes for converting LFG and other biomass are required in order to deal with the depletion of fossil fuels. This dissertation focuses on the development of a graphical technique that allows various technologies to be developed with syngas

production as an intermediate step and considers mass balances to determine the stoichiometric region for syngas production. Energy balance limit the stoichiometric region to autothermal operation, whilst carbon boundaries identify further restrictions on the stoichiometric region, and contours of Higher Heating Values (HHV) identify regions to obtain high calorific value syngas.

2 Literature review

2.1 Landfills

Landfills are huge pieces of land that are used for waste disposal and degeneration. The waste is sorted and managed so as to create the decomposition of waste. Through the decomposition of waste, LFG is produced and studies have shown that by extracting these gases, one can produce a source of renewable energy. There are many types of landfills depending on the class of waste. In the landfill classification system, a landfill is classified in terms of waste class, size of operation, and potential for significant leachate generation, all of which influence the risk it poses to the environment (Department of Water Affairs and Forestry, 1998). Waste types are grouped into two categories, General and Hazardous waste; hence landfills have to be grouped accordingly. General waste can be disposed of at any permitted landfill, however it is important to note that should it be disposed of on a hazardous landfill site, the charges for waste disposal are much higher. Hazardous waste is classified into 4 classes for landfill disposal:

- Hazard Rating 1: Extreme Hazard
- Hazard Rating 2: High Hazard
- Hazard Rating 3: Moderate Hazard
- Hazard Rating 4: Low Hazard

Each hazard rating has a different treatment and disposal requirement hence hazardous landfills are divided into two types according to their hazard rating, namely High hazardous landfill (H:H) and low hazardous landfill (H:h). H:H landfills can accept all hazard ratings of waste, while H:h landfills can only accept Hazard Ratings 3 and 4 and general wastes. Only non-hazardous landfill sites can be used for LFG utilization projects.

Before landfill gas energy projects can be rendered viable, initial assessments must be conducted to estimate the LFG recovery potential. This includes determining whether the landfill produces enough methane to support the energy recovery project as this is the main gas source. Below are the criteria for feasible landfill gas energy projects:

- The site should have at least 1 million tons of Municipal solid waste (MSW);
- Must have a depth of 50 feet (15.24 meters) or more;
- Must determine whether the site is open or recently closed; and
- The site should also have at least 25 inches (63.5 cm) of precipitation annually.

Landfills meeting the above criteria generally have enough methane gas to support a LFG energy project (U.S. EPA LMOP, n.d).

2.2 Gas Composition

Landfill gas is a natural by-product of anaerobic decomposition of solid waste. It is produced when biodegradable waste is broken down by micro-organisms (Swanepoel, 2009). The quantity and quality of LFG varies with the landfills content i.e. the characteristics of the waste and is dependent on many factors such as age of the landfill, weather conditions and design of the landfill to name a few. The total time and phase duration of gas generation varies with these landfill conditions. This can be seen in Figure 2.1 below. It is noted that maximum production is achieved between 10-15 years which also corresponds to the end of a landfill site lifespan. It is thus imperative to be able to have a viable project with sensible production rates between 3-5 years into a landfill site.

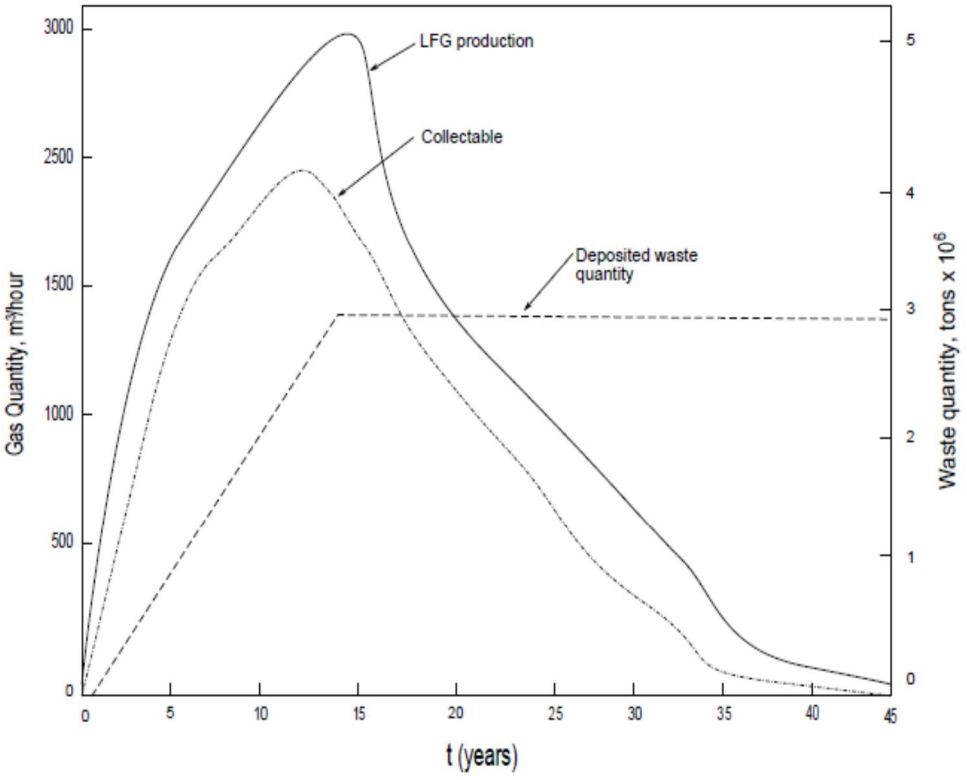


Figure 2.1: Landfill gas production over the course of time (Koch, 2001)

LFG is primarily CH_4 and CO_2 with traces of non-methane organic compounds and inorganic compounds. The various phases that LFG production processes undergo depend on factors such as humidity, temperature and atmospheric pressures. Berger and Mann, 2001, suggest four phases of bacterial decomposition of landfill waste and this is shown in Figure 2.2 below. The four phases as described by Berger and Mann, 2001 are:

- Phase I: Aerobic bacteria consume oxygen that is present in the landfill as well as proteins, lipids and complex carbohydrates that are found in the organic waste. Large amounts of nitrogen are found in this phase, whilst oxygen is still present. Carbon dioxide is the by-product of the aerobic decomposition of waste and lasts for days or months, depending on the waste content.
- Phase II: Once all the oxygen has been consumed by the aerobic decomposition of waste, compounds created in Phase I are converted into methanol, ethanol, acetic acid and lactic acid in an anaerobic process. No

methane is produced during this phase. This phase usually lasts a week at most but will return to Phase I if the process is disturbed or oxygen is introduced into the landfill.

- Phase III: The acids produced in Phase II are converted through anaerobic decomposition into acetate, an organic acid. The unstable production of methane gas is the main constituent during this phase and is driven by the production of the organic acid i.e. the acid producing bacteria form acids which is the methane producing bacteria's main energy source. The acid producing bacteria cannot survive in an acidic environment; hence by consuming acetate and carbon dioxide, the methanogenic bacteria help keep a neutral pH throughout the landfill.
- Phase IV: This phase begins when LFG is produced at a stable rate, and can last between twenty to fifty years after the cell initially started receiving waste.

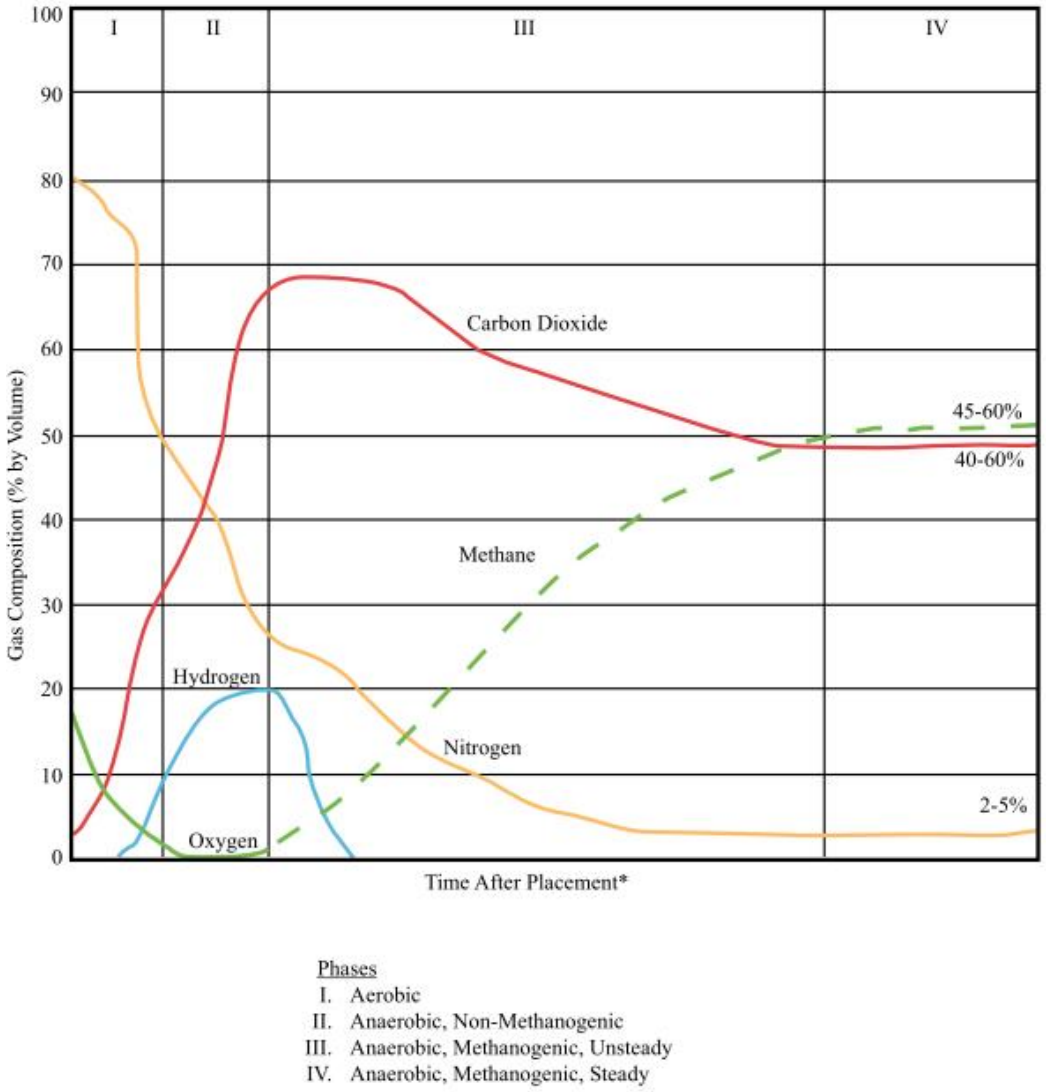


Figure 2.2: Changes in Typical LFG composition after Waste disposal (Berger and Mann, 2001)

Generally the amounts of methane and carbon dioxide produced are approximately 50% each, but this varies with every landfill. It is the methane content within the gas that makes it a viable source of re-usable energy (Last, 2009). Carbon dioxide and methane are greenhouse gases, however, methane is highly flammable in large quantities and is 21 times more potent than carbon dioxide and therefore has a higher impact on global warming (Weyant et al., 1999). Thus LFG poses a serious threat to the environment and needs to be managed accordingly.

2.3 Landfill gas extraction process

Gas extraction from landfills is done using gas wells and these come in two forms namely, vertical and horizontal wells. These are explained in detail below.

2.3.1 Gas Wells

Gas collection begins after a portion of the landfill is closed. This is known as a cell. The gases can be extracted by sinking a number of wells or boreholes into the landfill and collecting the gases through pipes (Last, 2009). It is important to note that every cells contains different types of waste that is at different stages of decomposition (Strachan et al., 2005), hence the flow rate of extracting LFG fluctuates. Gas fluctuation also occurs due to gas wells being installed in newly developed landfill cells. Landfills generally receive waste over a period of 20 to 30 years, which means that waste in an older inactive cell of the landfill could be in the final phase of LFG production, whilst a new active cell may only be starting to produce LFG (Berger and Mann, 2001). To ensure that as much of the extracted LFG can be used, cell development timing is crucial to aid in removing as much LFG as possible.

The type of gas wells that are to be drilled depend on the shape and volume of the cell, however cost implications also play a role (Swanepoel, 2009). The two main types of wells that are currently in use are vertical and horizontal gas wells. Some collection systems use a combination of vertical and horizontal wells. Well-designed systems of either type of wells are effective in collecting LFG.

Swanepoel, 2009, gives a comparison between vertical and horizontal gas wells indicating the typical costs incurred in constructing and operating the wells. This can be seen in Table 2.1 below.

Table 2.1: Comparison between Vertical and Horizontal gas wells (Swanepoel, 2009)

	Vertical Wells	Horizontal Wells
Capital costs (per hectare)	R 1.0 million	R 0.7 million
Operational Costs (per hectare annually)	R 2 678	R 3 480
Active or inactive cell	Inactive	Active
Spacing	Radius of 25m	30m horizontally, 10m vertically

Vertical Wells

Vertical gas wells are installed once an inactive cell is filled up. To install the vertical wells, 0.5m diameter holes are drilled 3 to 50 m deep, depending on the depth of the landfill. They have a sphere of influence with a radius of approximately 25m. This can be seen in Figure 2.3 and 2.5 below.

Horizontal Wells

Horizontal gas wells are placed in a cell that is still receiving waste and is referred to as an active cell. These wells are installed 30m apart horizontally and placed in layers 10m apart vertically as the cell is filled up with waste (Swanepoel, 2009), and is seen in Figure 2.4 and 2.6 below.

Each well head is connected to lateral piping, which transports the gas to the main collection header, regardless of whether the wells are used. This is seen in Figure 2.7 below. The design of the collection system should be done in such a way so as to allow the operator to monitor and adjust the gas flow. The creation of these wells is expensive and existing projects indicate that the individual flow rates of the various wells vary significantly. A preliminary study is crucial to determine the amount of methane generation in the landfill and to investigate whether the project of extracting gas is even viable.

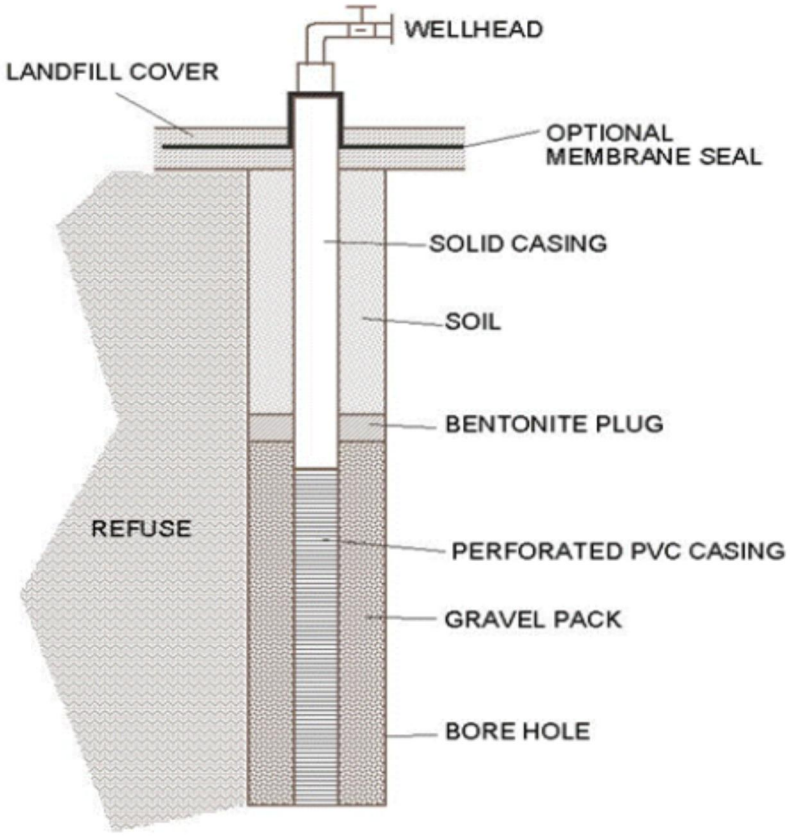


Figure 2.3: Vertical LFG extraction wells (U.S. EPA LMOP, n.d)

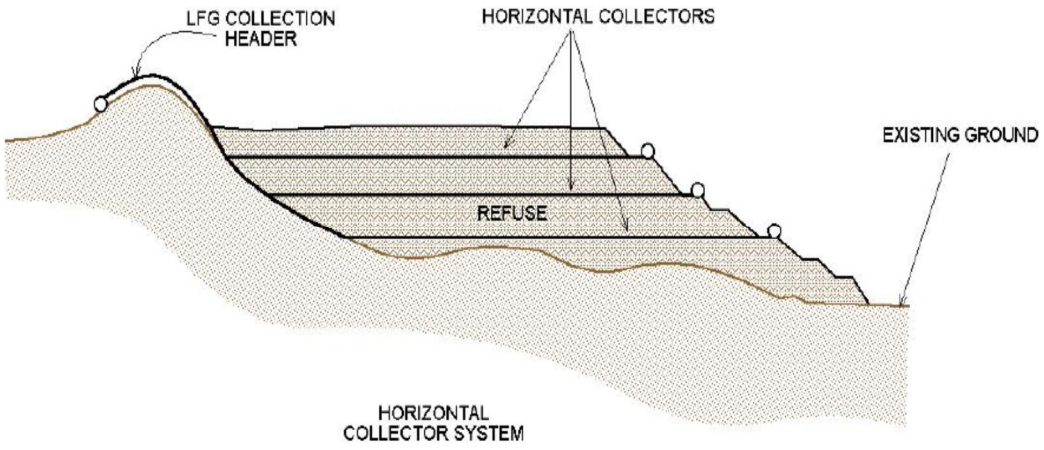


Figure 2.4: LFG Collection system with horizontal Trenches (U.S. EPA LMOP, n.d)

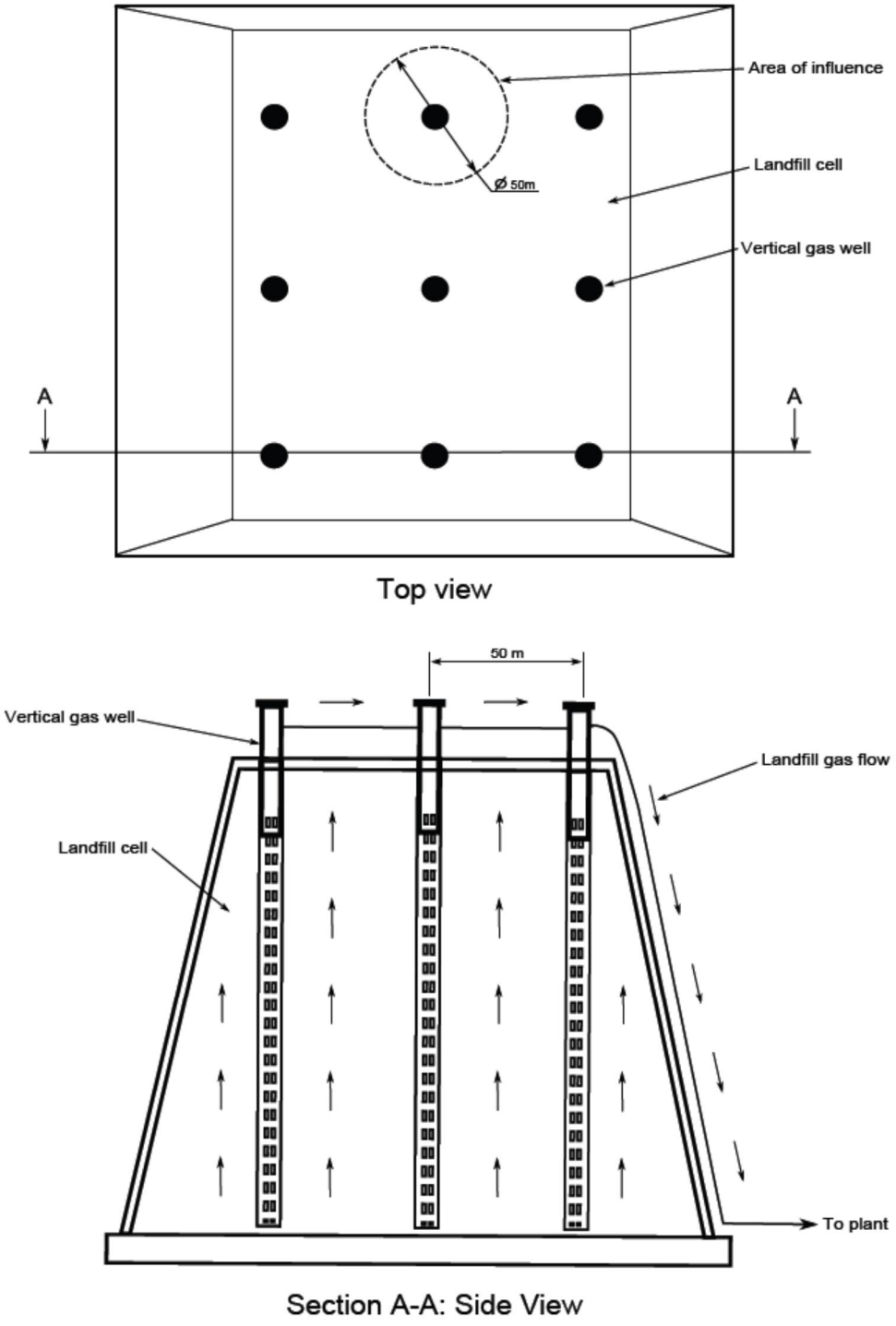


Figure 2.5: The area of influence and spacing of vertical gas wells (Swanepoel, 2009)

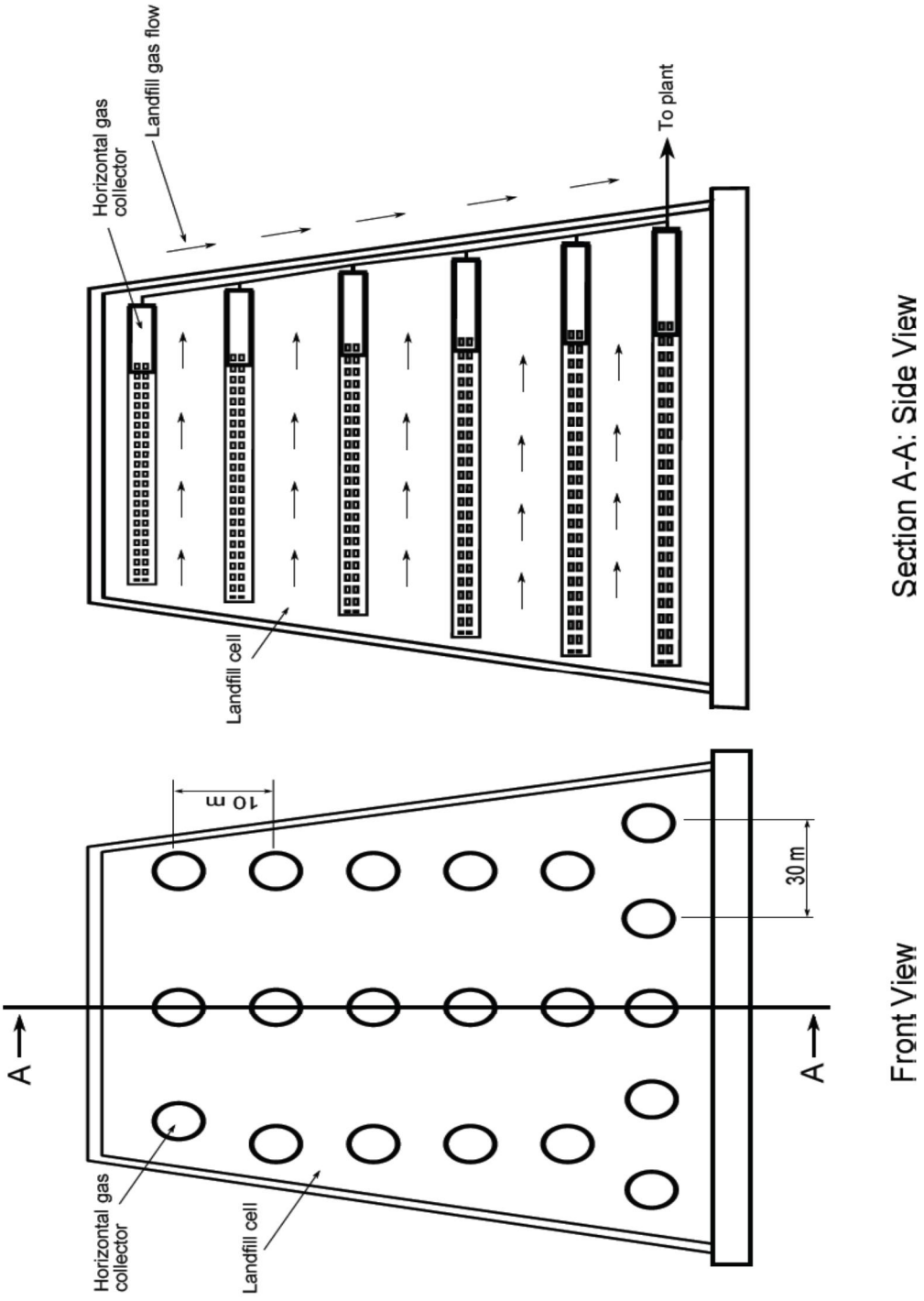


Figure 2.6: The area of influence and spacing of horizontal gas wells (Swanepoel, 2009)

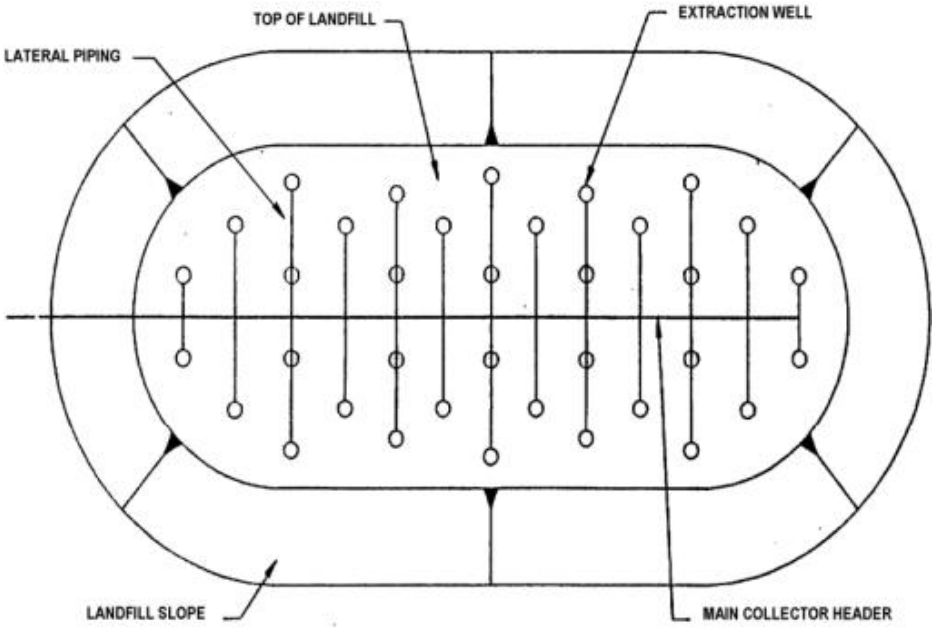


Figure 2.7: LFG Extraction site plan (U.S. EPA LMOP, n.d)

2.3.2 Leachate

One of the main problems associated with landfills is leachate generation. It occurs through water drainage through decomposing waste. The quantity and composition of the leachate vary significantly between landfills and is a factor of geographical location, seasons and rate of decomposition to name a few. Four groups of pollutants are usually found in leachate: dissolved organic matter, inorganic macro-components, heavy metals, and xenobiotic organic compounds (Greenman et al., 2009). Due to the complexity of components found in leachate and the inconsistency in quality and quantity of the wastewater, treatment of the wastewater becomes exceptionally difficult and expensive. U.S. EPA LMOP, n.d suggests that leachate evaporation is a good option when treatment becomes expensive. Evaporators are available in a number of sizes and reduce the volume of the leachate collected by concentrating the wastewater. This allows for a more manageable disposal volume. The downfall to this is that high capital costs are associated with projects like this. Greenman et al., 2009 suggests that by using a microbial fuel cell (MFC), wastewater treatment and electricity production can be

accomplished. This technology is still in the early stages of its development and hence will not be discussed further in this dissertation.

2.4 Gas Cleaning

Once the gas has been extracted and before it can be converted for energy usage, the gas must undergo different cleaning processes. Treatment requirements depend on the end use application. Minimal treatment is required for direct use of the gas in boilers, furnaces or kilns. If the gas is used for electricity purposes, treatment systems include a series of filters to remove contaminants such as siloxanes that could damage engines and turbines and reduce the efficiency (Ajhar et al., 2010). If the gas is converted into pipeline quality gas, more extensive treatment is required such as adsorption and absorption and thus becomes expensive. The type of cleaning mechanisms used thus depends on the end product, changes in air quality and regulations and emission limits that are placed on all processes.

Cleaning of the gas can be divided into primary and secondary treatment processing. Primary cleaning processes usually include de-watering and filtration of the gas to remove moisture and particulates. Newer projects now use gas cooling and compression to remove moisture. Secondary treatment processes depend on the end use of the gas and the contaminants that need to be removed for the end use of the gas. The three main trace contaminants are siloxane, sulphur compounds and halogens (Deed et al., 2004).

2.4.1 Primary Cleaning

Primary treatment processes use simple physical process operations and represent the first stage of reducing the amounts of contaminants in LFG. The main constituents removed are condensate (water) and particulates.

Condensate Knock-out

The presence of condensate in landfill gas can have a negative impact on plant performance such as accumulation of water reduces gas flow space, raises the pressure loss, the two-phase flow is unstable and can cause oscillations which make it difficult to achieve a steady state and controllable operation (Deed et al., 2004). Three components of the gas can be treated, namely, slugs of liquid, gas-liquid foam and uncondensed water vapour. In-line dewatering is commonly used by landfill operators. The final element of de-watering is the condensate knock out pot and is situated as close to the inlet gas booster as possible. The purpose of the knockout drum is to decrease the gas velocity to create a "dropout" of liquid. The liquid is then drained and pumped to discharge. Demisting meshes are used for refinement of water. The meshes are placed in gas pipes entering and leaving a condensate knockout drum. Foam is trapped in these meshes and is prevented from getting carried over. Uncondensed water vapour is removed through gas cooling and compression. Typical temperatures for gas cooling are between 2 to 10 $^{\circ}$C, whilst gas compression ranges from 69 to over 690 KPa, depending on the input pressure and distance to energy recovery system requirements (U.S. EPA LMOP, n.d and Deed et al., 2004).

Particulate filtration

Particulates found in landfill gas must be removed during primary cleaning as it may cause damage to systems and equipment on plants downstream. Particulates are removed by passing the gas through wired filter pads or using a cyclone separator. Both systems are prone to blockage due to the fine particulate matter; hence require frequent maintenance to remove solid build up (Deed et al., 2004).

2.4.2 Secondary Cleaning

Processes which include both physical and chemical processes are known as secondary treatment. Secondary treatment processes are sometimes made up of multiple clean up processes and are designed to provide greater gas cleaning than

primary treatment processes alone (U.S. EPA LMOP, n.d and Deed et al., 2004). The cleaning of landfill gas is done prior to combustion; hence it has no effect on bulk emissions of CO and NO_x. It is only used to reduce destructive gas components that will reduce the engine efficiency or cause unacceptable levels of emissions (Deed et al., 2004). Secondary cleaning processes depend on the constituents that need to be removed for the desired end use. Dry scrubbing and wet scrubbing are mainly used to remove H_2S from the gas, although wet scrubbing can be used to remove a number of other compounds. Dry scrubbing uses solid chemical treatment for H_2S, whereas wet scrubbing uses dry or liquid chemicals for cleaning and may be applied in batch contactor towers or injected directly into the gas pipeline. During wet scrubbing, the by-product of the reaction is generally separated and disposed of, the chemical is consumed and the absorbent can be regenerated. Membrane separation techniques, pressure swing processes, liquid absorption/solvent scrubbing processes, water scrubbing processes and cryogenic processes are used to remove impurities like CO_2, N_2 and other trace components.

H_2S Removal

Hydrogen sulphide has been known to accumulate in landfills as a result of decomposition of material. The concentration of H_2S in the LFG depends largely on the material being disposed of in a particular landfill site. Studies have shown that high concentrations of H_2S were recorded in construction and demolition (C&D) debris landfills. One particular material responsible for high concentrations of H_2S in LFG was found to be gypsum, which is a good fire barrier and is used in buildings for interior walls (Panza and Belgiorna, 2010). H_2S has a characteristic rotten egg smell and can be detected by humans in concentrations as low as 0.21 ppb, with concentrations greater than 30 ppm affecting the human nervous and respiratory system as stated in Panza and Belgiorna, 2010. H_2S concentration in a typical landfill can account for 0.01% of the total landfill gas on a dry volume basis (Malik et al., 1987). Sites containing gypsum is known to produce considerable amount of H_2S gas ranging from 7ppm

to 100ppm (Panza and Belgiorna, 2010), and in some extreme cases, concentrations as high as 5000 – 12 000 ppm can be detected (Reinhart and Townsend, 2002; Haarstad et al., 2003 and Lee et al., 2006). H_2S has also proven to be corrosive in the presence of moisture. The removal of H_2S along with heavy organic contaminants poses the greatest concern, and is generally removed in two separate stages, depending on the end use of the gas and the concentration of H_2S found in the gas. In the first stage of the process, LFG is passed through a scrubber where the bulk of the H_2S is removed. In the second stage, the scrubbed and dried LFG is passed through a multiple bed adsorption unit where halogenated hydrocarbons, organic sulphurs and most of the heavy hydrocarbon are removed. The adsorption unit can also be fitted with a layer of impregnated carbon for additional H_2S removal. A representative H_2S specification for pipeline quality methane is approximately ¼ grain per 100 SCF (standard cubic feet) (2.63Nm^3) (Malik et al., 1987). A basic representative of H_2S removal can be seen in Figure 2.8 below.

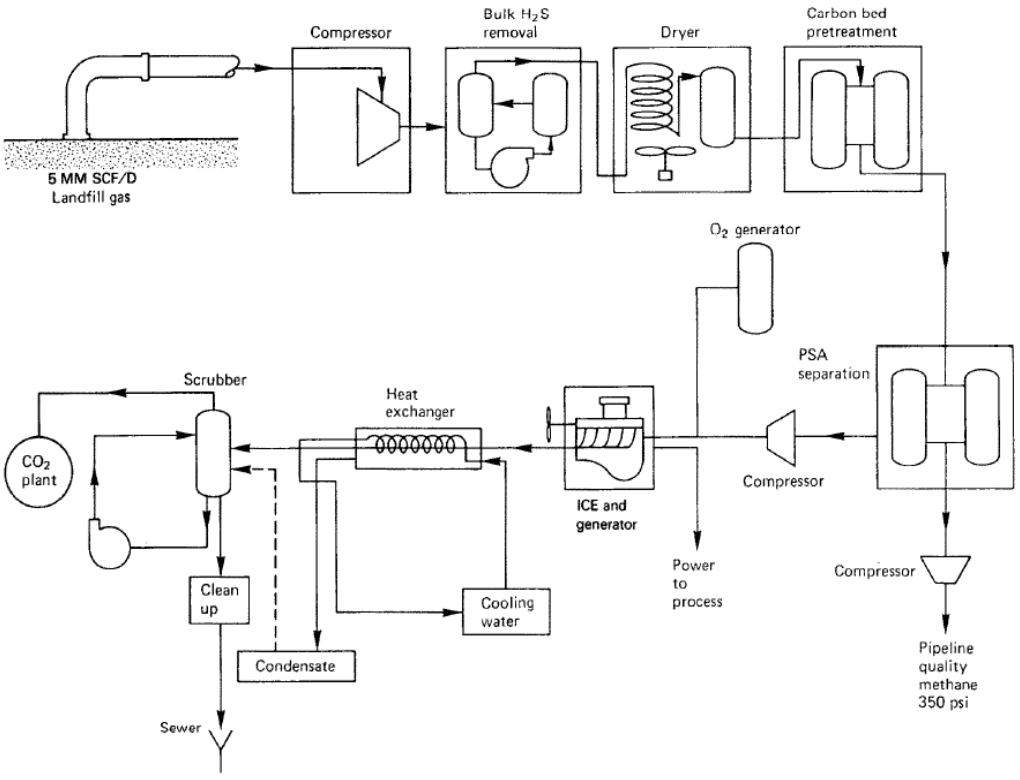


Figure 2.8: Removal of H_2S for CO_2, methane and electricity production (Malik et al., 1987)

Siloxane Removal

Siloxanes are found in household and commercial products such as cosmetics, deodorants, food additives and some soap to name a few, and end up in solid waste and wastewater (Xebec Adsorption Inc., 2007 and U.S. EPA LMOP, n.d). According to Xebec Adsorption Inc., 2007, one third of all landfill sites have a severe siloxane problem and this can be seen in Figure 2.9 below. Traces of siloxanes are found in LFG and these are converted into silicon dioxide, the main constituent of sand. The general organic concentration of silicon compounds found in typical landfill sites are in the range of 3 – 24 mg/m^3 (Ajhar et al., 2006). The silicon dioxide collects on the inside of internal combustion engines, gas turbines and on boiler tubes and in turn reduces the performance of the equipment. Figure 2.10 shows silica build-up on heads and scrapped pistons of engines. Other undesired effects include poisoning of catalysts that are used in steam reforming (Finocchio et al., 2009) or fuel cells (Haga et al., 2008), as well as the deactivation of catalysts for pre-combustion and post-combustion of gas purification (Urban et al., 2009). This also leads to higher maintenance costs. Commercially available technologies used for siloxane removal are adsorption, absorption and deep chilling. Other technologies that have not yet gained access to commercial biogas purification include bio-trickling filters, catalysts and membranes (Ajhar et al., 2006). Siloxane removal however depends on the energy technology selected as well the composition of the siloxanes in the gas, and this varies with every landfill.

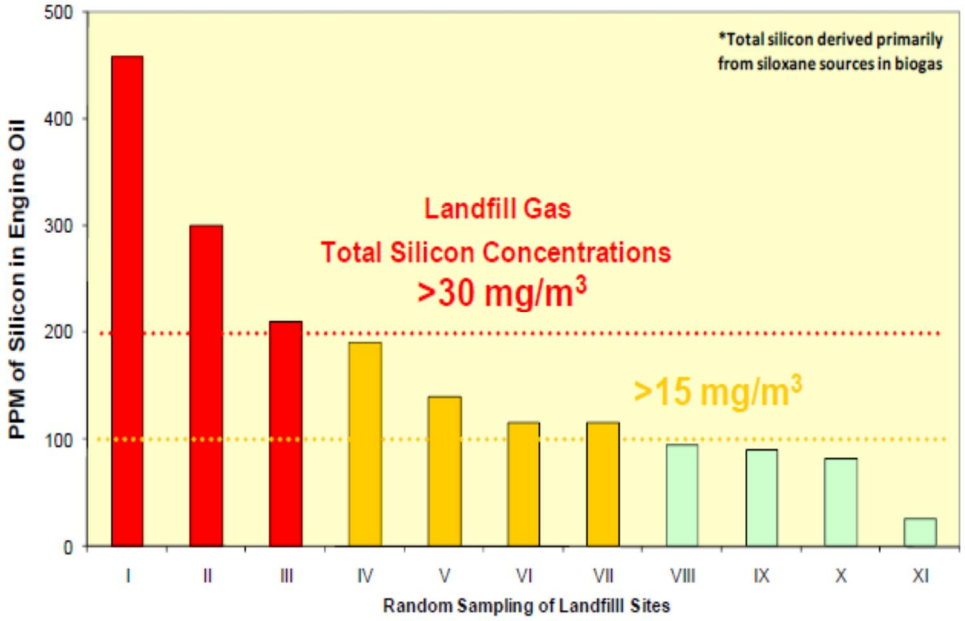


Figure 2.9: One third of all landfill sites have a severe siloxane problem (Xebec Adsorption Inc., 2007)



Figure 2.10: Silica build up on heads and scrapped pistons of Caterpillar and Jenbacher engines (Xebec Adsorption Inc., 2007)

As discussed above, a low, medium or high grade fuel produced from LFG is dependent on the different methods of cleaning. Each grade of fuel has a specific heating value. Low and medium grade fuel produced from LFG has a heating value of approximately 16.8MJ/m^3 and is roughly half the heating value of natural gas. High grade fuel that has been processed and treated further has a higher heating value as compared to low and medium grade fuels of approximately 37.3MJ/m^3. Due to its high heating value, high grade fuel produced from LFG can be substituted directly for natural gas in pipeline applications. (CRA, n.d).

2.5 Electricity

2.5.1 Electricity generation

One of the most common ways of converting landfill gas into useful energy is the production of electricity. Electricity is produced by burning the gas using internal combustion engines, gas turbines or micro-turbines. Each of these is discussed in Table 2.2. Figure 2.11 represents a basic flow diagram of electricity generation.

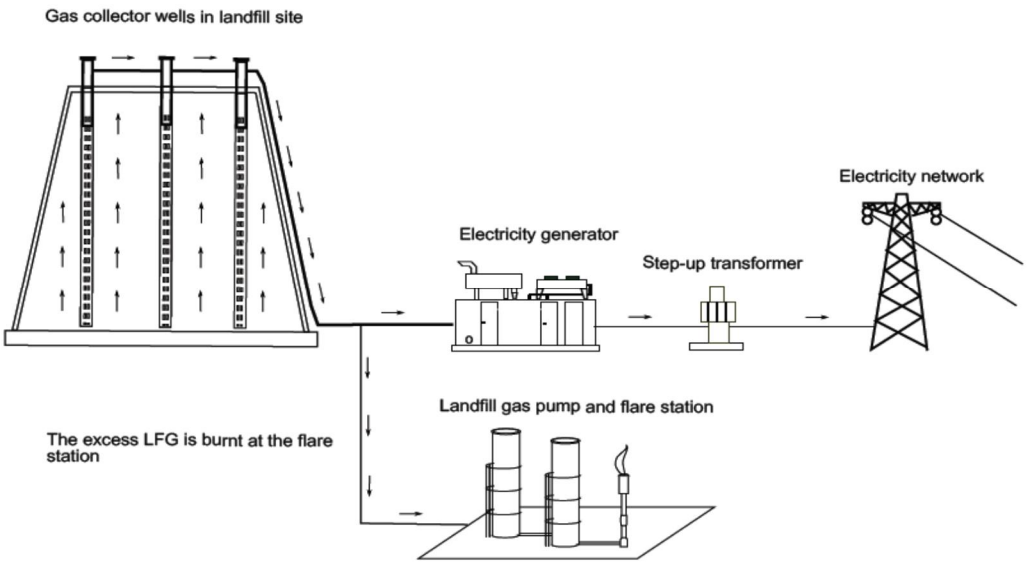


Figure 2.11: The flow of LFG from extraction to electricity generation (Swanepoel, 2009)

As can be seen from Figure 2.11, LFG is extracted from the landfill through wells. The gas then goes into electricity generators where it is converted into electricity. The gas does not need to be cleaned for electricity purposes. Excess gas gets flared, whilst the gas that is converted into electricity gets transmitted onto transmission lines.

Table 2.2: Comparison of electricity production technologies (U.S. EPA LMOP, n.d)

Technology	Advantages	Disadvantages
■ **Internal combustion engine** ■ **Sizing: 800kW to 3 MW per engine**	■ High efficiency compared to gas and micro turbines ■ Good size match with the output of gas of many landfills ■ Relatively low costs when compared with gas and micro turbines on a kW installed capacity basis ■ Increased efficiency when waste heat is recovered ■ Engines can be added or removed to follow gas recovery trends	■ Maintenance costs are relatively high ■ Relatively high air emissions ■ Economics may be marginal in areas with low electricity costs
■ **Gas turbine** ■ **Sizing: 1 – 10 MW per gas turbine**	■ Economies of scale, since the cost per kW of generating capacity drops as the gas turbine size increases and the efficiency improves. ■ Increased efficiency when heat is recovered ■ More resistant to corrosion damage ■ Low nitrogen oxides emissions ■ Compact	■ Reduced efficiency when the unit is running at partial load ■ High gas compression required ■ High parasitic loads ■ Economics may be marginal in areas with low electricity

Technology	Advantages	Disadvantages
		costs
■ **Micro-turbine** ■ **Sizing: 30 – 250 kW per micro-turbine**	■ Lower gas flow required ■ Can function with low methane percentage ■ Low nitrogen oxides emissions ■ Relatively easy interconnection ■ Unit can be readily added or removed as availability of gas quantity changes	■ Extensive pre-treatment of LFG is required ■ Economics may be marginal in areas with low electricity costs

The cost for the above mentioned comparisons can be seen in Table 2.3 below. From this it can be seen that gas turbines are the cheapest way to generate electricity with micro-turbines being the most expensive.

Table 2.3: Typical Costs associated with electricity production technologies (U.S. EPA LMOP, n.d)

Technology	Estimated Capital Costs R/kW)*	Estimated Annual OandM Costs (R/kW)*
Internal combustion engine (>800kW)	R 13 898.37	R 1 471.29
Small internal combustion engine (<1MW)	R 18 803.07	R 1 716.51
Gas turbine (>3MW)	R 11 443.74	R 1 062.45
Micro-turbine (<1MW)	R 44 957.55	R 3 105.62

* Based on 2010 dollars, with 2012 exchange rate

Another alternative to produce electricity is also available, this being fuel cells. Fuel cells generate electricity by means of a chemical reaction. Every fuel cell is made up of two electrodes, namely, the cathode which is the positive electrode and anode, the negative electrode. The chemical reactions which produce

electricity occur at the electrodes. Fuel cells also contain electrolyte which carry electrically charged particles from one electrode to the next. The type of fuel cell developed, the design of electrodes and the fuel type used depends on the type of electrolyte used. The main electrolyte types are: alkali; molten carbonate; phosphoric acid; proton exchange membranes (PEM) and solid oxide. PEM and solid oxide are solid electrolytes, whilst the rest are liquid. In this dissertation, solid oxide fuel cells (SOFCs) are investigated to determine its yield on electricity production and the emissions produced thereof.

2.5.2 Solid Oxide Fuel Cells

SOFCs use solid metal oxides such as calcium or zirconium as electrolytes. Hydrogen is the basic fuel used in fuel cells, however, with the SOFC, hydrocarbon fuels can be used due to the CO not depositing on the anode (Ye et al., 2010 and Lorente et al., 2012). Furthermore, very little pollutants are emitted as compared with other conventional technologies such as combustion engines and since they create electricity without combustion, they extract more energy from fuels (Minh, 2004).

The basic principal of the fuel cell is that the fuel enters the fuel cell at the anode, where H_2 is stripped of their electrons and become ionized, carrying a positive electrical charge. Oxygen or air enters the fuel cell through the cathode and picks up electrons as they travel through the electrolyte to the anode where it combines with the H_2 ions (Minh, 2004). The electrolyte plays an important role as it must allow the correct amount of ions to pass between the electrodes. If free electrons or other substances travel through the electrolyte, the chemical reaction is interrupted and electricity is not produced. A simple configuration is shown in Figure 2.12 below.

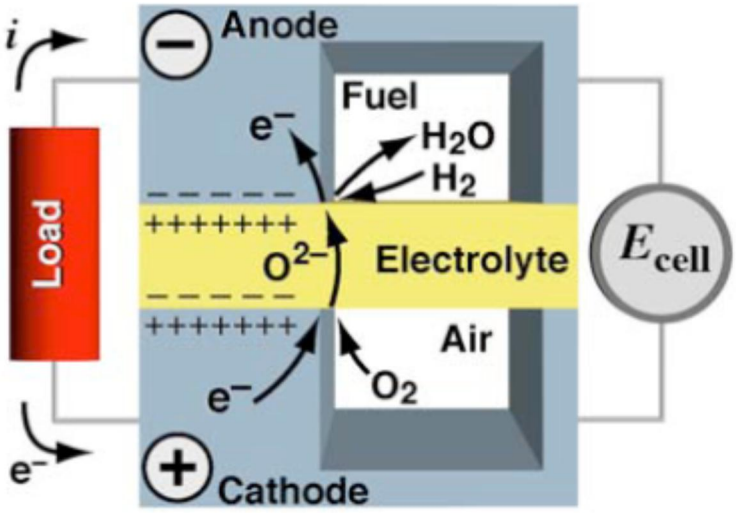


Figure 2.12: Practical SOFC with three phase boundary to facilitate charge transfer (Kee et al., 2004)

SOFCs operate at high temperatures of about 700°C to 1000 °C and has an efficiency and cell output of approximately 70% and 100kW respectively (Minh, 2004). Due to such high temperatures, a reformer does not need to be used to extract the hydrogen from the fuel, and waste heat can be recycled advancing system efficiency further. A catalyst is used to speed up the reaction rate. Disadvantages to SOFCs are as a result of the high temperatures and limitations to SOFC applications. The sizes of the fuel cells are quite large and although the electrolyte cannot leak due to it being solid, it can crack.

The results of the following sections examined look at syngas as a fuel source. The reactions that will be analyzed are as follows:

$$2\,H_2 + O_2 \rightarrow 2H_2O \qquad 2.1$$

$$CO + H_2O \rightarrow H_2 + CO_2 \qquad 2.2$$

Equation 2.1 occurs as a result of the general chemical reaction of the fuel cell where hydrogen reacts with oxygen to produce electricity and a byproduct, water. The CO from the syngas reacts with the produced water according to the water-gas shift reaction (Equation 2.2), and forms further H_2 which can be converted into electricity. The emission from Equation 2.2 is CO_2.

2.6 Electro-Catalytic reduction of CO_2

Landfill gases are made up of typically CO_2 and CH_4. It is said that methane is highly flammable in large quantities and is 21 times more potent than carbon dioxide and therefore has a higher impact on global warming (Weyant et al., 1999). However, methane makes a good fuel source, therefore, if the CO_2 from landfills are converted into methane, the methane content from landfills can be doubled, to produce a greater fuel volume. This application is used largely in space based operations, however it can be used to solve the problem of global warming and the sustainable energy shortage simultaneously as discussed in Izumi, 2010 and Brooks et al., 2006. A process using the electro-catalytic reduction of landfill CO_2 to methane is investigated in the sections that follow using literature from Lyndon, 2008 and Dey et al., 2004, to see if the processes are economically viable. According to Lyndon, 2008 the reaction occurs at room temperature and includes a polymer solid-electrolyte membrane, onto which are deposited cathode and anode films. CO_2 is circulated past the cathode film, which is catalytic for electrolytic reduction of CO_2, whilst water is circulated past the platinum anode.

The overall reaction is as follows:

$$CO_2 + 2H_2O \rightarrow CH_4 + 2O_2 \qquad 2.3$$

This process seems highly attractive at first glance, however studies have shown that the activation energy required for this reaction is considerably high with ΔH = 891 KJ/mol. Furthermore, electrolytic reactions prove to be more expensive than reactions that happen spontaneously or reactions that require a catalyst only.

Equation 2.3 can also occur through the photo-catalytic reduction of CO_2. Izumi, 2010, explains the photo-catalytic enhancement of TiO_2 using highly dispersed active Ti ion species. Two tests were compared: Ti species anchored on PVG prepared from $TiCl_4$ and the second, highly dispersed TiO_2 powder in the photo-catalytic reduction of CO_2. The TiO_2 powder proved to produce only methane with a formation rate of 0.17 $\mu mol.h^{-1}.g_{cat}^{-1}$, whilst the Ti-PVG catalyst produced methane, methanol and CO, with the formation rate of methane being 1.6 nmol.h^{-}

$^{1}.g_{cat}^{-1}$. By using semiconductor photocatalysts such as Pt-promoted perovskite $NaNbO_3$, Izumi, 2010 reported to produce methane at a rate of 4.9 µmol.$h^{-1}.g_{cat}^{-1}$. The photo-catalysis reaction mechanism is still not commercialised and hence not well understood, and there is not enough theoretical understanding to explain the product selectivity using TiO_2.

The photo-electro-catalytic conversion of CO_2 in water is only sustainable when electrons and protons needed for the reaction are supplied using renewable resources such as solar energy and wind energy (Centi and Perathoner, 2009). Furthermore, based on the results obtained to date, it is evident that the development of a more efficient photocatalyst is required for the use of the photo catalytic reduction of CO_2 to be a possible solution for global warming. Figure 2.13 shows a representative of a photo-electro-catalytic device for CO_2 reduction to fuels using solar energy.

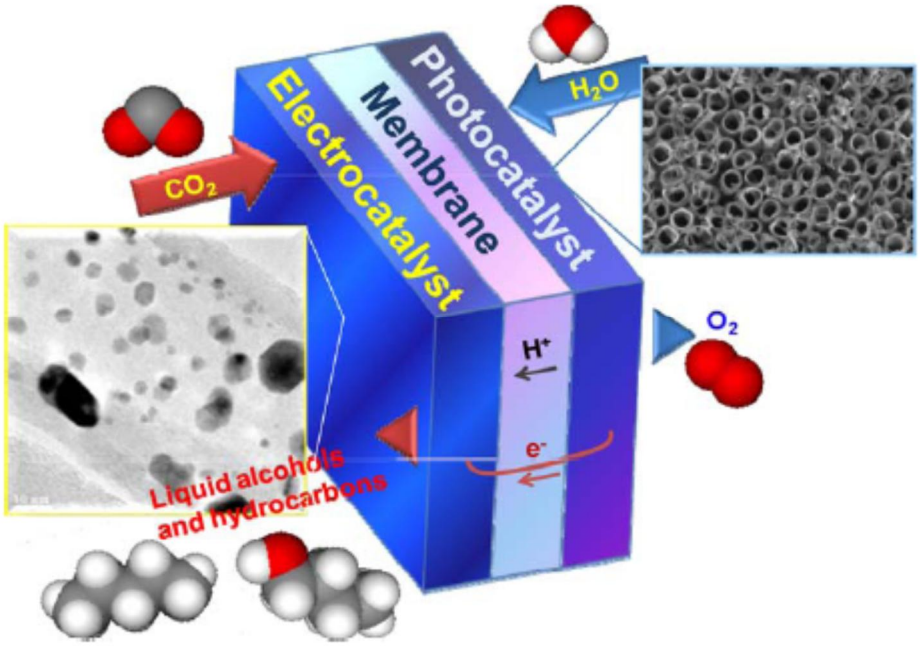


Figure 2.13: Simplified scheme of a photo-electro-catalytic device for CO_2 reduction to fuels using solar energy (Centi and Perathoner, 2009

Centi and Perathoner, 2009, investigated the use of Nitrogen-doped TiO_2 nanotubes array for solar conversion of CO_2 and water vapour to produce methane and other hydrocarbons. The Nitrogen-doped nanotube sample hardened at a

temperature of 600°C, film thickness about 50µm, and Cu as the co-catalyst (52% of the surface area decorated with Cu particles), yielded the following products shown in Figure 2.14 below.

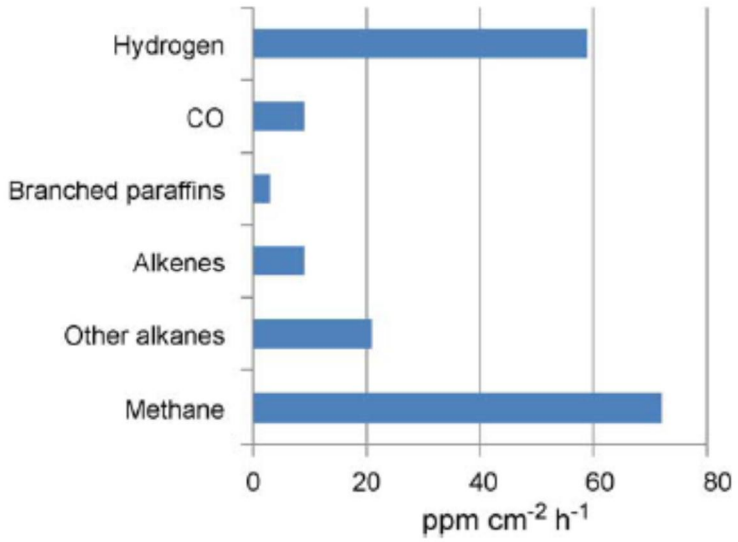


Figure 2.14: Product yield from Nitrogen-doped nanotubes (Centi and Perathoner, 2009)

Electro-catalytic reduction of CO_2 using H_2 proved theoretically to be a better option than CO_2 with water. The reaction is as follows (Gür et al., 1990):

$$2\,H_2 + \ CO_2 \ \rightarrow \ CH_4 + \ O_2 \qquad 2.4$$

Equation 2.4 gives only gaseous products, oxygen and methane, which are collected separately. The dissociation of CO_2 accompanied by the transportation of O_2 across a solid electrolyte in the presence of an applied field occurs first. This is followed by a rapid hydrogenation of the surface carbon, which is formed as a result of the reaction of CO_2 with H_2. This reaction does not produce any graphite as a by-product because the carbon is highly reactive toward H_2, and the resident time on the metal surface is too short for any nucleation to take place (Gür et al., 1990).

Brooks et al., 2006, investigated the Sabatier reaction which is represented by Equation 2.5 below, where water is produced, instead of oxygen.

$$4\,H_2 + \ CO_2 \ \leftrightarrow \ CH_4 + \ 2\,H_2O \qquad 2.5$$

This reaction is exothermic (ΔH = -167 kJ/mol), and advances at relatively low temperatures of about 400°C in the presence of a catalyst such as ruthenium. The Sabatier process is usually carried out in a packed bed reactor or porous-foam reactor configuration. It can be incorporated into a number of industrial processes using a source of low cost hydrogen.

2.7 Synfuels Production

Synthetic liquid hydrocarbons (Synfuels) have been produced for more than three quarters of a century from non-liquid feedstock. It is currently produced from fossil fuels through coal gasification to form synthesised gas (syngas – H_2 and CO) which then undergoes dry reforming (also known as the Fischer-Tropsch Process) to produce synfuels (Olah et al., 2009). Depending on the catalyst used, carbon deposition can occur during dry reforming and may lead to the deactivation of the catalyst surface. Ni catalysts in particular are subject to such carbon deposition at temperatures below 900°C (Kennema, 2014).

The general reactions associated with synfuels are:

- Gasification of carbon in fossil fuels
- Water gas shift reactions
- Reverse water gas shift reactions
- Fischer-Tropsch Reaction

Synfuels are generically $(CH_2)_n$, where the value of n distinguishes between the various synfuels. The elementary olefin molecule is represented by CH_2 and the various synthetic polymers such as ethylene (C_2H_4) and propylene (C_3H_6) are formed from this ((Olah et al., 2009 and Uhrig et al., 2007). By using fossil fuels such as coal, one atom of carbon is produced as CO_2 for every atom produced as CH_2 in the synfuel (Schultz et al., n.d). Therefore the atoms of CO_2 produced, always equal that of the desired product, CH_2. Renewable production of synfuels

can help reduce CO_2 emissions and address the growing shortage of petroleum. The general concern associated with synfuels is that the capital and operating costs must be competitive with alternative fuels. As a result, Sasol Advanced Synthol (SAS) in South Africa have reduced their consumption of catalysts by 60% and plant maintenance by 85% as compared to their 1980 plants (Uhrig et al., 2007). The synfuel processes analysed below looks at reducing the amount of CO_2 produced, or to eliminate it altogether; thereby producing a synthetic fuel which is not made from fossil fuels and has minimal carbon emissions.

2.8 DME production

The production of Dimethyl Ether (DME) will also be considered and investigated to see if it can be used as a fuel source. It can be produced from hydrocarbon sources including natural gas. It is a benign, nontoxic organic compound and when combusted, it produces minimal NO_x and CO, though hydrocarbons (HC) and soot formation is significant. DME in itself is not a greenhouse gas and can act as a clean fuel when burnt in engines optimised for DME and are excellent transportation fuels for internal combustion engines and fuel cells (Olah et al., 2009). If DME is produced in large quantities, and sold at lower costs to LPG, this fuel can contribute positively to solving energy supply problems and environmental problems. Having a cetane number between 55 – 60, DME is substantially higher than conventional fuels whose cetane numbers range between 40 – 55 (Olah et al., 2009). This makes it a more superior fuel to methanol. Due to the fact that it is a liquid at 6 bar (Olah et al., 2009), existing LPG infrastructure can be used. The boiling point of DME is – 24.9 $^{\circ}$C, making it a gas under ambient conditions. However, it can be stored in pressurized tanks as a liquid, similarly to liquefied petroleum gas. DME is also a convenient starting material for synthetic hydrocarbons and their diverse products.

A demonstration plant producing 100t/day exists in Asia and is used for testing by JFE. The schematic diagram of it can be seen below in Figure 2.15.

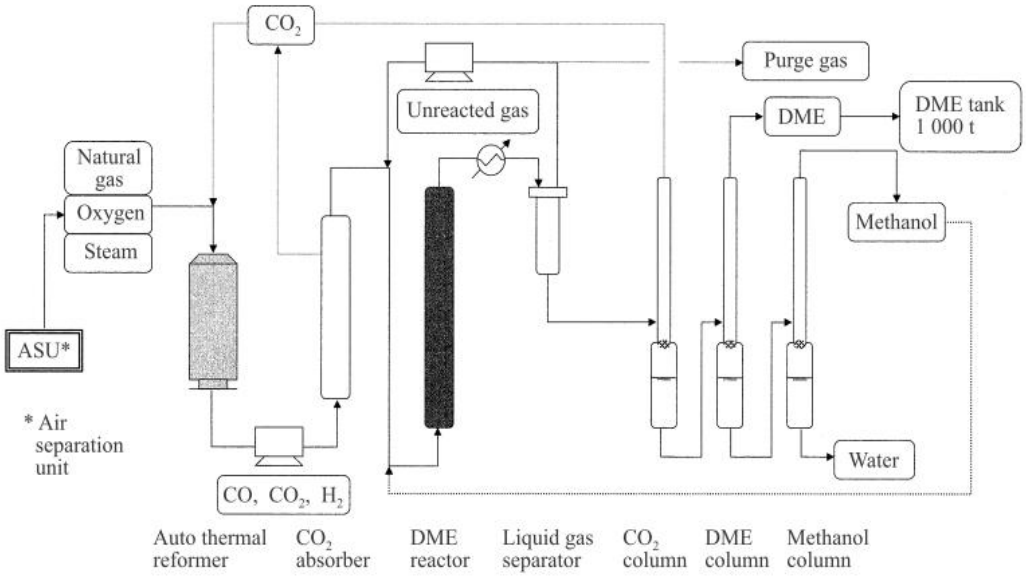


Figure 2.15: Process flow diagram of 100 t/day DME synthesis plant (Yotaro et al., 2006)

As explained in the JFE Process (Yotaro et al., 2006), the equations for DME production using authothermal dry reforming are as follows:

$$2\,CO + 4H_2 \rightarrow 2\,CH_3OH \quad (2.6)$$

$$2\,CH_3OH \rightarrow CH_3OCH_3 + H_2O \quad (2.7)$$

$$CO + H_2O \rightarrow CO_2 + H_2 \quad (2.8)$$

$$3\,CO + 3\,H_2 \rightarrow CH_3OCH_3 + CO_2 \quad (2.9)$$

Equation 2.9 is the overall reaction producing CO_2 in proportion to the desired product DME. When natural gas such as CO_2 and CH_4 is used as a feedstock, the CO_2 produced from the overall reaction, Equation 2.9, can be recycled back into the process with the CO_2 feedstock. The reaction is as follows:

$$2\,CH_4 + O_2 + CO_2 \rightarrow 3\,CO + 3\,H_2 + H_2O \quad (2.10)$$

$$CH_4 + CO_2 \rightarrow 2\,CO + 2\,H_2 \quad (2.11)$$

In order for Equation 2.10 to take place, the natural gas has to undergo steam reforming or authothermal dry reforming as in the JFE Process to produce syngas.

Dry reforming as can be seen by Equation 2.11 can also be used but has not been done to great extents as yet (Olah et al., 2009). Equation 2.6 to 2.9 will then follow Equation 2.10 or 2.11 for DME production.

Due to landfills generally having a composition of carbon dioxide and methane of approximately 50%/ 50% respectively, methane dry reforming as explained by Olah et al., 2009, would be a good alternative as both the methane and the CO_2 will be used as feedstock. This process does not require steam and no hydrogen is lost in the by-product water. The overall reaction is as follows:

$$3\,CH_4 + 3\,CO_2 \rightarrow 6\,CO + 6H_2 \qquad 2.12$$

$$6\,CO + 6\,H_2 \rightarrow 2\,CH_3OCH_3 + 2\,CO_2 \qquad 2.13$$

$$3\,CH_4 + CO_2 \rightarrow 2\,CH_3OCH_3 \qquad 2.14$$

Equation 2.14 has an enthalpy value of ΔH = 59 kcal/mol or ΔH°_{298K} = 247.3 KJ/mol as described by Jiang et al., 2010, which is significantly more endothermic than steam reforming which has an enthalpy of ΔH = 49 kcal/mol. Dry reforming of methane is typically carried out at temperatures between 800 – 1000 $^{\circ}$C. Nickel based catalyst is the most suitable for these types of reactions (Yasyerli et al., 2011); hence for the dry reforming process explained above catalysts such as Ni/MgO, or Ni/$MgAl_2O_4$ are used (Olah et al., 2009). Excess CO_2 can be recycled back into the process.

3 Methodology and Clean Development Mechanism Projects

3.1 Methodology

Figure 3.1 illustrates the basic process flow diagram of the methodology for establishing the best procedure for converting landfill gas into useful products. The diagram is explained in details below.

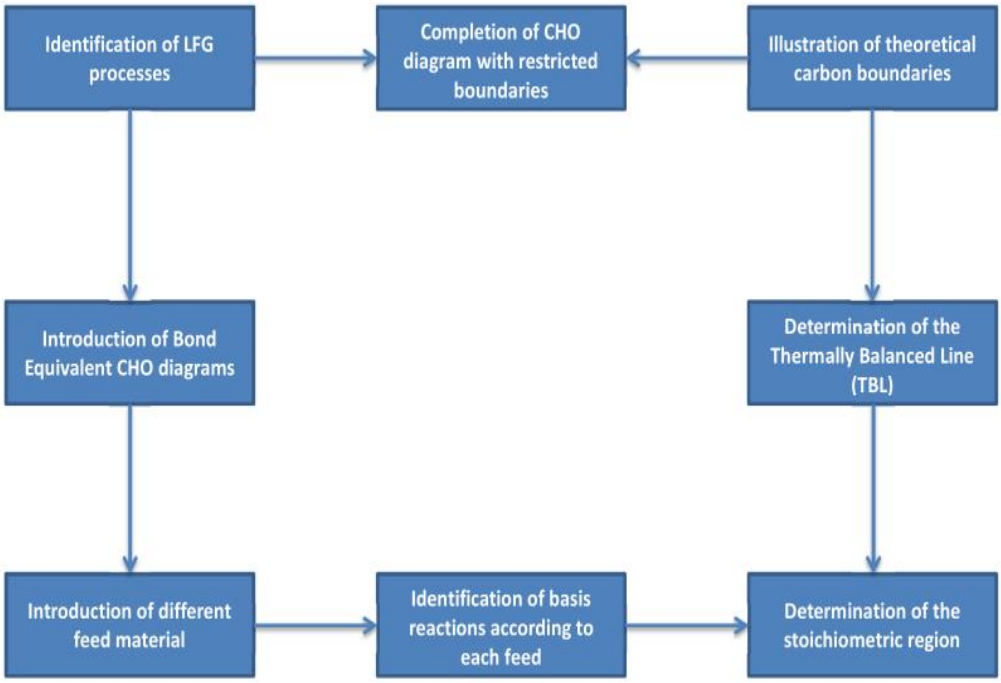


Figure 3.1: Flow chart of the Methodology

A desktop review of various processes consisting of CO_2 and CH_4 as feedstock were examined to identify the best practical method of converting landfill gas into a useful product such as electricity, pipeline gas and even fuel. Four main processes were identified as examples:

i. Electricity generation;
ii. Electro-catalytic reduction of CO_2;
iii. Synfuel production; and
iv. DME production.

To establish a feasible region of operation for landfill gas, Bond-Equivalent Carbon-Hydrogen-Oxygen (CHO) diagrams were introduced to determine a stoichiometric region in which landfill gas can be converted into useful products. LFG was then represented as a point within the diagram using bond-equivalent percentages. All possible reactions that could occur within the CHO diagram were represented. Reactions were then eliminated based on the rules that govern the basis reactions which were:

I. The reactions must be able to attain other reactions by positive linear combinations;
II. The reactions should not form the original feed.

Three feed types were chosen and by satisfying these two rules, the basis reactions were identified for each feed type and represented graphically in Figures 4.3, 4.4 and 4.5 below. The stoichiometric region for each feed type was thus established and the TBL which makes the processes autothermal were found. The TBL restricts the stoichiometric region. Carbon boundaries were also introduced which further restricted the stoichiometric region to operate within the carbon boundary.

The three processes identified were then illustrated on the CHO diagram and were analysed with each feed type to establish the region in which to operate. From this, conclusions could be made as to which process would be best suited for conversion of LFG into useful products with the least amount of CO_2 emissions and which feed type would be most applicable for the conversion.

3.2 Clean Development Mechanism Projects

Landfill gas projects are known as Clean Development Mechanism (CDM) projects as one can earn saleable certified emission reduction (CER) credits from these projects. Each certificate is equivalent to one tonne of CO_2, which can be counted toward Kyoto Protocol targets (United Nations Framework Convention on Climate Change, 2012). Before this is done however, and before carbon credits can be sold, the project must be validated against the requirements of the CDM

and then approved by the host country (Environ Holdings, 2012). Once this is done, a letter of approval is sent to the CDM Executive Board. Generation of CERs can only be achieved once the CDM Executive Board accepts the project.

The CDM has been in existence since 2006 and has registered more than 1 650 projects and is expected to produce CER's amounting to more than 2.9 billion tonnes of CO_2 equivalent in the first commitment period of the Kyoto Protocol, 2008 – 2012 (United Nations Framework Convention on Climate Change, 2012) .

4 Theory

In this chapter, a geometric method to analyse industrial system is developed and will enable industries using LFG as a feedstock to operate processes in an optimum region where reactions can occur adiabatically or exothermically, with the aim to produce optimal results such as fewer emissions and producing products with little required energy. The concept of CHO diagrams is introduced, and the desired stoichiometric region for LFG is established with different feed material. Operating condition and parameters which should be used while operating in the stoichiometric region such as temperatures, carbon boundaries and calorific values are demonstrated to achieve optimal process results.

4.1 History of Bond Equivalent diagrams

One of the first CHO diagrams was represented as the Van Krevelen plot. It used atomic ratios of O/C and H/C to determine a carbon boundary isotherm. It demonstrates the usefulness of trajectories and identifies the dominating chemical changes in coal conversion processes (Kauchali, 2012). The Van Krevelen diagram has its disadvantages in that it can only be used for materials containing C:H. Hydrogen, oxygen and water cannot be plotted using the chart.

The Van Krevelen diagram led to the formation of the CHO diagrams which were introduced by Cairns and Tevebaugh, 1964, in order to represent the carbon deposition boundaries on fuel cells for temperatures between 25 – 1227 °C, at atmospheric pressure. These ternary diagrams, better known as CHO diagrams were seen as a useful tool in representing organic chemical processes (Tay et al., 2011). The equilibrium composition for a given CH_4 partial pressure was then determined by Broers and Treijtel, 1965 whilst Gruber and Princeton, no date, also represents compositions of CO, CO_2, H_2, H_2O and CH_4 on a single co-ordinate system in the ternary diagram.

The Bond Equivalent diagram was introduced by Battaerd and Evans (1979) and demonstrates the bonding capability of each element in the system (Kauchali, 2012), and shows important points on the CHO diagram. Through the application

of the CHO diagram, it can be shown that a constrained region can be allocated to a coal gasification process, using stoichiometry. By assessing energy considerations, the coal gasification process can be constrained further to a line or plane (Wei, 1979). This theoretical development thus gives insight into complex reaction schemes before complex reactor design and operations can be considered (Kauchali, 2012). This approach will be used to determine the conversion of landfill gas into useful energy by providing the constrained region where efficient conversion will take place.

4.2 Bond Equivalent Diagrams

Bond Equivalent (BE) diagrams provides a representation of how components, particularly carbon, (C), hydrogen (H_2), oxygen (O_2), methane (CH_4), carbon dioxide (CO_2), carbon monoxide (CO) and water (H_2O) react with each other. Figure 4.1 represents the CHO Diagram and the basic components found on it with two arbitrary points A and B which represent mixtures. Simple reactions can be represented on the diagram such as de-methanation (lines radiating from CH_4), dehydration (lines radiating from H_2O), decarboxylation (lines radiating from CO_2), de-oxidation (lines radiating from O_2) and dehydrogenation (Lines radiating from H_2).

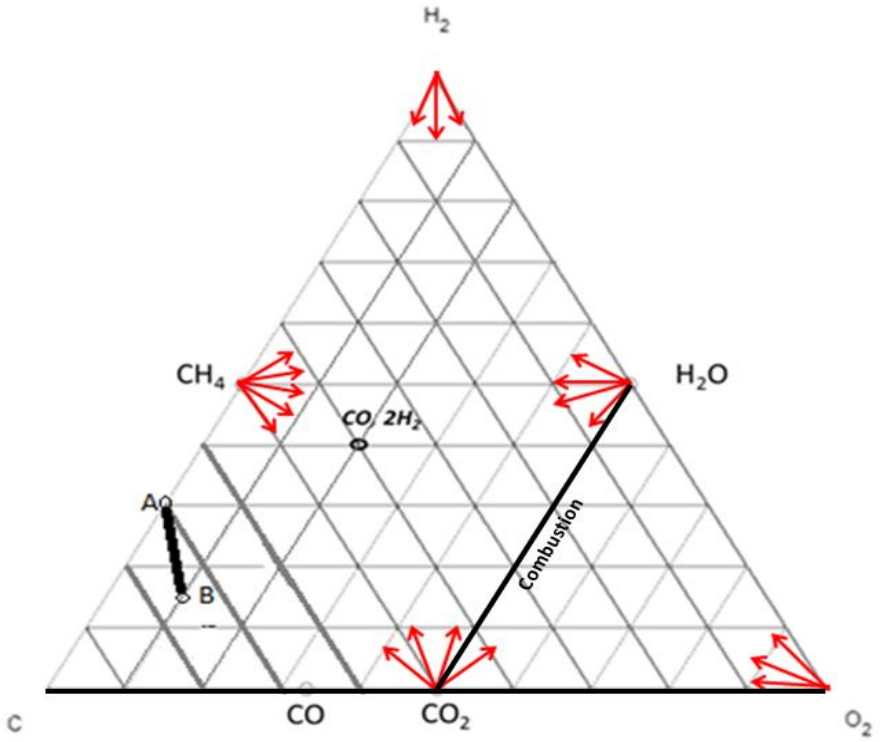


Figure 4.1: CHO Diagram

BE percentages are represented by molar percentages by multiplying the mole fraction of the main constituents C, O_2 and H_2 by their valent electrons 4, 2 and 1 respectively as shown by Battaerd and Evans, 1978. These are shown below:

$$C = \frac{4x_C}{4x_C + x_{H_2} + 2x_{O_2}} \quad 4.1$$

$$O = \frac{2x_{O_2}}{4x_C + x_{H_2} + +2x_{O_2}} \quad 4.2$$

$$H = \frac{x_{H_2}}{4x_C + x_{H_2} + +2x_{O_2}} \quad 4.3$$

In order to plot a chemical compound and determine the reaction, the BE percentages of each component in the compound must be found. For example,

CH_4 is represented by C=4/(4+4) and H=4/(4+4), which then places CH_4 at a point midway between H-C. Similarly, H_2O and CO_2 are found midway between H-O and C-O respectively. Mixtures can also be represented using the same technique, such as point B which contains 69% C, 5% H_2 and 26% O_2 by mass. Refer to Appendix A for a detailed explanation and representation.

It is important to note that for a specific output a direct route does not necessarily have to be followed (e.g. B to A in Figure 4.1); however alternative routes can become thermodynamically difficult and less efficient. The combustion line occurs as a result of C and O_2 reacting to form CO_2 and H_2O. This line represents any combustion reaction occurring within the CHO diagram as any component must react with O_2 to burn and will produce combustion byproducts CO_2 and H_2O. Any path leading toward the combustion line will experience efficiency penalties as energy is required for combustion to occur. BE diagrams show what the aims and drivers of a certain process need to be, however it does not show how to reach a specific aim. The pathway chosen to achieve a certain reaction must be determined by production costs, mining costs and system efficiencies to name a few.

4.3 Representing species on the CHO Diagram

The CHO diagram allows species to be indicated as points on the diagram as shown in Figure 4.2, point B, as well as for reactions to be represented as the intersection of two lines, one line representing the reactants whilst the other represents the products. If an equilateral triangle is drawn for the CHO diagram like the one shown in Figure 4.2 below, a star can be represented by joining the points on the CHO diagram to represent H_2, CH_4, CO, CO_2 and H_2O. C and O_2 are not represented on the star. This star can be used to determine gasification and reforming reactions and is known as the star of gasification (Kauchali, 2012). Although known as the star of gasification, reforming reactions can also be shown on the diagram as the star also symbolizes natural gases. Syngas (CO:H_2 = 1:1 ratio) is represented as point C on Figure 4.2, as it is the intersection of the reactants (C and H_2O) and products (CO and H_2).

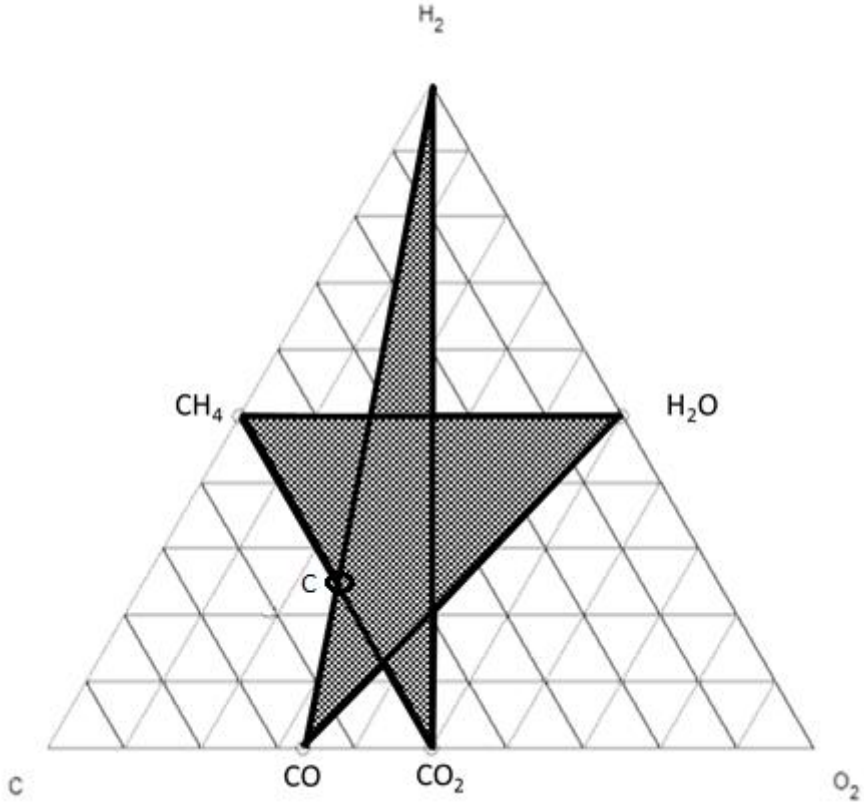


Figure 4.2: The Star of Gasification

4.4 Stoichiometric region of operation for LFG

Many reactions occur in reforming processes and this can become complex to analyze. The change and product distribution for the overall process is constrained by the considerations of stoichiometry. The feasible region of operation for LFG is determined by the analysis of LFG containing 60% CH_4 and 40% CO_2. Hydrogen sulfide, nitrogen and trace components are considered inert within the CHO diagram. By considering different reforming reactions for landfill gas, a theoretical region can be developed for a method of converting LFG into useful energy or products. By taking into account thermal balances between exothermic and endothermic reactions, further limits the results to the Thermally Balanced Line (TBL).

4.4.1 Reforming Reactions using the CHO Diagram

The following are important reforming reactions that occur for landfill gas and will aid in determining the feasible region in which LFG can be converted into useful energy. The CHO diagram restrict the amount of products that can be produced to the components found on the CHO diagram, namely, CO, CO_2, H_2O, CH_4 and H_2 (Desrosiers, 1979 and Prins, 2003). In order to show that the product distributions fall on a predicted narrow band, full scale and pilot data based on mass and energy balances only should be compared. These distributions however are obtained before any considerations of thermodynamic equilibrium, reaction kinetics and extent of reaction or reaction design and operation (Kauchali, 2012).

The reactions shown below are reactions that intersect with each other. In the case where reactants do not intersect with products, reactions were omitted. It should be noted that LFG is represented by $C_{2.5}O_2H_6$ (a mixture of 60% CH_4 and 40% CO_2).

For the landfill gas system, the following reactions at 650K will thus be considered:

Combustion

$$r_1: C_{2.5}O_2H_6 + 3\,O_2 \rightarrow 2.5\,CO_2 + 3\,H_2O \qquad -1\,200\ kJ/mol$$

$$r_2: C_{2.5}O_2H_6 + 1.5\,O_2 \rightarrow 3\,H_2 + 2.5\,CO_2 \qquad -464.4\ kJ/mol$$

$$r_3: C_{2.5}O_2H_6 + 0.25\,O_2 \rightarrow 3\,H_2 + 2.5\,CO \qquad 244.9\ kJ/mol$$

$$r_4: C_{2.5}O_2H_6 + 1.75\,O_2 \rightarrow 2.5\,CO + 3\,H_2O \qquad -491.4\ kJ/mol$$

Reforming

These reactions are based on the reactions between LFG and steam, CO_2, or H_2.

$$r_5: C_{2.5}O_2H_6 + 3\,H_2O \rightarrow 6\,H_2 + 2.5\,CO_2 \qquad 271.8\ kJ/mol$$

$$r_6: C_{2.5}O_2H_6 + 0.5\,H_2O \rightarrow 3.5\,H_2 + 2.5\,CO \qquad 367.6\ kJ/mol$$

$$r_7: C_{2.5}O_2H_6 + 2\,H_2O \rightarrow 2.5\,CH_4 + 2\,O_2 \qquad 800.4\ kJ/mol$$

$$r_8: C_{2.5}O_2H_6 + 0.5\,CO_2 \rightarrow 3\,H_2 + 3\,CO \qquad 386.7\ kJ/mol$$

$$r_9: C_{2.5}O_2H_6 + 3.5\,CO_2 \rightarrow 3\,H_2O + 6\,CO \qquad 501.6\ kJ/mol$$

$$r_{10}: C_{2.5}O_2H_6 + 2\,H_2 \rightarrow 2.5\,CH_4 + O_2 \qquad 309.6\ kJ/mol$$

$$r_{11}: C_{2.5}O_2H_6 + 4\,H_2 \rightarrow 2.5\,CH_4 + 2\,H_2O \qquad -181.2\ kJ/mol$$

Gas Combustion

$$r_{12}: H_2 + 0.5\,O_2 \rightarrow H_2O \qquad -245.4\ kJ/mol$$

$$r_{13}: CO + 0.5\,O_2 \rightarrow CO_2 \qquad -283.7\ kJ/mol$$

Gas Reactions

$$r_{14}: H_2O + CO \leftrightarrow H_2 + CO_2 \qquad -38.3\ kJ/mol$$

$$r_{15}: CO + 3H_2 \leftrightarrow CH_4 + H_2O \qquad -219.5\ kJ/mol$$

For the LFG to be used in reforming processes, all of the equations listed above may not be feasible. Furthermore, some reactions are dependent on each other. The analysis of the reforming system requires that the reactions that should be taken into consideration are those reactions that form the basis reactions and must satisfy two rules:

1. They must be able to attain other reactions by positive linear combination, and
2. These reactions should not form combustion through the original feed and carbon.

Three feeds to the process are considered, with landfill gas being the key component in each feed. It is important to note that in this dissertation, landfill gas is considered and represented as $C_{2.5}O_2H_6$ and not as individual components of CH_4 and CO_2 unless otherwise stated.

The three feeds are given below as:

Feed 1:	**Feed 2:**	**Feed 3:**
$C_{2.5}O_2H_6$	$C_{2.5}O_2H_6$	$C_{2.5}O_2H_6$
O_2	O_2	O_2
CO_2	H_2O	CO_2
		H_2O

For the rules to be obeyed, from Feed 1, oxygen and carbon dioxide must not be produced; from Feed 2, oxygen and water must not be produced and from Feed 3, oxygen, carbon dioxide and water must not be produced. Furthermore, reactions undergoing methane and carbon generation will not be considered. This reduces the above set of equations to the following basis reactions seen below, depending on the feed to the system.

The main reactions for a system containing Feed 1 are obtained by linear combination of the following basis reactions:

$$r_3: C_{2.5}O_2H_6 + 0.25\,O_2 \rightarrow 3\,H_2 + 2.5\,CO \qquad 244.9\ kJ/mol$$

$$r_4: C_{2.5}O_2H_6 + 1.75\,O_2 \rightarrow 2.5\,CO + 3\,H_2O \qquad -491.4\ kJ/mol$$

$$r_8: C_{2.5}O_2H_6 + 0.5\,CO_2 \rightarrow 3\,H_2 + 3\,CO \qquad 386.7\ kJ/mol$$

$$r_9: C_{2.5}O_2H_6 + 3.5\,CO_2 \rightarrow 3\,H_2O + 6\,CO \qquad 501.6\ kJ/mol$$

The linear combinations that make up the basis reactions for Feed 2 are:

$$r_2: C_{2.5}O_2H_6 + 1.5\,O_2 \rightarrow 3\,H_2 + 2.5\,CO_2 \qquad -464.4\ kJ/mol$$

$$r_3: C_{2.5}O_2H_6 + 0.25\,O_2 \rightarrow 3\,H_2 + 2.5\,CO \qquad 244.9\ kJ/mol$$

$$r_5: C_{2.5}O_2H_6 + 3\,H_2O \rightarrow 6\,H_2 + 2.5\,CO_2 \qquad 271.8\ kJ/mol$$

$$r_6: C_{2.5}O_2H_6 + 0.5\,H_2O \rightarrow 3.5\,H_2 + 2.5\,CO \qquad 367.6\ kJ/mol$$

Linear basis reactions associated with Feed 3 are:

$$r_3: C_{2.5}O_2H_6 + 0.25\,O_2 \rightarrow 3\,H_2 + 2.5\,CO \qquad 244.9\ kJ/mol$$

$$r_6: C_{2.5}O_2H_6 + 0.5\,H_2O \rightarrow 3.5\,H_2 + 2.5\,CO \qquad 367.6\ kJ/mol$$

$$r_8: C_{2.5}O_2H_6 + 0.5\,CO_2 \rightarrow 3\,H_2 + 3\,CO \qquad 386.7\ kJ/mol$$

All three combinations of feed will be analyzed to determine the stoichiometric region for each feed type.

4.5 Graphical Representation of Reactions

The reactions listed above can be represented as points on the CHO diagram. For example, In Figure 4.3 below, point r_3 represents Equation $r_{3:}$

$$r_3: C_{2.5}O_2H_6 + 0.25\,O_2 \rightarrow 3\,H_2 + 2.5\,CO \qquad 244.9\ kJ/mol$$

The above reactions for each feed type are plotted on the CHO diagrams shown in Figure 4.3, 4.4 and 4.5 below. The solid lines represent reforming reactions and the square dotted lines represent combustion reactions. It is noted that these reactions form the extreme boundary for all possible stoichiometry that convert LFG to useful gases (such as synthetic gas).

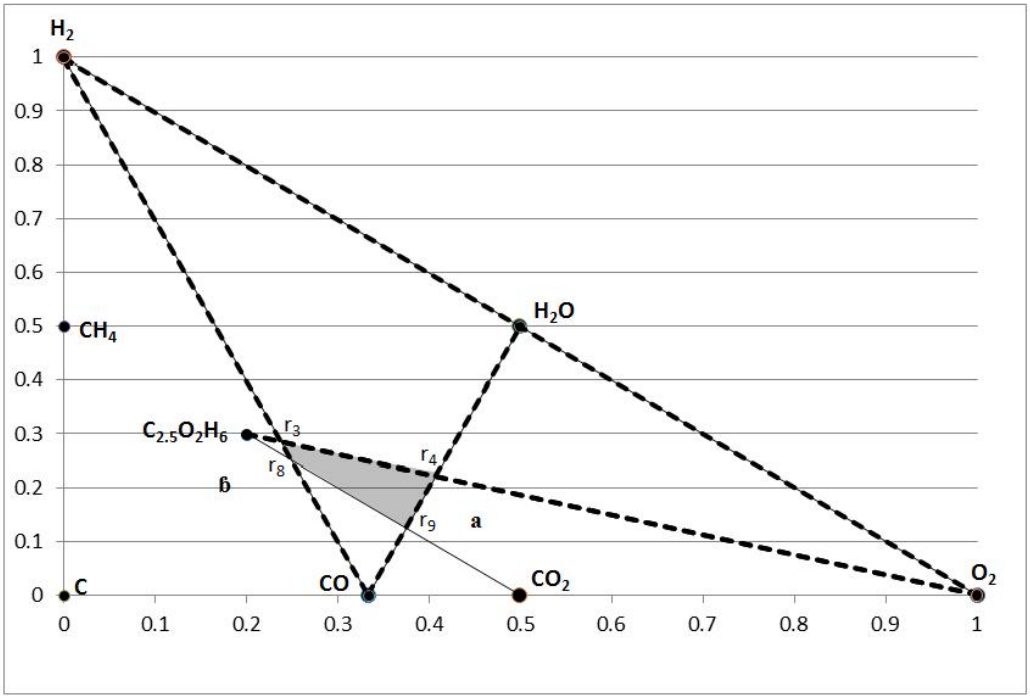


Figure 4.3: Graphical representation of LFG reactions using Feed 1

The shaded region represented in Figure 4.3, indicates all possible mass balances achievable for different Feed 1. Operating outside this region, for example operating in Area a or ɓ, either implies using too much O_2/ CO_2 (area a), or using too much LFG (area ɓ), which implies unreacted reactants at the exit of the reactor, therefore the sensible operation is bound by r_3, r_4, r_8 and r_9.

Figure 4.4 represents LFG reactions using Feed 2. The stoichiometric region is shown by the shaded region r_2, r_3, r_5 and r_6.

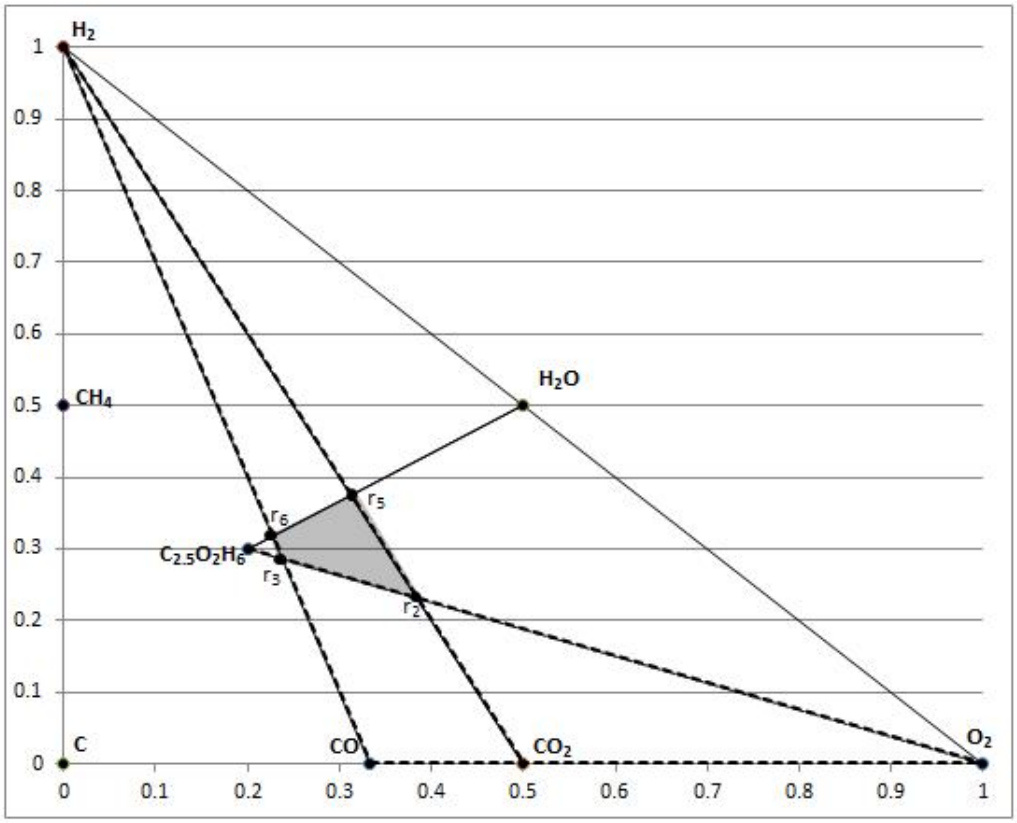


Figure 4.4: Graphical representation of LFG reactions using Feed 2

Any interior point inside the shaded region can be obtained by linear combinations of reactions r_2, r_3, r_5 and r_6 where the final products will be a combination of H_2, CO_2 and CO only. The edges of the shaded region in both Figures 4.3 and 4.4 comprise of reforming processes using O_2 on the lower side (r_9 for Figure 4.3 and r_2 for Figure 4.4), and steam on the top side (r_4 for Figure 4.3 and r_5 for Figure 4.4).

Figure 4.5 shows a graphical representation of LFG reactions using Feed 3.

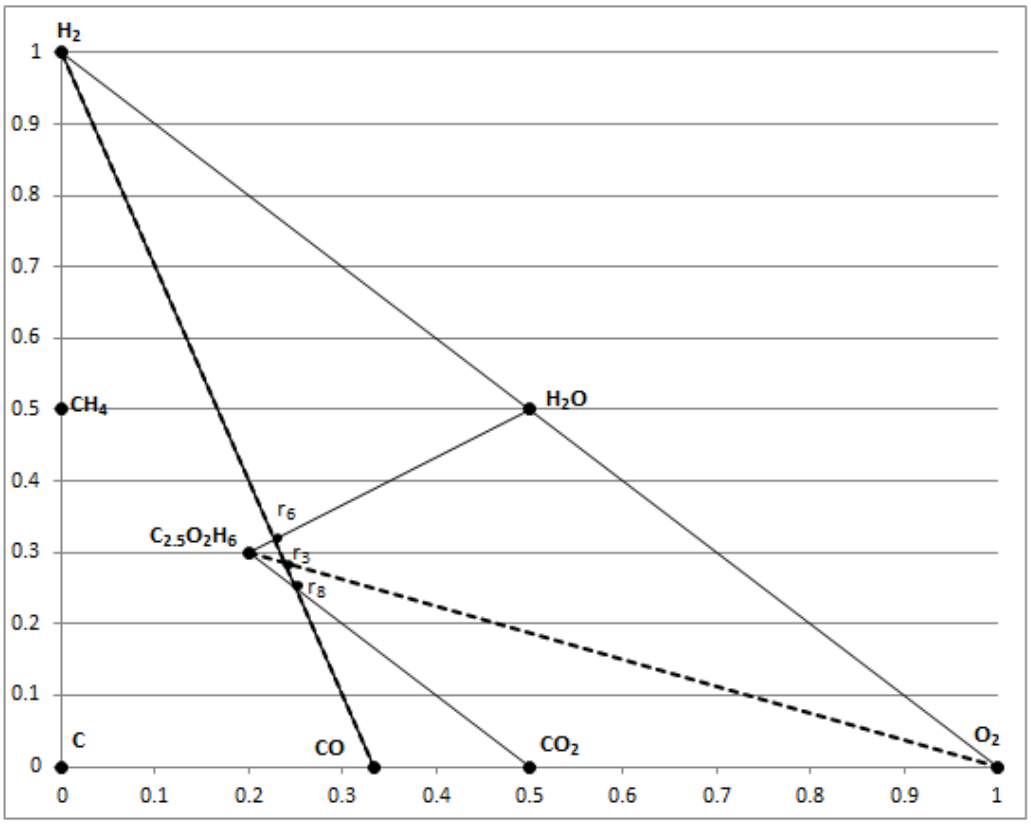


Figure 4.5: Graphical representation of LFG reactions using Feed 3

In the case of Feed 3 the stoichiometric region is represented by a straight line shown by point's r_3, r_6 and r_8, and therefore a stoichiometric region does not exist. Linear combinations of r_3, r_6 and r_8 can therefore be found along the straight line $r_6 - r_8$.

5 Energy Balance Considerations

5.1 Auto-thermal Operations

When heat is not added to or lost from the operation, the system is said to be adiabatic (Wei, 1979 and Kauchali, 2012). This is when exothermic reactions are balanced out by the endothermic reactions. Appendix B shows that there are seven reactions (r_3, r_4, r_5, r_6, r_8 and r_9) that make up the systems found within this dissertation and these reactions were categorized as endothermic or exothermic reaction. The enthalpies for the reactions were found for each equation according to detailed calculations shown in Appendix B. By using the enthalpies found, a ratio was calculated for each exothermic reaction with each endothermic reaction (refer to Appendix B). The exothermic reactions for Feed 1 are given by r_4 due to its negative enthalpies, whilst the endothermic reactions are given by r_3, r_8 and r_9 because of their positive enthalpies, therefore reaction r_4 is balanced by reactions r_3, r_8 and r_9. Once the ratios were obtained, the necessary equations were multiplied by the ratio to achieve and end result of zero enthalpy once the endothermic and exothermic reactions were added together (refer to Appendix B for detailed calculations and representations). From this, the TBL for Feed 1 is given by line AB in Figure 5.1, and this is representative of the product temperature equating to the inlet temperature (Wei, 1979). The equations representing the TBL can be characterized by two points on the CHO diagram, namely A and B and is given below.

$$A: \quad C_{2.5}O_2H_6 + 1.73\,CO_2 + 0.88\,O_2 \rightarrow 4.23\,CO + 3H_2O \qquad 0\ kJ/mol$$

$$B: \quad C_{2.5}O_2H_6 + 0.75\,O_2 \rightarrow 2.5\,CO + H_2O + 2H_2 \qquad 0\ kJ/mol$$

A third point making up the TBL does exist in this case and this is given as point C below. Point C however lies so close to line AB that the deviance from line AB is 0.0021 and is considered to be insignificant. For this reason, the TBL is given as a straight line AB and not as a region ABC.

$$C: C_{2.5}O_2H_6 + 0.28\,CO_2 + 0.77\,O_2 \rightarrow 2.78\,CO + 1.32\,H_2O + 1.68H_2 \quad 0\ kJ/mol$$

The TBL AB is represented below in Figure 5.1. Point C is represented only to indicate the third point making up the TBL, however will be eliminated through the remainder of this dissertation due to a deviance of 0.0021 which is considered to be negligible.

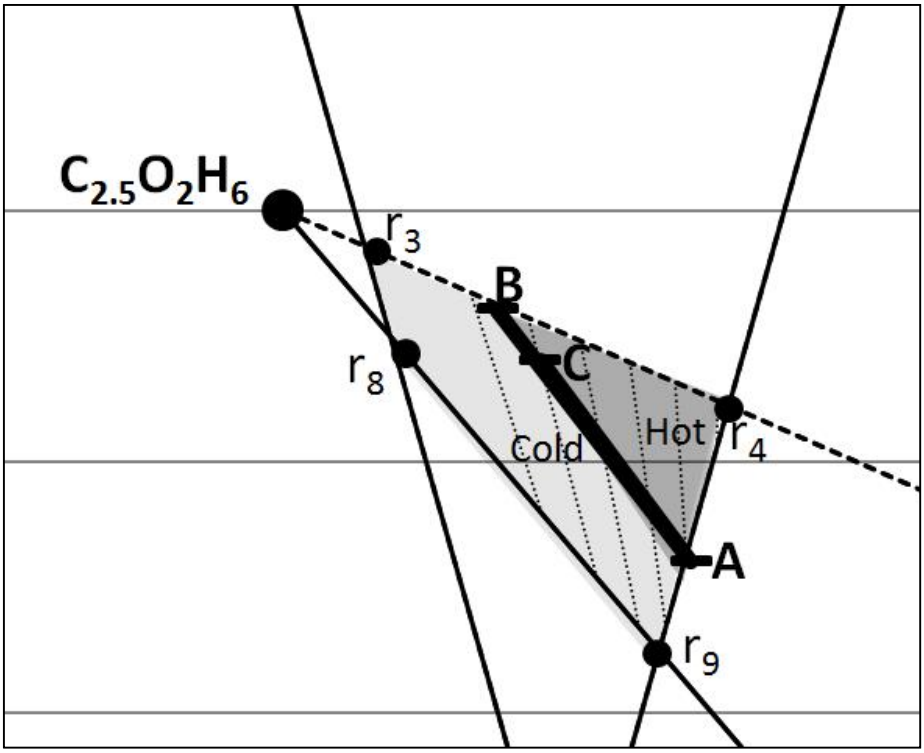


Figure 5.1: Indicating the TBL - Feed 1

According to Wei, 1979, reactions occur colder above the TBL and hotter below it and most coal gasification processes occur within the hotter region, below the TBL. This is not the case with the LFG process for Feed 1. Above the TBL, products will emerge hotter as opposed to Wei, 1979 due to the nature of r_4 which is exothermic whilst products will emerge colder below the TBL. Therefore in this case, it would be preferred to operate above the TBL in the hotter region. Operating below the TBL would require external heat sources to drive the endothermic reactions and this could lead to increased costs.

A similar case can be seen for Feed 2 in Figure 5.2. The TBL for Feeds 2 is tabulated below in Table 5.1. The TBL for Feed 2 also has 3 points with the middle point D significantly close to the end points. The deviance from line EF is

0.0020 and therefore it is assumed that point D lies on line EF. Hence the TBL for Feed 2 is given as line EF. A detailed summary on how the TBL was formed can be seen in Appendix B.

Table 5.1: Equations representing the Thermally Balanced Line for Feed 2

Feed 2	
$\boldsymbol{D: C_{2.5}O_2H_6 + 0.28\,H_2O + 0.66\,O_2 \rightarrow 1.40\,CO + 1.10\,CO_2 + 3.28\,H_2}$	$\boldsymbol{0\ kJ/mol}$
$\boldsymbol{E: C_{2.5}O_2H_6 + 1.90\,H_2O + 0.55\,O_2 \rightarrow 2.5\,CO_2 + 4.89\,H_2}$	$\boldsymbol{0\ kJ/mol}$
$\boldsymbol{F: C_{2.5}O_2H_6 + 0.68\,O_2 \rightarrow 1.64\,CO + 0.86\,CO_2 + 3\,H_2}$	$\boldsymbol{0\ kJ/mol}$

The TBL EF is represented below in Figure 5.2. Point D is represented only to indicate the third point making up the TBL for Feed 2, however will be eliminated through the remainder of this dissertation due to a deviance of 0.0020 which is considered to be negligible.

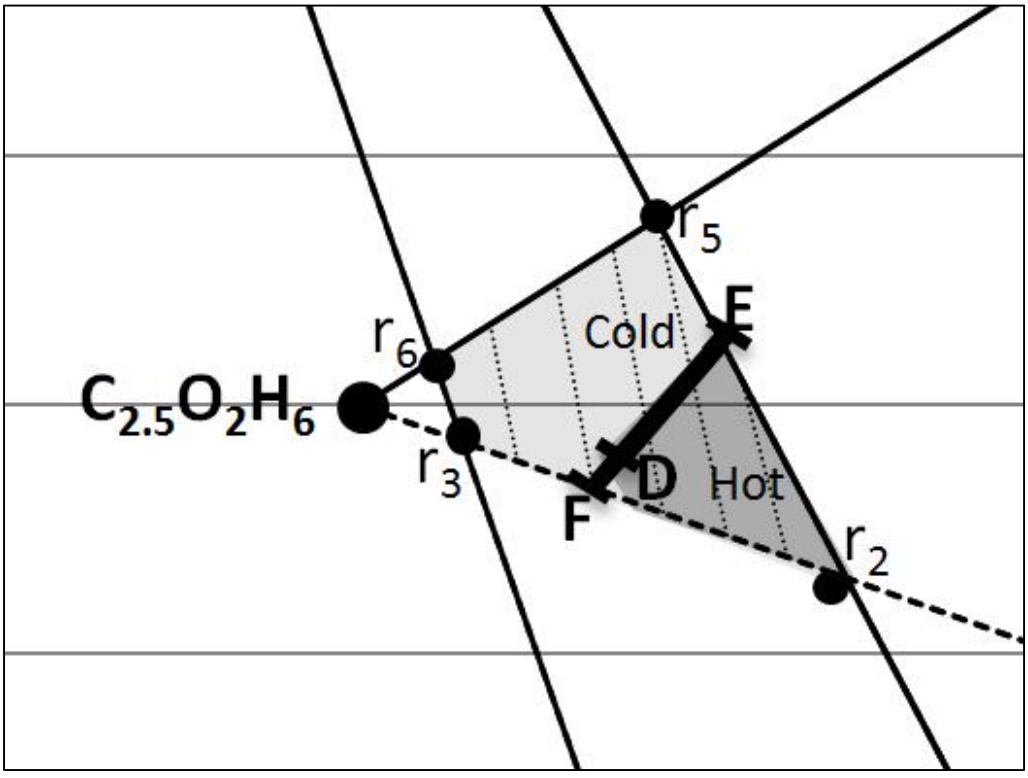


Figure 5.2: Indicating the TBL - Feed 2

In the case of Feed 2, the results are as Wei, 1979 describes. Products will emerge colder above the TBL and hotter below the TBL as r_2 is an exothermic reaction. A system with feed 3 will not be considered further in this dissertation as it does not have a TBL and would require additional energy and heat sources to drive the reactions as only endothermic reactions exist for this system.

Feed 3 does not have a thermally balanced line; instead it has 3 individual points which represent the endothermic reactions and can be seen in Figure 4.5 above by r_3, r_6 and r_8. No exothermic reactions or TBL exists for this process. The Equations for these points are represented in Table 5.2 below.

Table 5.2: Endothermic reactions for Feed 3

Feed 3		
r_3:	$C_{2.5}O_2H_6 + 0.25\,O_2 \rightarrow 3\,H_2 + 2.5\,CO$	$244.9\,kJ/mol$
r_7:	$C_{2.5}O_2H_6 + 0.5\,H_2O \rightarrow 3.5\,H_2 + 2.5\,CO$	$367.6\,kJ/mol$
r_{10}:	$C_{2.5}O_2H_6 + 0.5\,CO_2 \rightarrow 3\,H_2 + 3\,CO$	$386.7\,kJ/mol$

5.2 Idealised Stoichiometric Region (Calorific Values)

Calorific value contours were plotted for the idealised stoichiometric region using pure O_2 as a combustion medium and nitrogen and other components of air was seen as negligible. The contours of the calorific values found below are based on the method of Li et al., 2004. High heating values (HHVs) for each reaction is initially assumed and this is used to calculate the values of α and β for each reaction using an iterative calculation as can be seen in Appendix C. The Equations are shown below with a detailed description and detailed calculations shown in Appendix C:

$$HHV_1 = \alpha \times r_4 + (1 - \alpha) \times r_3 \quad 5.1$$

$$HHV_2 = \beta \times r_4 + (1 - \beta) \times r_8 \quad 5.2$$

The contours are plotted for 6–11MJ/m^3 for Feed 1 (Figure 5.3) and 7–12MJ/m^3 for Feed 2 (Figure 5.4).

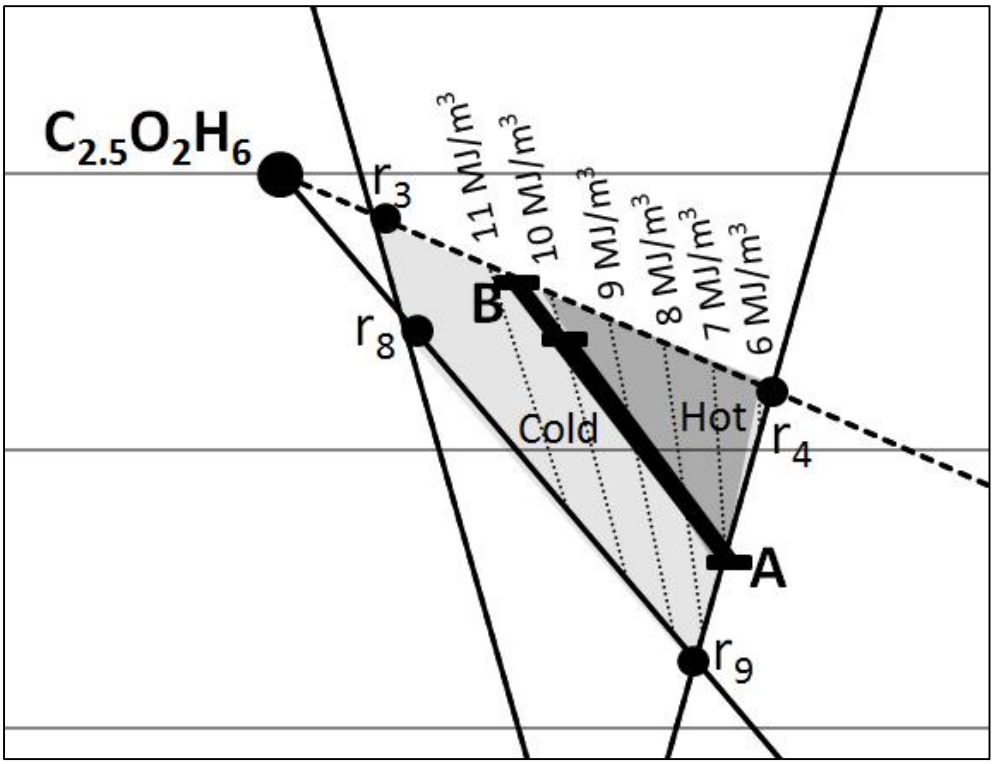


Figure 5.3: Close up Representation of HHV – Feed 1

Figure 5.3 shows processes within the stoichiometric region operating at 11MJ/m^3 will be endothermic reactions as they are found on the cold side. Although the calorific value may be high, the process would require a significant amount of energy to go to completion. Hence it is better to operate between 6 – 10MJ/m^3 on the hotter side of the TBL.

Figure 5.4 shows calorific values obtained using Feed 2.

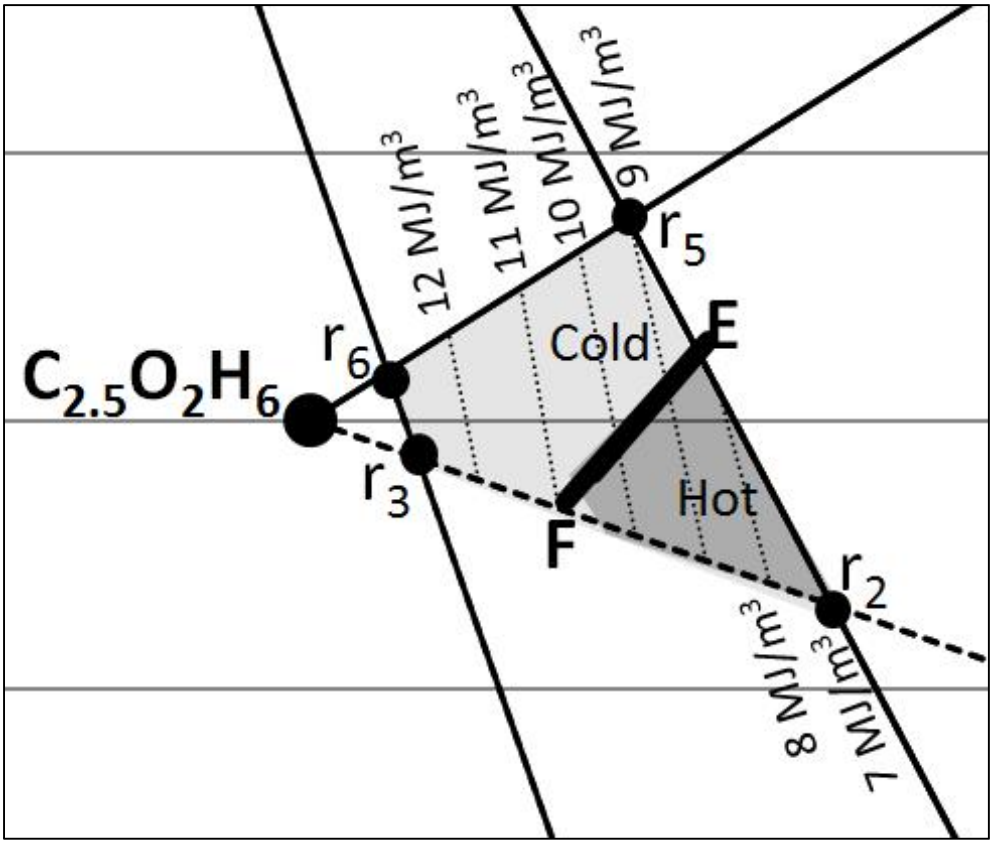


Figure 5.4: Close up Representation of HHV – Feed 2

It is evident from Figure 5.4 that operation within the stoichiometric region should be between 7 – 11MJ/m^3 and on the hotter side of the TBL, as anything above this would be an energy intensive process.

These values are useful when choosing a targeted calorific value and determining the reaction stream requirements. The higher the calorific value, the more energy can be drawn from the process, hence it makes sense to operate at higher calorific values rather than lower values. This however should still meet the requirements of the carbon boundary (discussed below) and the TBL. Sometimes, operating at high calorific values may not always be feasible as you may be operating within the carbon boundary, causing carbon deposition. It could also mean operating in endothermic conditions, which will require energy input into the system. It is important to note that it is however acceptable in some cases to operate at, or near the intersection of the TBL and carbon boundary as this is where the high heating

value is the highest. All these factors need to be considered carefully when choosing the ideal region to work within.

5.3 Carbon Boundary

Determining a carbon boundary within a process gives insight to whether or not unreacted carbon will be present in the product stream. These carbon boundaries can be represented on the CHO diagram as isotherms at constant pressure. The isotherms represented in Figures 5.5 and 5.6 were taken from Prins et al., 2003 for 733K and Li et al., 2001 for 900K, 1000K and 1100K.

The effect of temperature and pressure on carbon formation in gasification systems has been studied and it has been found according to Li et al., 2001 that it is not uncommon for carbon to partially gasify. It was also found that solid carbon does not reach equilibrium due to kinetic limitations. Operating within a carbon boundary for a reforming or gasification process indicates that a possibility exists for unreacted carbon to collect in the product stream. Hence, it is highly desirable to operate in a carbon free region as this will results in high carbon conversions. When operating at 733K, it can be seen that the process falls within the carbon boundary. Over time, carbon deposition is bound to occur resulting in a low efficiency process. If higher temperatures such as 1000K and 1100K are used, the process does not fall within the carbon boundary region and the carbon boundaries do not even touch the TBL. To find the most desirable conditions, it is best to choose a temperature to operate at, which is out of the carbon boundary but also touches the TBL. When operating at temperatures such as 900K for Feed 1 which is typical temperatures of operation for gasification or reforming, the stoichiometric region in which it is desirable to operate a reforming system is further reduced, however this touches the TBL. Hence no carbon deposition will occur and one will be able to operate on the TBL. For a 100% carbon conversion in an autothermal reforming process, the feasible region for operation for Feed 1 is defined by GHB (Figure 5.5).

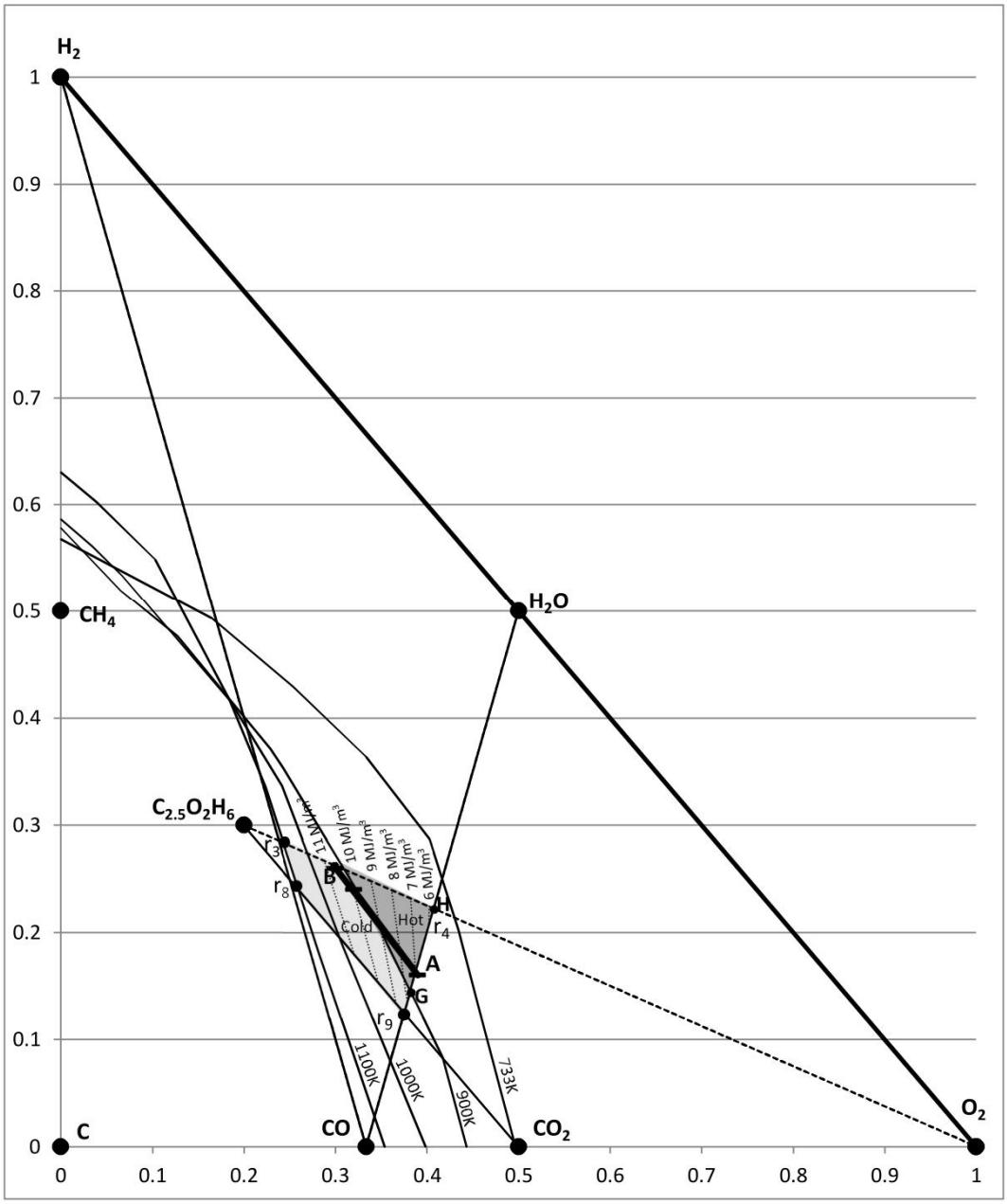


Figure 5.5: Thermally balanced line, carbon boundaries and calorific value contours for Feed 1

From Figure 5.5 (Feed 1), the idealized stoichiometric region for operation is GHB. The calorific values found in this region are 6 – 10MJ/m^3. The optimum conditions to run operations should be at 900K, operating at 9 - 10MJ/m^3 as this falls on the TBL and indicates that no carbon will be deposited.

A similarly case was assessed for Feed 2. In this case the carbon boundary at 900K touches the TBL at 11MJ/m^3. A carbon boundary at 800K (Li et al, 2001)

was also analyzed. This also touches the TBL, but at a lower calorific value, 10MJ/m^3 as opposed to 11MJ/m^3.

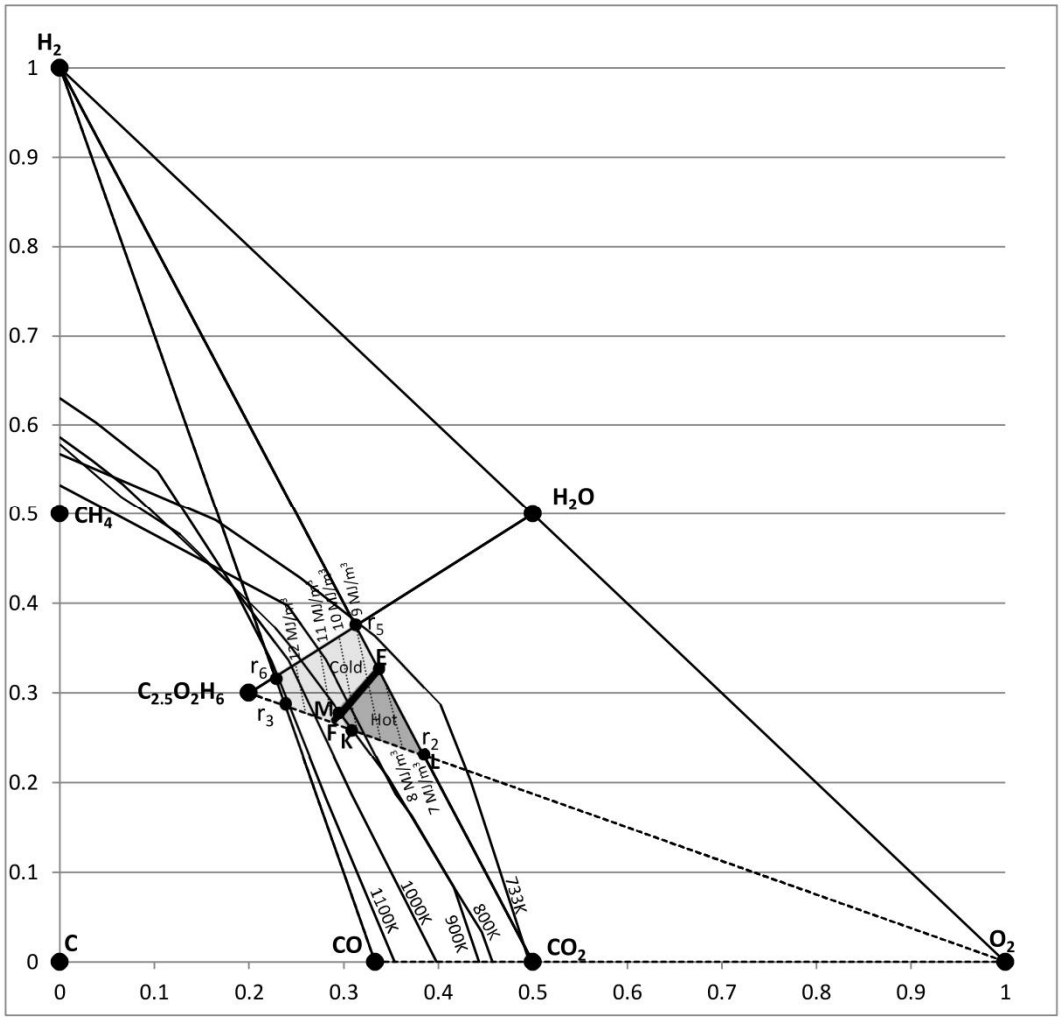


Figure 5.6: Thermally balanced line, carbon boundaries and calorific value contours for Feed 2

For Feed 2, the idealized stoichiometric region is shown as KLEM in Figure 5.6. The calorific values found in this region are 7 – 10MJ/m^3, however one can operate close to 11MJ/m^3.

In this instance, both 900K and 800K would be sufficient; however the 800K would further reduce the stoichiometric region in which a desirable reforming system can operate, hence limiting the calorific value to a maximum of 10MJ/m^3.

A maximum temperature that can be achieved must thus be determined in order to assess the location of the carbon boundary. Li et al., 2001 provide a method for determining the carbon boundary using the Gibb's minimization technique which is not explained in this report, but the position of the boundary has been taken from Li et al., 2001.

6 Results

The sections below investigate different processes of converting landfill gas into useful energy such as electricity, pipeline rich fuel in the form of methane, synfuels and dimethyl ether (DME) production which can be sold as a fuel.

6.1 Electricity generation using an Internal Combustion Engine

Electricity generation using internal combustion engines is a fairly simple process and is used widely around the world. Most landfills which produce electricity use some sort of combustion engine to generate electricity. The benefits of such combustion engines is that the incoming gases do not have to be as clean as in the case of pipeline rich gases and hence cleaning processes and the costs associated with these are eliminated. The downfall of this however, is that with fewer cleaning processes, the wear and tear on the engines increase and have to be maintained and replaced regularly. The efficiencies of the engines are also known to be quite low. Below are the results obtained from the combustion of LFG using a combustion engine.

6.1.1 Basic Flow diagrams

Figure 6.1 illustrates the basic process for combustion of LFG into electricity. Cleaning steps are not shown and it is assumed that the inlet stream to the combustion engine contains CH_4 and CO_2 only in the ratio 60:40 respectively. Furthermore, secondary cleaning of the gas is not required since the gas is burnt for electricity purposes. Contaminants found in the gas may be assumed as negligible.

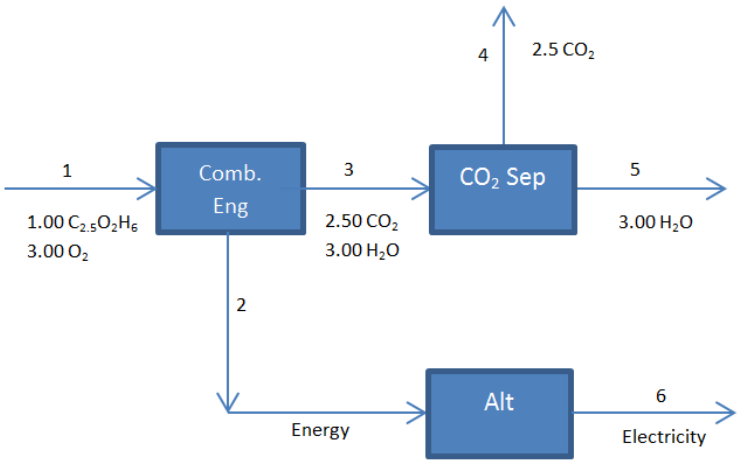


Figure 6.1: Electricity generation using an Internal Combustion Engine.

From Figure 6.1, LFG and oxygen enter the combustion engine where the LFG gets burnt completely to produce CO_2 and H_2O. The efficiency of the combustion engine is in the range of 25-35% (LMOP, n.d and Roberts et al, 2014). Assuming all the gas gets burnt, the remaining gases such a CO_2 and water vapour leave as waste through stream 3. The CO_2 is separated and released into the atmosphere whilst the water is disposed of. This water can also be used as process water in the plant instead of discharging to sewer. Heat energy is generated and passed through an alternator to produce electricity which can be supplied to the grid. Point CE on the CHO diagram in Figure 6.6 and 6.7 below represents the above mass balance.

Mass balances available for combustion are given below as:

$$r_1: C_{2.5}O_2H_6 + 3\,O_2 \rightarrow 2.5\,CO_2 + 3\,H_2O$$

$$r_2: C_{2.5}O_2H_6 + 1.5\,O_2 \rightarrow 3\,H_2 + 2.5\,CO_2$$

$$r_3: C_{2.5}O_2H_6 + 0.25\,O_2 \rightarrow 3\,H_2 + 2.5\,CO$$

$$r_4: C_{2.5}O_2H_6 + 1.75\,O_2 \rightarrow 2.5\,CO + 3\,H_2O$$

For electricity generation, focus will only be on r_1.

The system described in Figure 6.1, is the basic process for combustion. If this process is used within the CHO diagram, it will fall out of the stoichiometric

region and on the combustion line as can be seen in Figure 6.6 and 6.7 below. By using the CHO diagram, the system can be modified according to the feed in order for the process to occur on the TBL.

The system described for Feed 1 is as follows and represented in Figure 6.2 below:

$$C_{2.5}O_2H_6 + 0.77\,O_2 + 0.28\,CO_2 \rightarrow 1.68\,H_2 + 2.78\,CO + 1.32\,H_2O \quad 6.1$$

$$1.68\,H_2 + 2.78\,CO + 2.23\,O_2 \rightarrow 2.78\,CO_2 + 1.68\,H_2O \quad 6.2$$

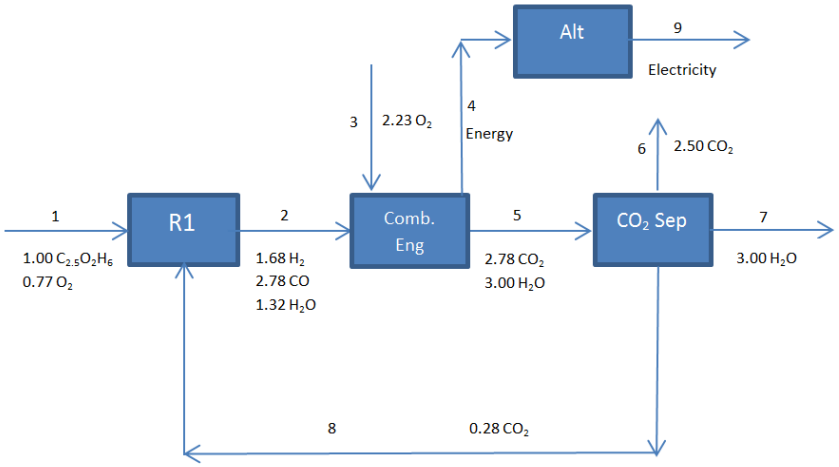


Figure 6.2: Electricity generation using an Internal Combustion Engine represented on the TBL – Feed 1.

The system is slightly different to the basic process for combustion in the sense that it has a CO_2 recycle stream and syngas is combusted rather than LFG. None the less, the CO_2 emitted to the atmosphere and the water generated is still the same as that for normal combustion. Equation 6.1 is the same as Equation C found on the TBL AB thus Equation 6.1 lies on the TBL AB.

If a different feed is introduced as in the case of Feed 2, the system will be as follows:

$$C_{2.5}O_2H_6 + 0.66\,O_2 \rightarrow 3\,H_2 + 1.64\,CO + 0.86\,CO_2 \quad (6.3)$$

$$3\,H_2 + 1.64\,CO + 2.32\,O_2 \rightarrow 1.64\,CO_2 + 3\,H_2O \quad (6.4)$$

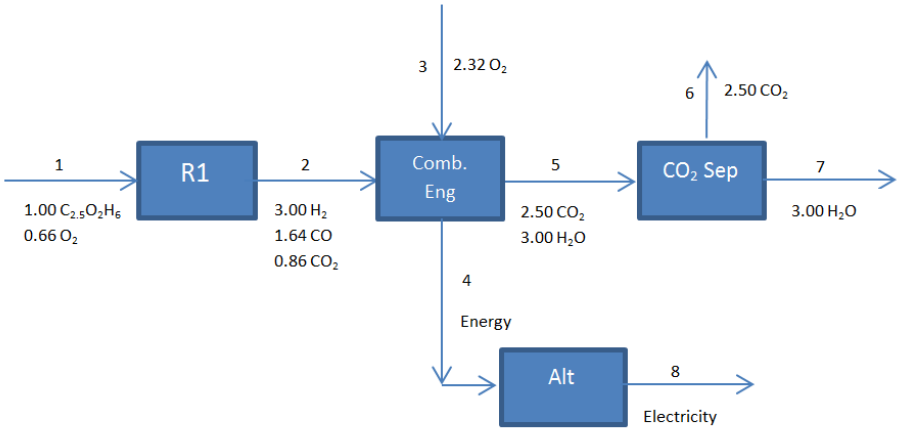


Figure 6.3: Electricity generation using an Internal Combustion Engine represented on the TBL – Feed 2

Figure 6.3 is similar to the basic combustion process as it does not have a recycle stream. The discharge streams of CO_2 and H_2O have also not changed.

In order to choose the best process, energy balances should be done on each process and on each piece of equipment in order to determine the energy losses from the system and to determine how much energy is actually converted into electricity. Wasted heat from the process can be used to drive the turbines which generate electricity.

The processes described above are depicted on the CHO diagram and can be seen in Figure 6.6 and 6.7 below.

6.2 Electricity generation using SOFC's

Solid oxide fuel cells (SOFC) are not widely used in industry. Unlike combustion engines, the gas entering the fuel cell has to be very clean so that impurities do not damage the catalyst. Intrinsic cleaning technologies can be used to remove these

impurities. If these impurities are not removed, not only does it damage the catalyst, but also has the potential to interact with and degrade the SOFC anode due to carbon deposition (Ye et al., 2010 and Lorente et al., 2012). This however makes the process more costly. If dry reforming is done prior to the fuel cell, syngas is produced and this then becomes the feed stream to the fuel cell. H_2 from the syngas needs O_2 to combust. The H_2 is burnt to produce electricity and the CO reacts according to the water-gas shift reaction to produce additional H_2 for electricity production and CO_2, hence the waste from the overall process is CO_2 and water. Below are the results obtained from the combustion of LFG using an SOFC.

6.2.1 Basic Flow Diagrams

Figure 6.4 illustrates the process for combustion of LFG into electricity though a fuel cell. Cleaning steps are not shown and it is assumed that the inlet stream to the dry reforming process contains CH_4 and CO_2 only in the ratio 60:40. Contaminants found in the gas may be assumed as negligible. It is also important to note that the gas should be cleaned thoroughly before it can pass through the fuel cell and hence secondary treatment of the gas is required.

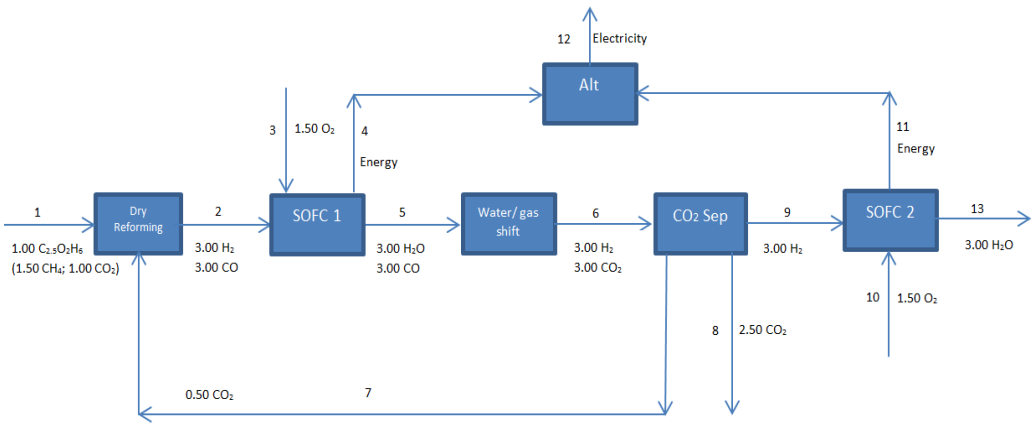


Figure 6.4: Electricity generations using SOFC's and dry reforming – Feed 1

From Figure 6.4, it can be seen that stream 1 brings in the cleaned LFG. The gases react in a dry reformer to produce syngas in stream 2. H_2 from the syngas needs oxygen to combust; therefore oxygen is fed into the system through stream 3. The

H_2 is burnt to produce electricity in SOFC 1 and the CO reacts according the water-gas shift reaction to produce additional H_2 which can be used for added electricity production through SOFC 2. The water-gas shift reaction occurs in the fuel cell (SOFC 1) simultaneously to the combustion reaction, however in order to access the situation, it is shown separately in this report. Due to the water-gas shift reaction, H_2 will always be in excess as all the H_2 produced during dry reforming according to reaction 6.5 reacts with O_2 to form electricity. The water-gas shift reaction produces additional H_2 than what is required; hence a constant bleed of H_2 would be required if a second SOFC is not used. Instead of removing the additional H_2 from the system, it may be worthwhile to pass the additional H_2 produced by the water gas shift reaction to a second fuel cell (SOFC 2). This eliminates the bleed of excess H_2 and instead produces double the electricity as can be seen in Figure 6.4. The waste materials from the process are CO_2 and water. The reactions for the process are shown below:

$$(1.5\,CH_4 + CO_2) + 0.5\,CO_2 \rightarrow 3.0\,CO + 3.0\,H_2 \quad 6.5$$

$$3.0\,H_2 + 1.5\,O_2 \rightarrow 3.0\,H_2O \quad 6.6$$

$$3.0\,CO + 3.0\,H_2O \rightarrow 3.0\,CO_2 + 3.0\,H_2 \quad 6.7$$

Reaction 6.5 is the dry reforming stage. CO_2 produced from the overall process can be recycled back into the system to make up for lack of CO_2 in the feed stream. Reaction 6.6 is the conversion of H_2 into electricity and water is formed as a by-product. Reaction 6.7 is the water-gas shift reaction which produces CO_2 and H_2 which is required for electricity generation. The above process can be used for Feed 1 and is depicted on the CHO diagram below.

For a feed type such as Feed 2, dry reforming does not need to be used as H_2 is produced on the TBL. The system for such a reaction will be as follows:

$$C_{2.5}O_2H_6 + 0.55O_2 + 1.9\,H_2O \rightarrow 4.90\,H_2 + 2.5\,CO_2 \quad 6.8$$

$$4.90\,H_2 + 2.45\,O_2 \rightarrow 4.90\,H_2O \quad 6.9$$

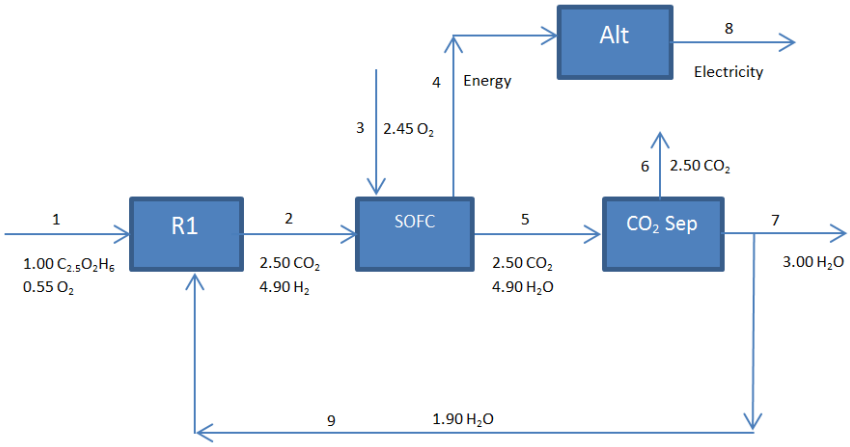


Figure 6.5: Electricity generations using SOFC's and Feed 2

From Figure 6.5 it can be seen that more CO_2 is produced as compared to the dry reforming process. H_2O is recycled back into the process. Although the CO_2 emissions may be greater, the process occurs on the TBL, hence the process runs under adiabatic conditions. More on this is explained on the CHO diagrams in Figure 6.6 and 6.7 below.

6.2.2 Electricity generation depicted on CHO diagram

The combustion reactions given by r_1 and reaction 6.6 was plotted on the CHO diagram. The results are shown below in Figure 6.6 for Feed 1 and Figure 6.7 for Feed 2.

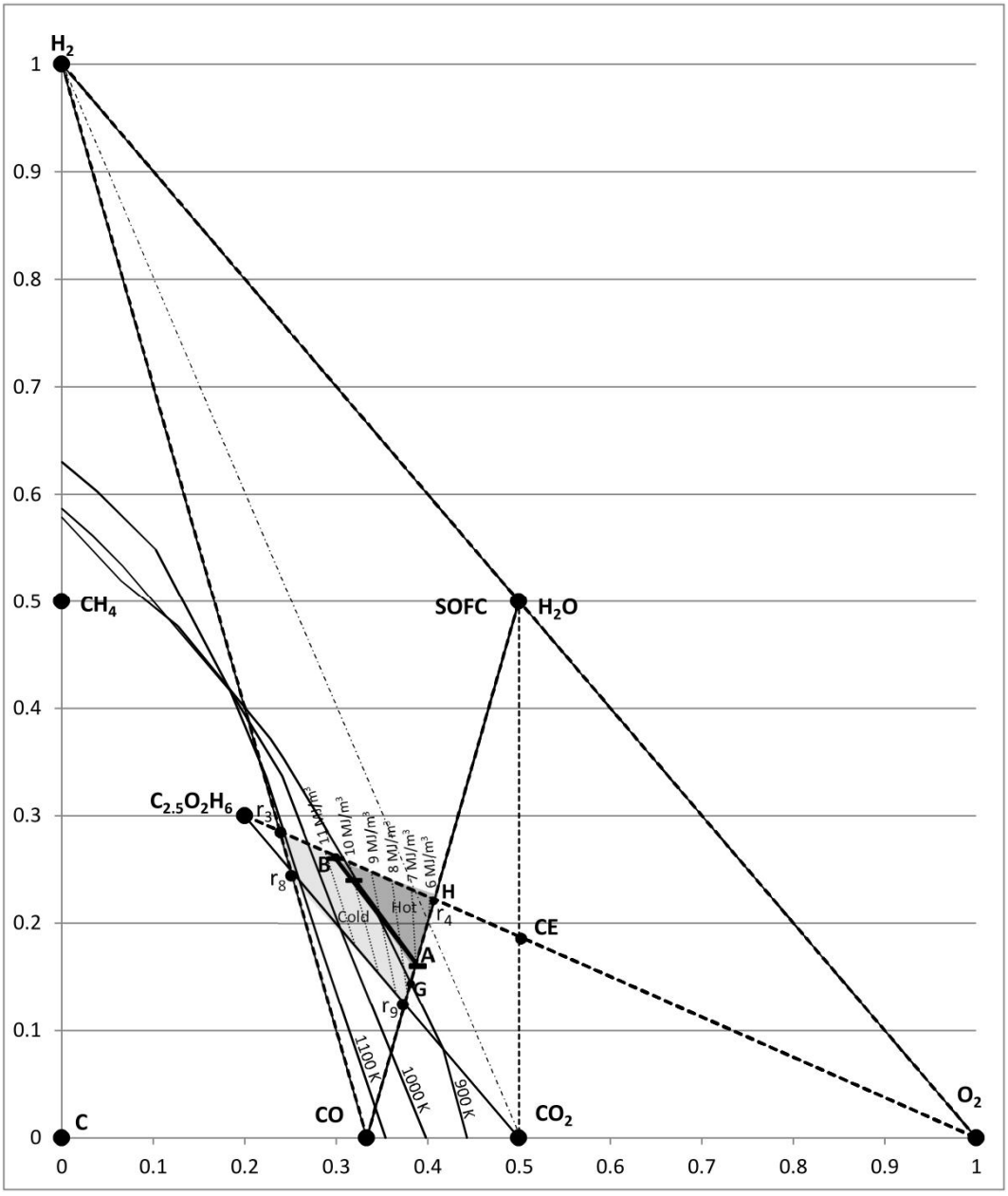


Figure 6.6: Electricity production using Feed 1

Figure 6.7 depicts the point that complete combustion occurs and this is shown by Point CE and represents Figure 6.1. The point labeled SOFC is representative of Figure 6.4; however this point takes into consideration the SOFC process only (Equation 6.6) and eliminates the dry reforming (Equation 6.5) and water gas shift reactions (Equation 6.7) which in turn assists with the generation of electricity. If the entire process shown in Figure 6.4 had to be taken into account, the overall balance would be represented by point CE. It is evident that the combustion and

the SOFC reactions fall out of the stoichiometric region defined for optimum operating conditions, however the combustion reaction occurs at a lower position on the CHO diagram as compared to the SOFC reaction when the electricity generation process is singled out from the rest of the process. Although the SOFC reaction occurs at a higher point than general combustion through an internal combustion engine (point CE), and may seem more attractive from an environmental point of view as less CO_2 emissions seem to form, it should be noted that if an overall balance is done on Figure 6.4 (as depicted by the dotted lines), it would be representative of point CE, therefore the process as a whole would still emit the same amount of CO_2 emissions as an internal combustion engine. This proves that if combustion is used to generate electricity, the overall mass balance will always yield the same amount of CO_2 emissions and will always be representative of point CE, despite the reactants or technology used for the intermediate reactions.

When Feed 1 is used for electricity generation as in the mass balance depicted by Figure 6.2, the process occurs on the TBL AB, however any point on the TBL is adiabatic and no energy is required for the process to occur. The calorific value at this point is 7MJ/m^3. If water is removed, the system ends up at point H. From there, O_2 is introduced for combustion to take place and the system is then forced to the combustion line to point CE. For this process combustion occurs only on point CE due to the reactants used. Should other reactants be considered, point CE will move, but only along the combustion line. Although with the TBL, the system ends up at the same point as normal combustion, the energy required for the reaction to occur would need to be calculated as well as the energy losses before a sound decision on which process proves to be a superior one can be established.

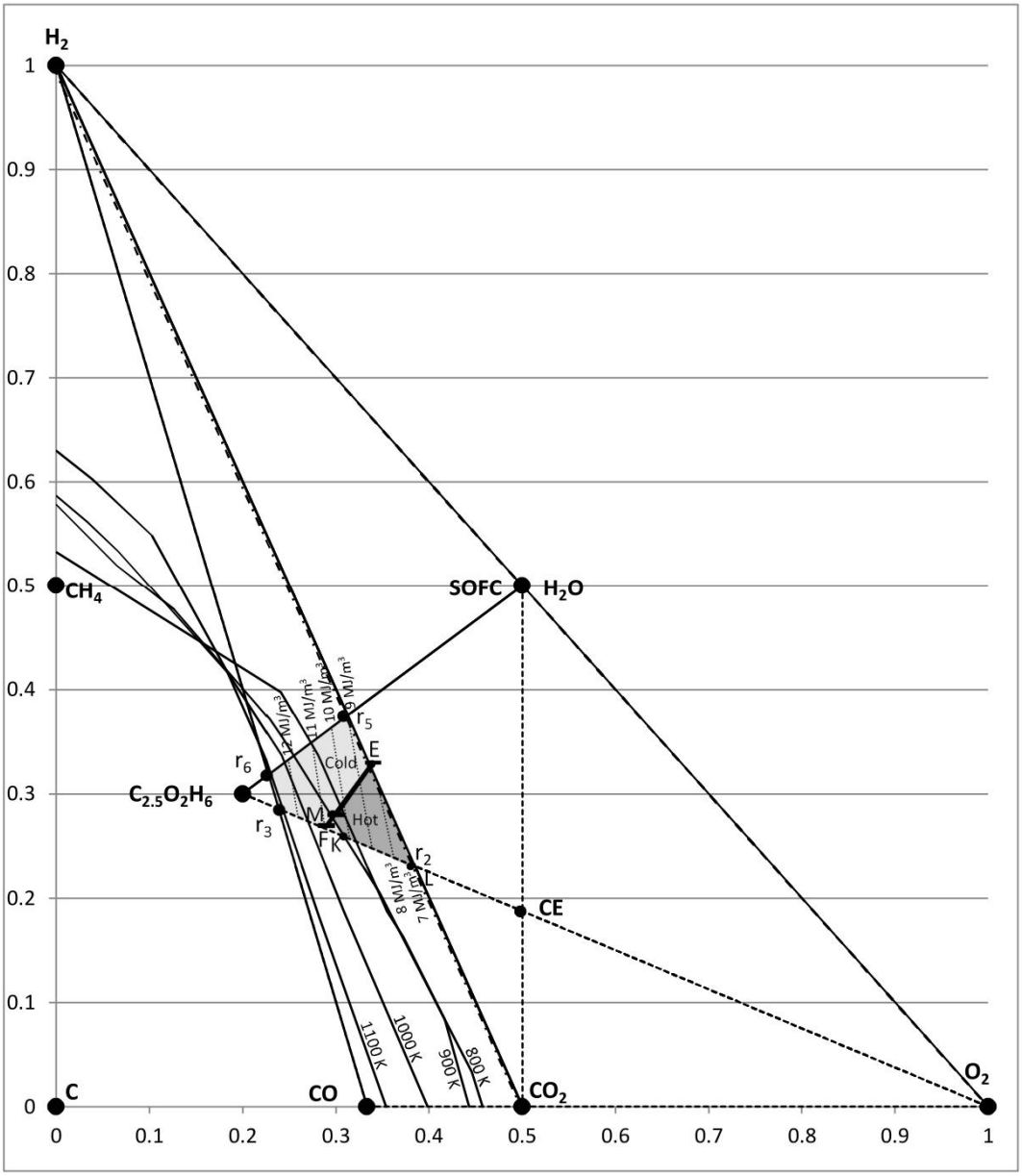


Figure 6.7: Electricity production using Feed 2

For combustion to occur according to Feed 2 which is represented by the mass balance in Figure 6.3, the system is found at point F, which lies on the TBL and an adiabatic process. The calorific value at this point is high and is found to be 11MJ/m^3. An HHV between 8.5 and 10.5MJ/m^3 can be achieved for electricity generation to occur once O_2 is introduced into the process for combustion to occur. The technique shown in Figure 6.7 allows options for steam to be added to the process. It can be seen that one can operate at 10MJ/m^3, however this is too exothermic. If H_2O is introduced, the system can operate on the same contour to

obtain the same HHV of 10MJ/m^3, but at a lower exit temperature as this process is less exothermic. For optimal operation, steam (H_2O) should be added to force the system to operate at the intersection of the TBL and the carbon boundary. Again, the energy required for electricity generation as well as losses and the amount of energy produced would need to be determined before a conclusion can be made on which process is preferable.

For the process represented by the mass balance in Figure 6.5, the system is found at point E on the TBL. The calorific value at this point is relatively low and is between 8 – 9MJ/m^3. If the CO_2 is removed and H_2 is reacted with O_2 for electricity production, the system will be forced to point SOFC.

From Figure 6.6, it shows that less energy is required for SOFC to be carried out, however in Figure 6.7, it shows that more energy is required for SOFC to be carried out as it is above the TBL and this is an endothermic region for Feed 2 (Figure 6.7). Despite the variation between the feeds, it is important to note that by choosing to produce electricity using an SOFC, a more optimal process will be established. SOFC's are operated at high temperatures between 973.15 K and 1273.15 K. Although the SOFC process does not fall within the stoichiometric region and the carbon boundaries defined, no carbon will deposit on the anodes if the gas is stripped of all impurities (Ye et al., 2010 and Lorente et al., 2012) and therefore hydrocarbons and landfill gas can be transformed into useful energy. Additionally, SOFC's use H_2 for electricity production; hence the efficiency obtained for the entire process is much greater than conventional combustion. SOFC's have an efficiency of approximately 70 % according to Minh, 2004 as compared to an internal combustion engine of just 25 to 35% as stated in LMOP, n.d and Roberts et al, 2014. Furthermore, if the TBL is used, the process becomes even more desirable as an adiabatic process is introduced.

The conventional route of using combustion engines may use traditional technologies but will give a far lower efficiency. The costs of installation and operation of an SOFC is considerably high as it requires the correct electrolytes and catalysts to drive the reaction to completion and a clean incoming stream of gas, however it offers greater value electricity production by upgrading the

efficiency from 35% to approximately 70 %. This is far greater than one can obtain from the same input stream as used by an internal combustion engine. A detailed energy balance around each process would need to be completed to determine the correct amounts of electricity produced as well as any energy losses.

6.3 Electro-Catalytic reduction of CO_2

Electro-catalytic reduction of CO_2 to produce oxygen and methane is common in space based operations, however not so much so in industrial processes. If this process is viable, it would be an attractive one due to the fact that the reaction occurs at room temperature, CO_2 is not emitted into the atmosphere and the products are oxygen and methane which can both be sold on the market. Below are the results obtained from the conversion of CO_2 into methane.

6.3.1 Basic Flow Diagram

The figures below illustrate the process for converting LFG into methane using electro-catalytic reduction of CO_2 with H_2O, H_2 and production of methane using the Sabatier Reaction respectively (discussed in detail under Section 2.6). Cleaning steps are not shown and it is assumed that the inlet stream to the process contains CH_4 and CO_2 only in the ratio 60:40. Contaminants found in the gas may be assumed as negligible. It is also assumed that the CO_2 separation is 100% efficient.

The reaction for methane production using electro-catalytic reduction of CO_2 with H_2O is as follows and represented by Figure 6.8 below:

$$0.40\ CO_2 + 0.80\ H_2O \rightarrow 0.40\ CH_4 + 0.80\ O_2 \qquad 6.10$$

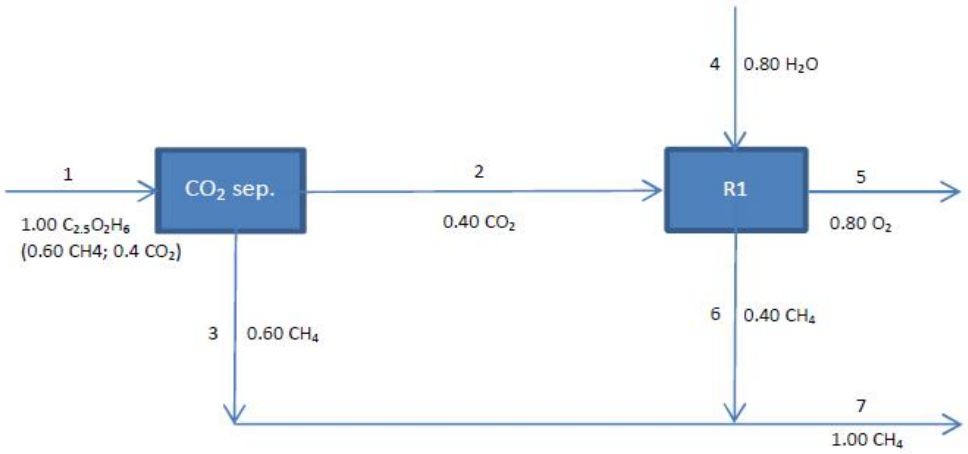


Figure 6.8: Electro-catalytic reduction of CO_2 using H_2O to produce methane

Figure 6.8 shows LFG entering the process with CH_4 and CO_2 in the ratio 0.60:0.40 respectively. The CO_2 is separated from the feed stream and enters the electro-catalytic reactor where it reacts with H_2O at room temperature to produce CH_4 and O_2. The O_2 is removed in stream 5 and can be used as a by-product to other processes which require combustion. The product methane from the reaction is removed with stream 6. CH_4 from the feed is combined to the CH_4 produced and is removed from the system as the desired product in stream 7. The CH_4 can be compressed to form liquid methane which is easy for storage and transportation. This reaction uses water which is highly accessible as compared to the electro-catalytic reduction of CO_2 with H_2.

The reaction for methane production using electro-catalytic reduction of CO_2 with H_2 is as follows and represented by Figure 6.9 below:

$$0.40\,CO_2 + 0.80\,H_2 \rightarrow 0.40\,CH_4 + 0.40\,O_2 \qquad 6.11$$

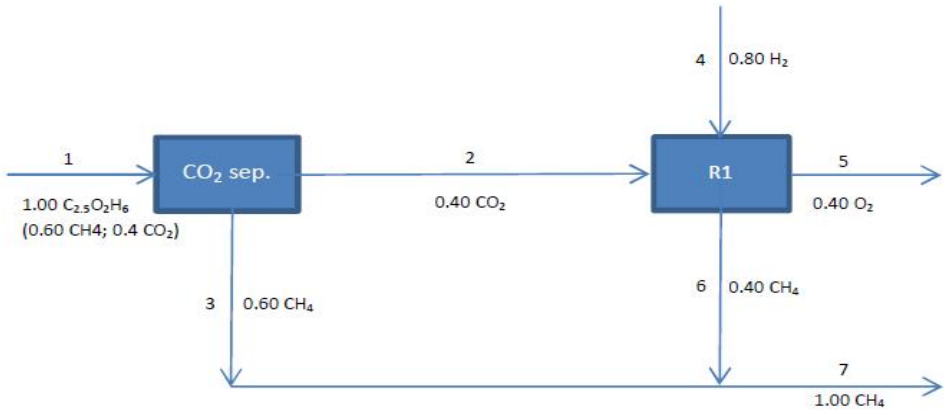


Figure 6.9: Electro-catalytic reduction of CO_2 using H_2 to produce methane

Figure 6.9 shows LFG entering the process with CH_4 and CO_2 in the ratio 0.60:0.40 respectively. The CO_2 is separated from the feed stream and enters the electro-catalytic reactor where it reacts with H_2 to produce CH_4 and O_2. The O_2 is removed in stream 5 and can be used as a by-product to other processes which require combustion. The product methane from the reaction is removed with stream 6. CH_4 from the feed is combined to the CH_4 produced and is removed from the system as the desired product in stream 7. The CH_4 can be compressed to form liquid methane which is easy for storage and transportation.

The reaction for methane production using Sabatier reaction is as follows and represented by Figure 6.10 below:

$$0.40\,CO_2 + 1.60\,H_2 \rightarrow 0.40\,CH_4 + 0.80\,H_2O \qquad 6.12$$

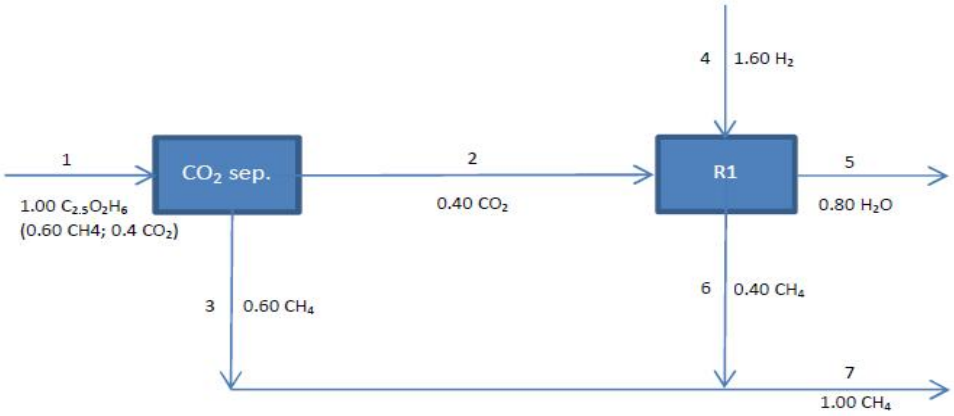


Figure 6.10: Production of methane using the Sabatier reaction

Figure 6.10 shows LFG entering the process with CH_4 and CO_2 in the ratio 0.60:0.40 respectively. The CO_2 is separated from the feed stream and enters the reactor where it reacts with H_2 to produce CH_4 and H_2O. The H_2O is removed in stream 5 and can be used as a by-product for other reactions or as process water. The product methane from the reaction is removed with stream 6. CH_4 from the feed is combined to the CH_4 produced and is removed from the system as the desired product in stream 7. The CH_4 can be compressed to form liquid methane which is easy for storage and transportation. The Sabatier reaction requires more H_2 to convert CO_2 into CH_4 as compared to the electro-catalytic reduction of CO_2 with H_2 and H_2O. It also produces H_2O as a by-product as compared to O_2 which could serve to be a much valuable by-product than H_2O.

6.3.2 Methane generation depicted on the CHO diagram

The reactions described above are represented on the CHO diagrams below for Feed 1 and 2 respectively.

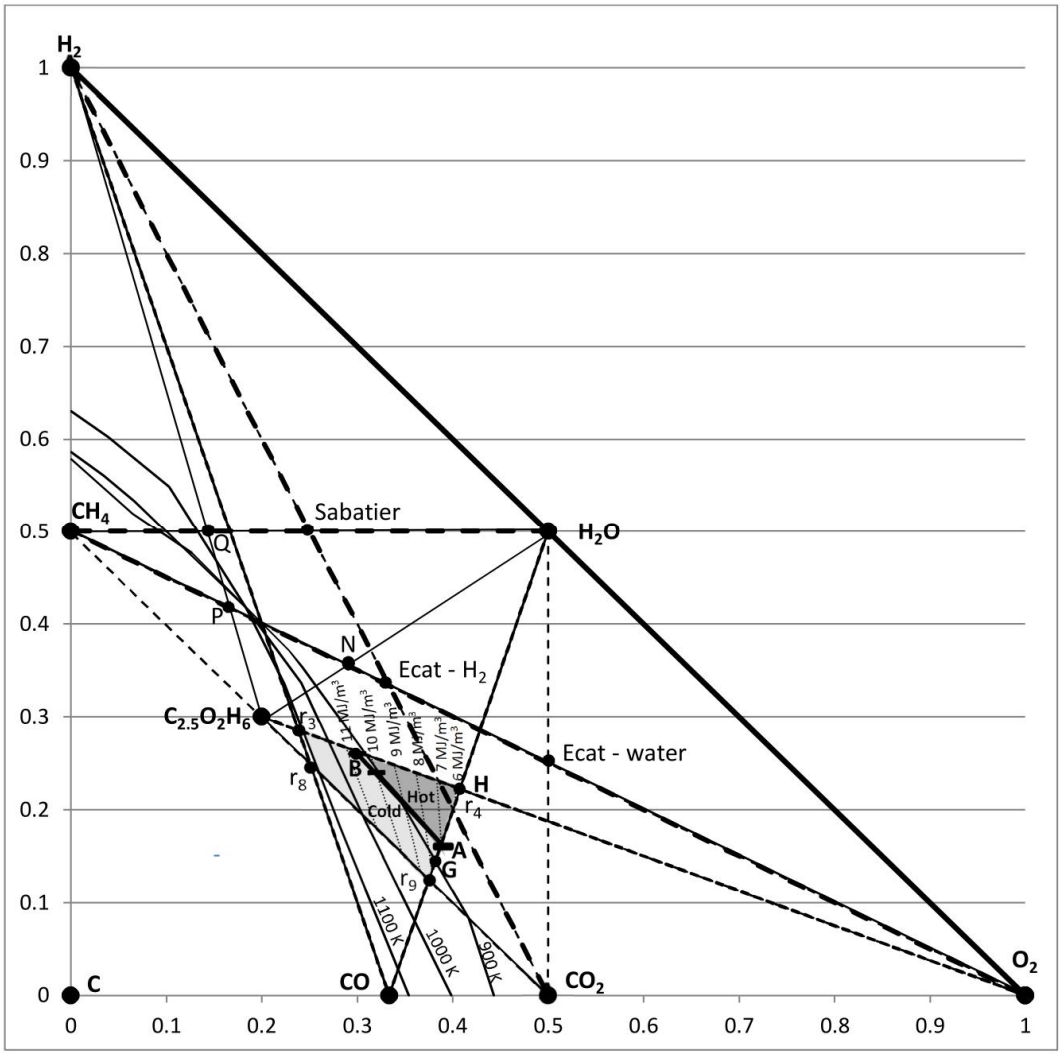


Figure 6.11: Methane generation using Feed 1

Methane generation brings about two completely different set of results for Feed 1 and 2. In both situations, CO_2 is separated from the LFG producing CH_4 and CO_2 in different streams. The CH_4 is sent to the product stream and the CO_2 reacts according to the different reactions shown in Section 6.3.1 to produce additional CH_4 and a by-product. By analysing Feed 1 represented by Figure 6.11, all three reactions occur out of the stoichiometric region. It should be noted that the overall process in Figure 6.8 represented by dotted lines in Figure 6.11 would yield a different point on the CHO diagram; however this process will also occur out of the stoichiometric region and can be seen by point N in Figure 6.11. The same applies for the overall processes represented in Figure 6.9 and 6.10 by dotted lines and are illustrated by points P and Q respectively in Figure 6.11. The purpose of

the stoichiometric region is to create syngas from LFG, or a mixture thereof, for example, the stoichiometric region in Figure 6.11 produces H_2, CO and H_2O. The syngas can then undergo electro-catalysis to form CH_4 and H_2O or O_2, depending on the reaction. In the case of Feed 1, none of the reactions occur within the stoichiometric boundary and hence are not considered favourable as syngas cannot be produced as an intermediate step.

By introducing Feed 2 into the system, the scenario changes to three different sets of results as can be seen in Figure 6.12. The electro-catalytic reduction of CO_2 using H_2O occurs below the TBL in the exothermic region (r_2 exothermic) therefore would require less energy for the reaction to go to completion; however it still remains out of the stoichiometric boundary. The Sabatier reaction occurs above the TBL, in the endothermic region and also does not fall within the stoichiometric region. The Sabatier reaction in this case would not be a good option to pursue as energy would be required to drive the endothermic process to completion and this would incur additional costs. The electro-catalytic reduction of CO_2 using hydrogen falls within the established stoichiometric region and lies on the TBL. This point falls between low calorific values of 8 – 9MJ/m^3 and is considered a reasonably good calorific value to operate at. A good process temperature would be 800K as one would be operating out of the carbon boundary leading to no carbon deposition. Furthermore, according to Gür et al., 1990, this reaction does not produce any graphite as a by-product because the carbon is highly reactive toward H_2, and the resident time on the metal surface is too short for any nucleation to take place.

In this instance, for the production of methane, only one option seems viable and that is using Feed 2 and allowing it to react according to the electro-catalytic reduction of CO_2 using H_2. This option allows H_2O to be converted to H_2 and CO_2, and secondary reactants are then converted into CH_4 and O_2 through electro-catalytic reduction of CO_2 using H_2 and this step is energy intensive. Although this option may be feasible it is a very energy intensive process therefore one needs to take the energy balance into account as well as account for increased costs involved for catalysts and electrodes used in the process. The reaction also

uses pure hydrogen and this further increases the cost as hydrogen first needs to be separated from the LFG through methane dry reforming as explained by Olah et al., 2009. Pure H_2 gas could also be purchased although there would be cost implications as H_2 is quite expensive.

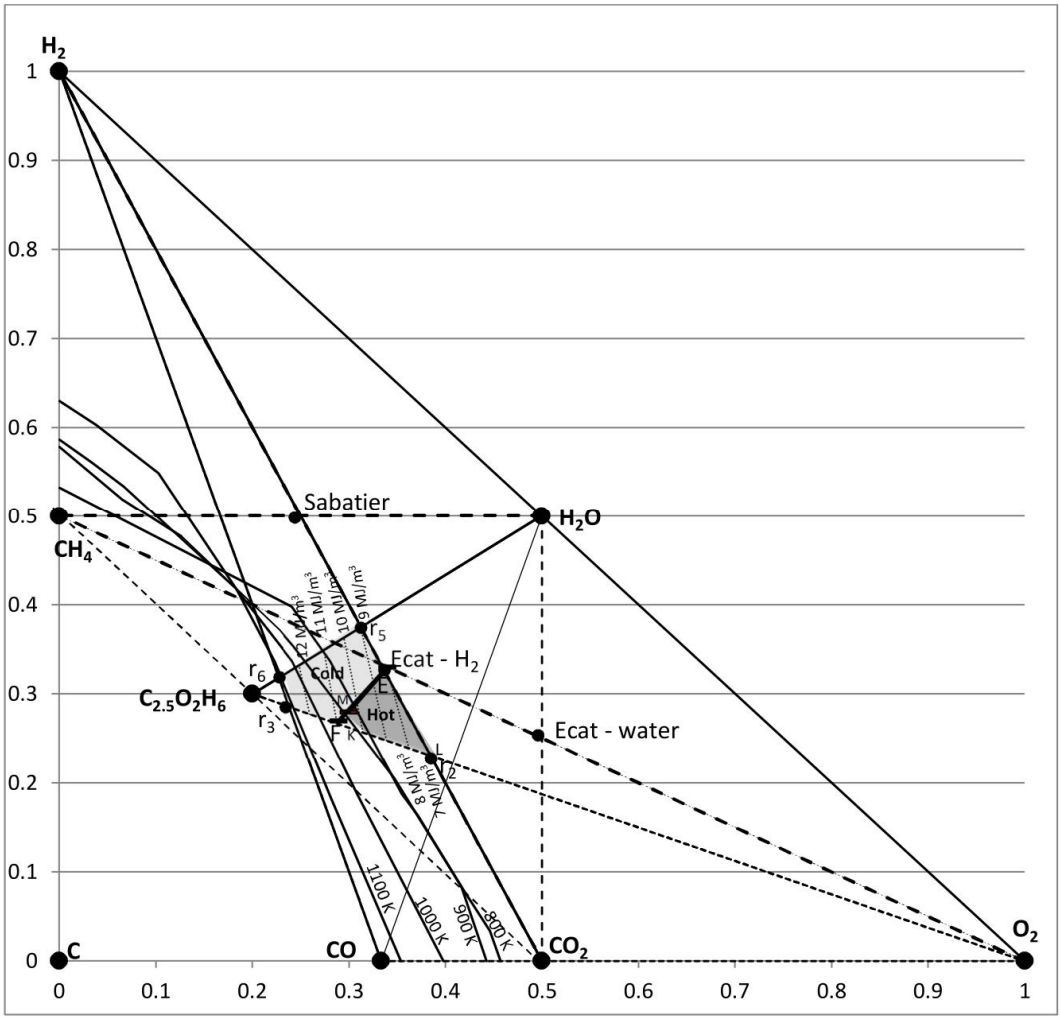


Figure 6.12: Methane generation using Feed 2

The process of converting CO_2 into CH_4 may seem attractive from an environmental perspective as all CO_2 is converted into a fuel source with no CO_2 emissions to the environment; however more energy is required for the process to reach completion. One therefore needs to consider all fuels that can be produced using LFG as a feedstock and to see which process would be best suited to produce a fuel with as little CO_2 emissions as possible and still being able to

operate within the stoichiometric region to obtain optimal results with reduced energy intensive processes.

6.4 Synfuel Production

Synfuels, currently produced from syngas still uses fossil fuels as a primary input source. For every atom of carbon used, one atom of CO_2 is produced for every atom of CH_2 produced (Schultz et al., n.d). Therefore the atoms of CO_2 produced, always equal that of the desired product, CH_2. The synfuel processes analysed below looks at reducing the amount of CO_2 produced, or to eliminate it altogether; thereby producing a synthetic fuel which is not made from fossil fuels and has minimal carbon emissions. Below are the results obtained from the production of synfuel from LFG.

6.4.1 Basic Flow Diagram

Figure 6.13 illustrates the process for converting LFG into synfuel with minimal carbon emissions. Cleaning steps are not shown and it is assumed that the inlet stream contains LFG in the ratio 60:40 of methane and carbon dioxide respectively. Contaminants found in the gas may be assumed as negligible.

In order for the process to occur on the TBL for Feed 1, the equations for the process must be as follows:

$$C_{2.5}O_2H_6 + 0.78\,O_2 + 0.45\,CO_2 \rightarrow 1.48\,H_2 + 2.95\,CO + 1.52\,H_2O \qquad 6.13$$

$$1.48\,H_2 + 2.95\,CO \rightarrow 1.48\,CH_2 + 1.48\,CO_2 \qquad 6.14$$

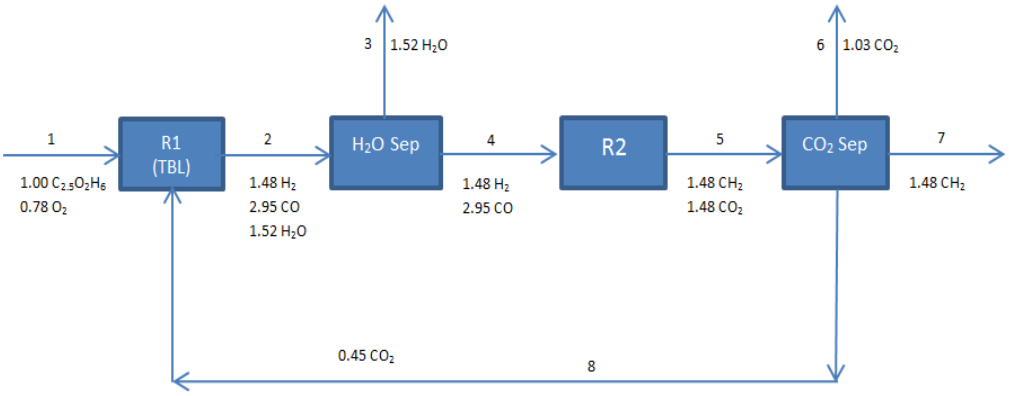


Figure 6.13: CH_2 production using Feed 1

From Figure 6.13 it can be seen that CO_2 is required for the reaction to occur on the TBL and this CO_2 is achieved through recycling waste CO_2. This means that fewer emissions are released into the atmosphere as the feed itself requires CO_2 to progress into products. Once the syngas is produced, and the water removed in stream 4, the syngas reacts to produce the desired product CH_2 and emissions of CO_2. It can be seen from Equation 6.14 and from Figure 6.13 in stream 6, that CH_2 and CO_2 are produced in the same ratio. This confirms the theory illustrated in Schultz et al., n.d. However, by using a recycle stream such as stream 9, the CO_2 emissions to the atmosphere are reduced. The H_2O and CO_2 separation process represented by Figure 6.13 are gas-liquid separation processes, hence it is easier to separate water from syngas and CO_2 from the CH_2 and it is less costly. This gives a greener and more sustainable process as less energy is required for the entire process to occur as the process occurs on the TBL.

If Feed 2 is used, the process is as follows for it to still occur on the TBL (Figure 6.14):

$$C_{2.5}O_2H_6 + 0.67\,O_2 + 0.10\,H_2O \rightarrow 3.10\,H_2 + 1.55\,CO + 0.95\,CO_2 \qquad 6.15$$

$$3.10\,H_2 + 1.55\,CO \rightarrow 1.55\,CH_2 + 1.55\,H_2O \qquad 6.16$$

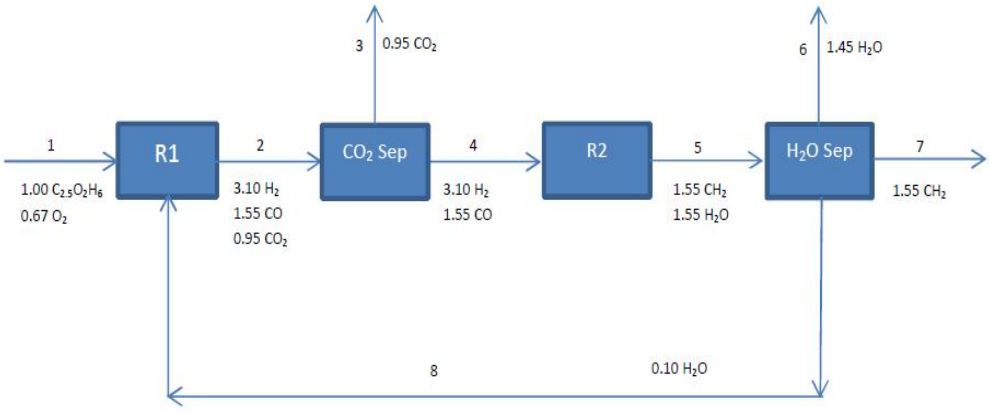


Figure 6.14: CH_2 production using Feed 2 with a H_2O recycle stream

Figure 6.14 and Equation 6.15 show that water is required in the feed if Feed 2 is used instead of CO_2 as in the case with Feed 1. The water produced along with the product CH_2 from Equation 6.16 is recycled to the feed stream. Syngas (H_2:CO) is produced in the ratio 2:1 along with 0.95 kmols/day of CO_2. The CO_2 produced is separated and emitted to the atmosphere. In this case, the CO_2 separation process is a gas-gas separation; therefore it is more difficult to separate the CO_2 from the syngas stream and requires more energy which makes this process expensive as compared to the process in Figure 6.13. Once the CO_2 is removed, the syngas reacts to completion to form the desired product CH_2 and H_2O in the same proportion. It is important to note that even though the CO_2 in this case is not recycled and is more difficult to separate from the gas stream, the amount produced and emitted to the atmosphere is in smaller proportions to the desired product CH_2 as compared to the process shown in Figure 6.13. The water that's not recycled can be reused within the plant as process water.

Another scenario exists for Feed 2 where the system does not operate on the TBL. The process is as follows and is depicted in Figure 6.15 below:

$$0.60\,CH_4 + 0.30\,O_2 \rightarrow 1.20\,H_2 + 0.60\,CO \qquad 6.17$$

$$1.20\,H_2 + 0.60\,CO \rightarrow 0.60\,CH_2 + 0.60\,H_2O \qquad 6.18$$

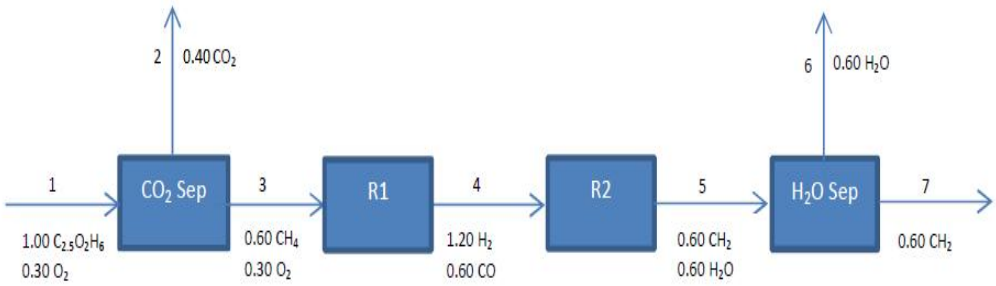


Figure 6.15: CH_2 production using Feed 2 – no recycle stream

The scenario shown in Figure 6.15 does not occur on the TBL. LFG that enters the system is stripped off its CO_2 and this is removed as emissions. The remaining CH_4 combusts to produce syngas (H_2:CO) in the ratio 2:1. This then reacts completely to form the desired product CH_2 and H_2O in the same ratios. The H_2O removed from the system can be used as process water in the plant. Although CO_2 is not recycled, the amount of CO_2 emitted to the atmosphere is much lower than the desired product. This is an idealised case and the CO_2 is reduced further as compared to Figure 6.14 although it is a more energy intensive process.

The processes described above all aim to reduce the levels of CO_2 discharged to the environment. The process found in Figure 6.14 and 6.15 move away from what is said in theory according to Schultz et al., n.d., stating that CO_2 produced is in the same ratios as that of CH_2. The process depicted in Figure 6.9 however is in line with theory as the same ratios of CO_2 and CH_2 are produced. The process is converted to a slightly greener process by recycling CO_2 back to the feed, thereby reducing carbon emissions. Each process explained above is depicted on the CHO diagrams below and explained in more detail.

6.4.2 CH_2 generation depicted on the CHO diagram

The production of CH_2 was plotted on the CHO diagram. The results for Feed 1 and Feed 2 are shown in Figure 6.16 to 6.17 respectively.

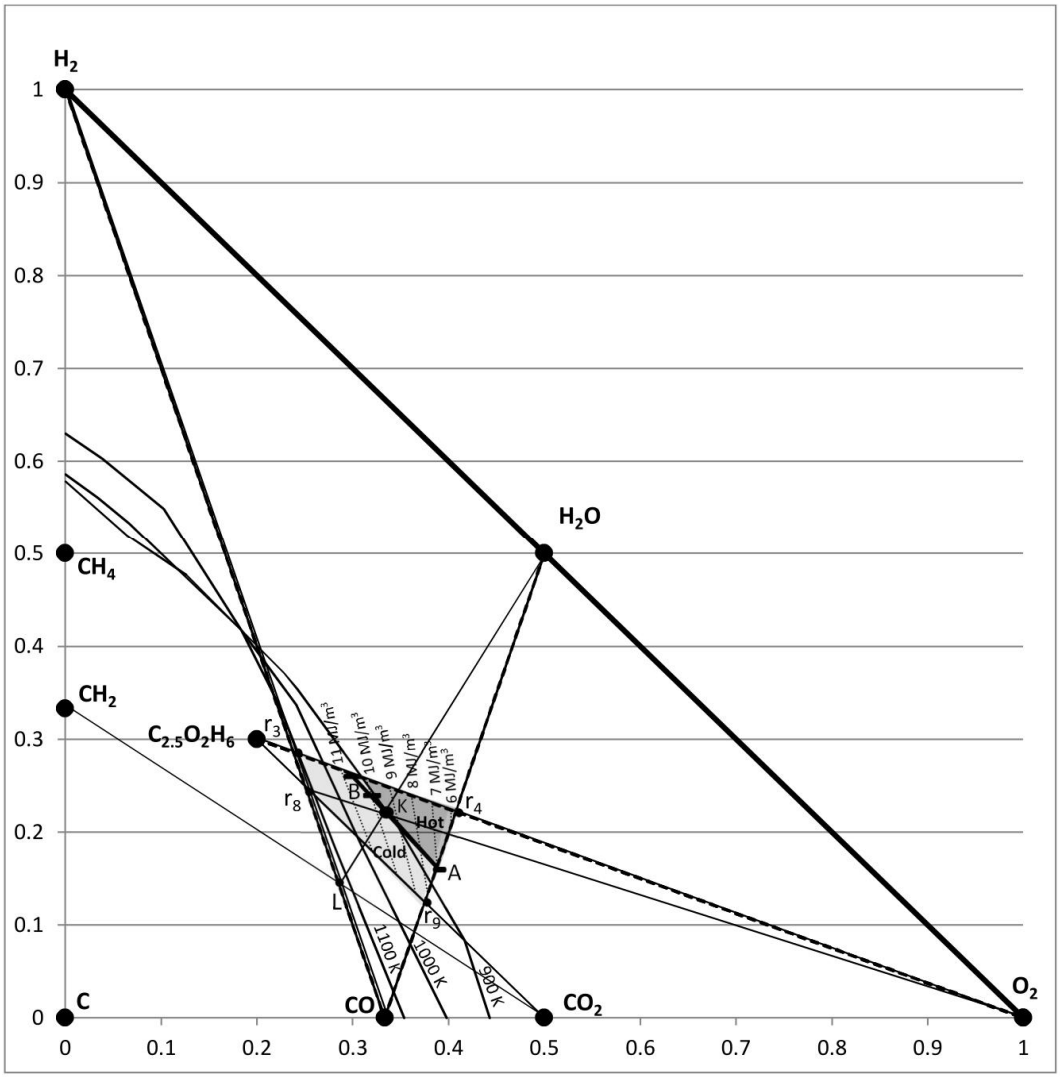


Figure 6.16: CH_2 production using Feed 1

From Figure 6.16, LFG ($C_{2.5}O_2H_6$) is mixed with additional CO_2 which brings the mixture of gases to point r_8. This then reacts with O_2 to produce H_2, CO and H_2O in the proportions as can be seen from the mass balance in Figure 6.13. The reason CO_2 is introduced into the reaction is to allow the system to operate on the TBL as can be seen by point K. The reaction occurs at a calorific value of approximately 9.5MJ/m^3 which is relatively high in this case. The reaction also takes place at 900K hence no deposition of carbon takes place. As a result of operating on the TBL, some water is formed with the CO and H_2. When the water is removed, the system is moved away from the TBL from point K to L producing a 0.5 ratio of H_2: CO (syngas). At the point L, the system is reacted according to

the Fischer Tropsch reaction to produce a synfuel. CO_2 is also formed during this process; however some of it can be recycled back into the process thereby emitting fewer emissions to the atmosphere. This example highlights the conversion of LFG to syngas for downstream processes.

From Figure 6.17 it can be seen that LFG reacts with O_2 and H_2O to form a mixture of syngas in the ratio 2:1 and CO_2. The formation of syngas and CO_2 is represented by point F. This reaction also occurs at 900K but at a higher calorific value (11MJ/m^3) than Figure 6.13. The CO_2 cannot be recycled and is forced to be removed, moving the system away from the TBL to point M where only syngas exists.

Figure 6.18 shows a system where landfill gas is separated into its main components CH_4 and CO_2. The process does not occur on the TBL. The CO_2 is removed completely and discharged to the atmosphere as it cannot be recycled. The remaining CH_4 is then combusted using O_2 to produce syngas and H_2O in the ratio 2:1 respectively at point N. No emissions are produced during this reaction. The syngas reacts completely to form equal quantities of CH_2 and H_2O.

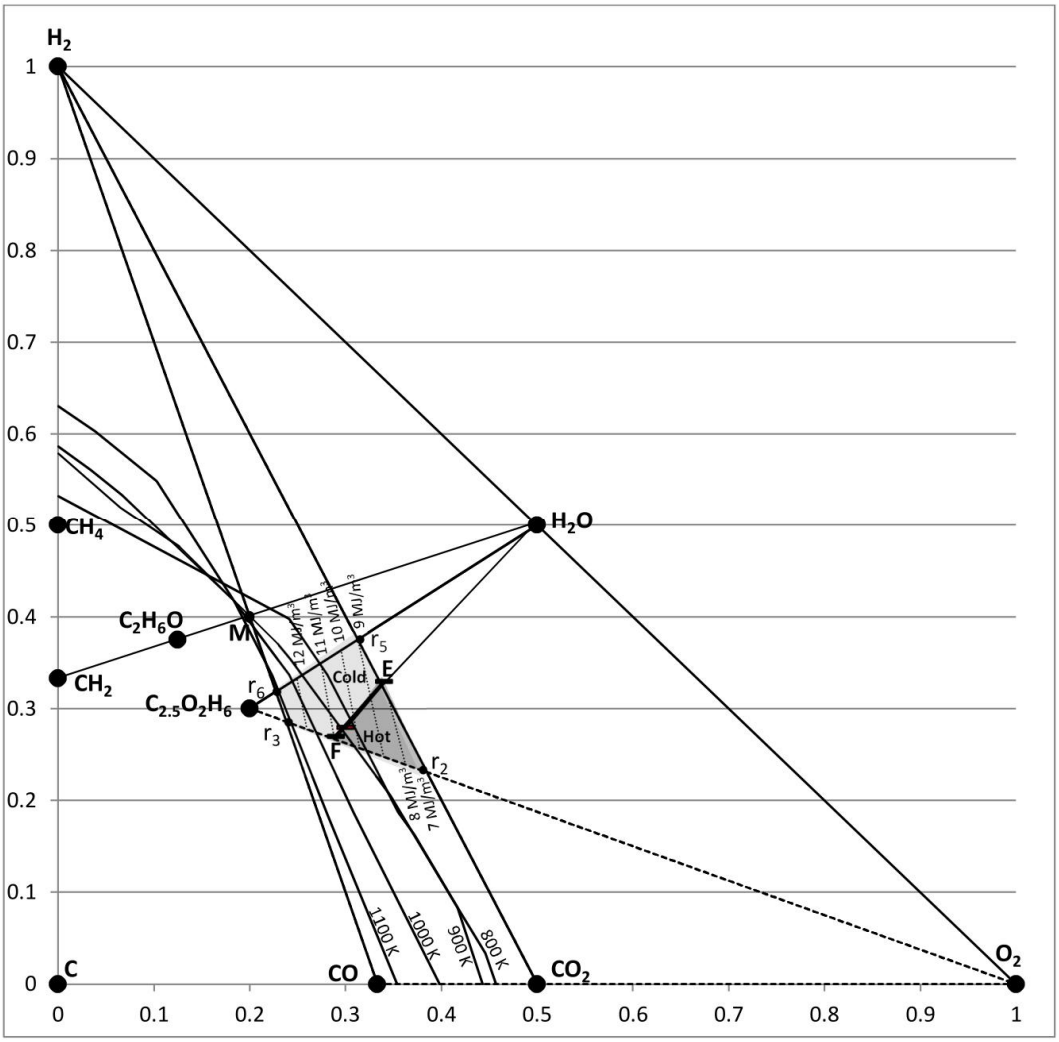


Figure 6.17: CH_2 production using Feed 2 with a H_2O recycle stream

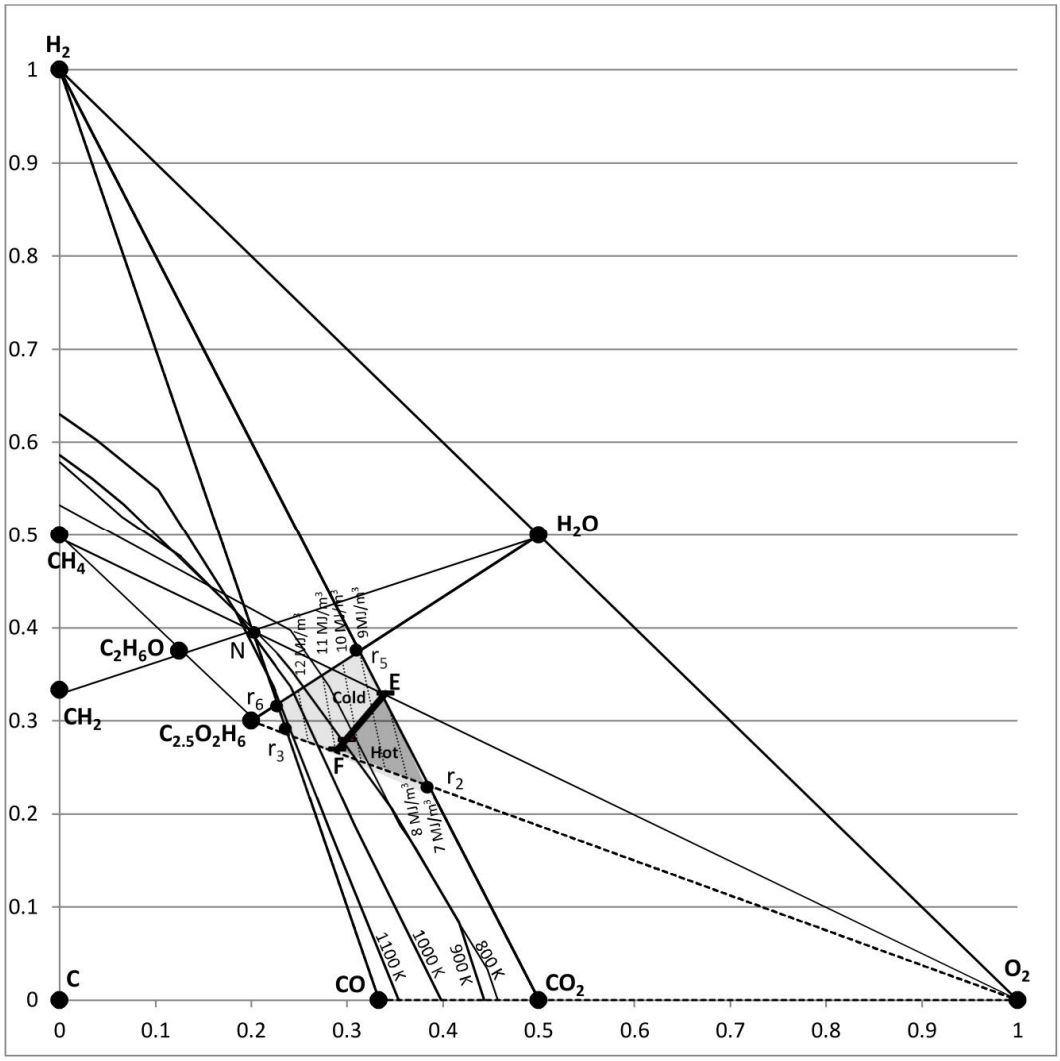


Figure 6.18: CH_2 production using Feed 2 – CO_2 elimination

6.5 DME production

DME produced from syngas is seen as a more superior fuel to methanol due to its high cetane number ranging between 55-60. It produces very few emissions as compared to other fuel processes and is easily stored (liquid at 6 Bar). Below are the results obtained from the production of DME from LFG using different processes.

6.5.1 Basic Flow Diagram

Figure 6.19 illustrates the process for converting LFG into DME using Feed 1 as a feed source. Cleaning steps are not shown and it is assumed that the inlet stream contains LFG in the ratio 60:40 of methane and carbon dioxide respectively. Contaminants found in the gas may be assumed as negligible.

In order for the process to occur on the TBL for Feed 1, the equations for the process must be as follows:

$$C_{2.5}O_2H_6 + 0.88\,O_2 + 1.73\,CO_2 \rightarrow 4.23\,CO + 3\,H_2O \quad 6.19$$

$$2.12\,CO + 2.12\,H_2O \rightarrow 2.12\,H_2 + 2.12\,CO_2 \quad 6.20$$

$$2.12\,CO + 2.12\,H_2 \rightarrow 0.71\,C_2H_6O + 0.71\,CO_2 \quad 6.21$$

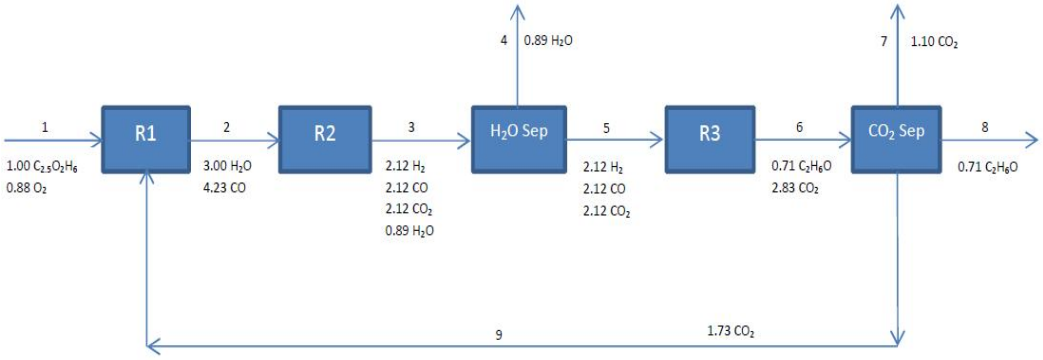


Figure 6.19: DME production using Feed 1 with a CO_2 recycle stream

According to Figure 6.19, CO_2 is required in the feed for reaction 6.19 to go to completion in Reactor 1 (R1); hence it is introduced to the feed stream by means of a recycle stream, stream 9. Half of the CO produced reacts according to the water gas shift reaction, reaction 6.20, to produce stoichiometric proportions of H_2 and CO_2 which is seen in stream 3. Excess water that does not react can be removed and reused as process water or can be discarded. The remaining CO then reacts with the H_2 produced to yield the desired product C_2H_6O (DME) and undesired CO_2. A build-up of CO_2 is expected as it is produced in equations 6.20 and 6.21 in Reactors 2 (R2) and 3 (R3) respectively. CO_2 that is required in the feed can be recycled and the rest will be discarded as CO_2 emissions. Although

this process yields high amounts of CO_2, it is still considerably less that the CO_2 emissions produced during combustion of LFG.

Another scenario exists for Feed 1 where a recycle stream is not used and the following reactions apply. The system is represented by Figure 6.20 below:

$$C_{2.5}O_2H_6 + 0.75\,O_2 \rightarrow 2\,H_2 + 2.5\,CO + H_2O \quad 6.22$$

$$0.25\,CO + 0.25\,H_2O \rightarrow 0.25\,H_2 + 0.25\,CO_2 \quad 6.23$$

$$2.25\,H_2 + 2.25\,CO \rightarrow 0.75\,C_2H_6O + 0.75\,CO_2 \quad 6.24$$

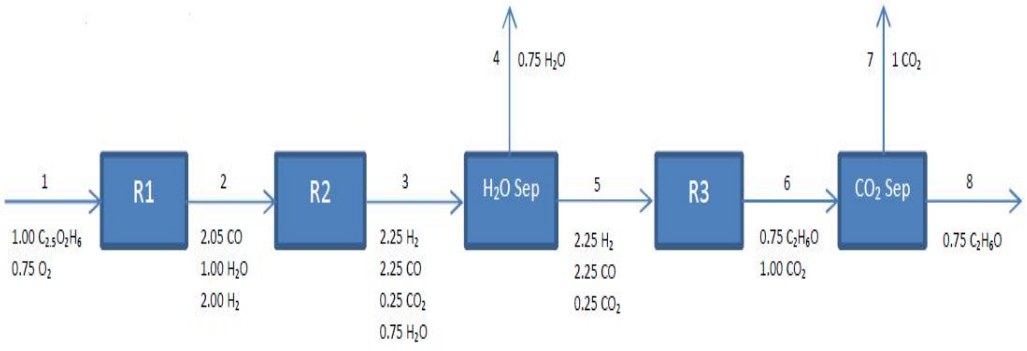


Figure 6.20: DME production using Feed 1 without a CO_2 recycle stream

The system represented in Figure 6.20 is a simple process as it has no recycle stream and does not require CO_2 in the feed to get it to the TBL. Instead, the reaction itself (Equation 6.22) occurs on the TBL producing syngas and H_2O. In order for DME to be produced according to Equation 6.24, H_2 and CO must be in stoichiometric proportion with each other and this is not the case with Equation 6.22. Therefore, 0.25 kmols/ day of CO are allowed to react with H_2O to produce 0.25 kmols/day of H_2 (Equation 6.23). This reaction also produces CO_2 in the same ratio as can be seen in Figure 6.20. The H_2 and CO are now in stoichiometric proportion and hence react according to Equation 6.24 to produce DME and additional CO_2. The CO_2 is removed from the system as an inert stream, stream 7.

When Feed 2 is used, a recycle stream of water is required to get the system on the TBL. The equations for the system represented by Figure 6.21 can be seen below:

$$C_{2.5}O_2H_6 + 0.67\,O_2 + 0.10\,H_2O \rightarrow 3.10\,H_2 + 1.55\,CO + 0.95\,CO_2 \quad 6.25$$

$$1.55\,CO + 3.10H_2 \rightarrow 0.78\,C_2H_6O + 0.78\,H_2O \quad 6.26$$

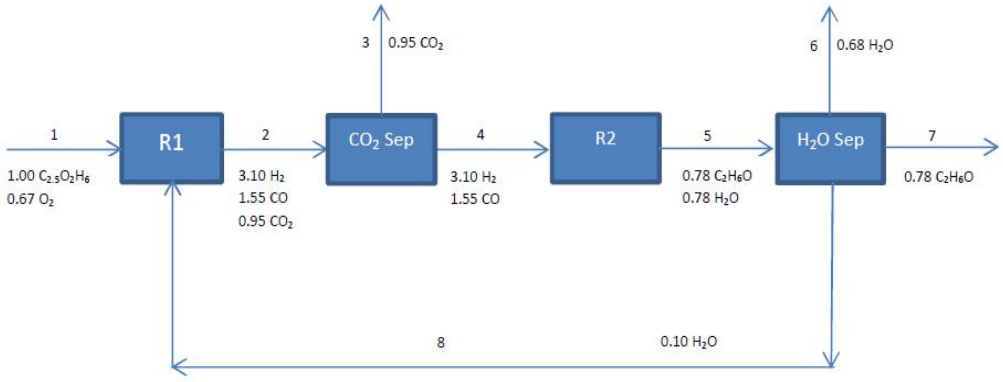


Figure 6.21: DME production using Feed 2

Reaction 6.25 which occurs on the TBL produces syngas in the ratio 2:1 and inert CO_2. The CO_2 can be removed immediately from the system (stream 3) as it is not required anywhere else in the process. The syngas then reacts completely to produce DME and H_2O. The product DME can be removed and stored for use, whilst some of the water is recycled to the feed stream and the remainder removed from the system.

6.5.2 DME generation depicted on the CHO diagram

DME production was plotted on the CHO diagram. The results are shown in Figure 6.22 and 6.23 below.

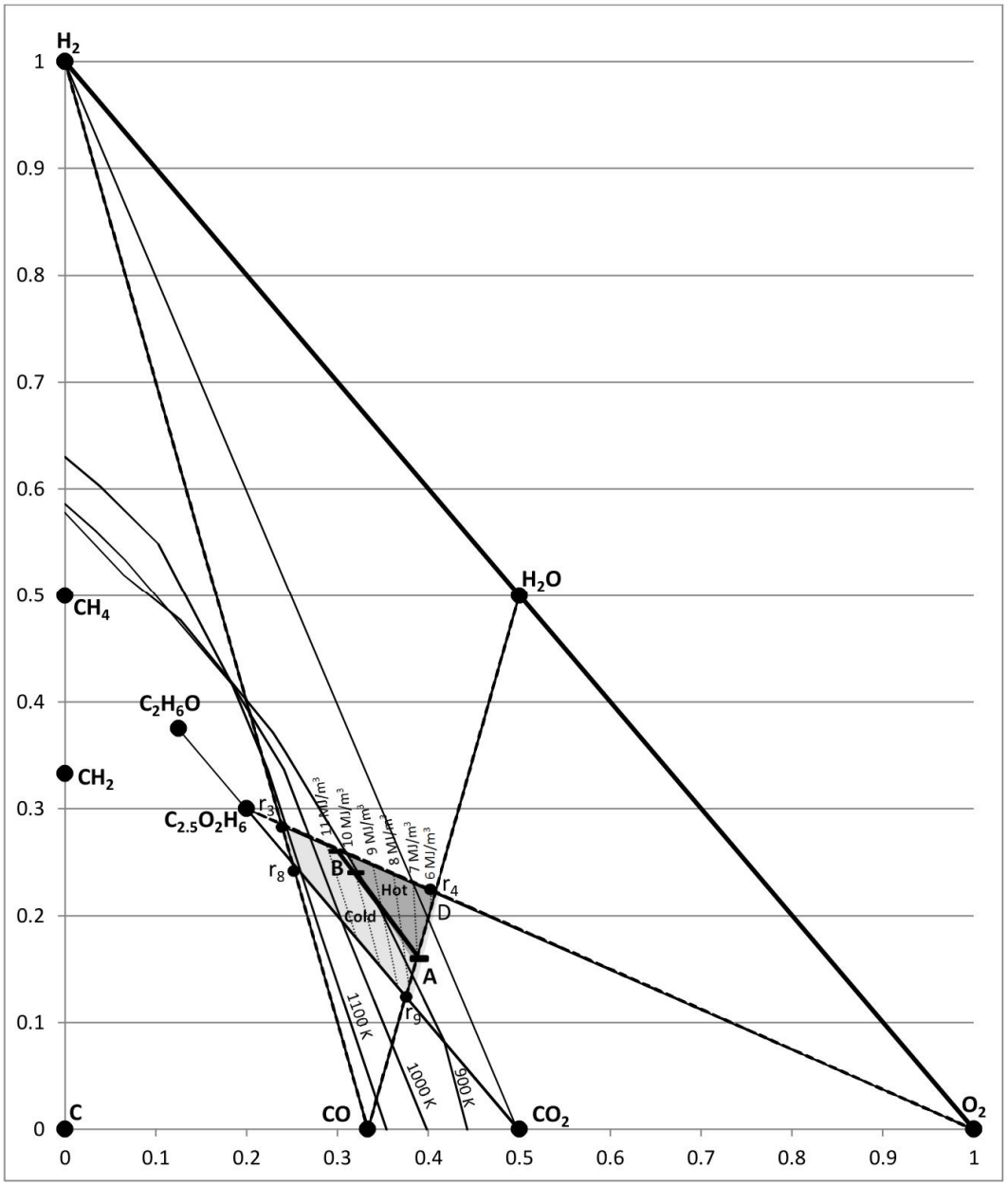


Figure 6.22: DME production using Feed 1 with a CO_2 recycle stream

The process shown in Figure 6.19 is depicted on the CHO diagram above (Figure 6.22). LFG is reacted with additional CO_2 and this gas burns in O_2 producing CO and H_2O. As the reaction goes to completion, it moves off the TBL and towards the exothermic region represented by point D. This reaction occurs at a low calorific value between 6 – 7MJ/m^3 and at a temperature lower than 900K hence no carbon deposition occurs. On the same point, some of the CO and H_2O react according to the water-gas shift reaction to form H_2 and CO_2. The H_2 produced

reacts with unreacted CO on the endothermic region (r_8) to produce DME and CO_2. The final reaction occurs at temperatures 1 100K and at calorific values greater than 11MJ/m^3.

In Figure 6.23 below, the process depicted in Figure 6.20 is shown. The initial reaction occurs on the TBL, between calorific values 10 and 11MJ/m^3. One can choose to operate the system at 900K, however slight carbon deposition may occur. An alternative may be to run the system at 1 000K. A bit of CO is allowed to react according to the water-gas shift reaction. This reaction occurs in the exothermic region (point D) and thus does not require energy input into the system. The syngas produced then reacts to form the desired product (DME) and CO_2. This reaction occurs out of the stoichiometric region and in the endothermic region. This means this would be an energy intensive process and fairly high temperatures about 1 100K would need to be used to operate the system. The overall processes shown in Figure 6.22 and 6.23 operate between the endothermic and exothermic region at both high and low calorific values.

The system shown in Figure 6.24 operates on the TBL on point F. LFG is mixed with H_2O and burned with O_2. This produces syngas and CO_2. Here, the system is operated at 1000K so that carbon deposition does not occur and has a calorific value 11MJ/m^3. If CO_2 is removed the system is forced out of the stoichiometric region to point G. Point G is in the endothermic region, hence energy would be required to drive the process to completion to form DME and H_2O.

Between these three processes, one would have to make a decision based on the following:

- The amount of energy inputted into the system;
- The operating temperatures and whether there is a chance of carbon deposition;
- Calorific values;
- Operating within the stoichiometric region; and
- Amount of carbon formed as compared to the desired product.

All three options vary slightly, however from the mass balances it can be seen that despite the process chosen, CO_2 will always be emitted to the atmosphere.

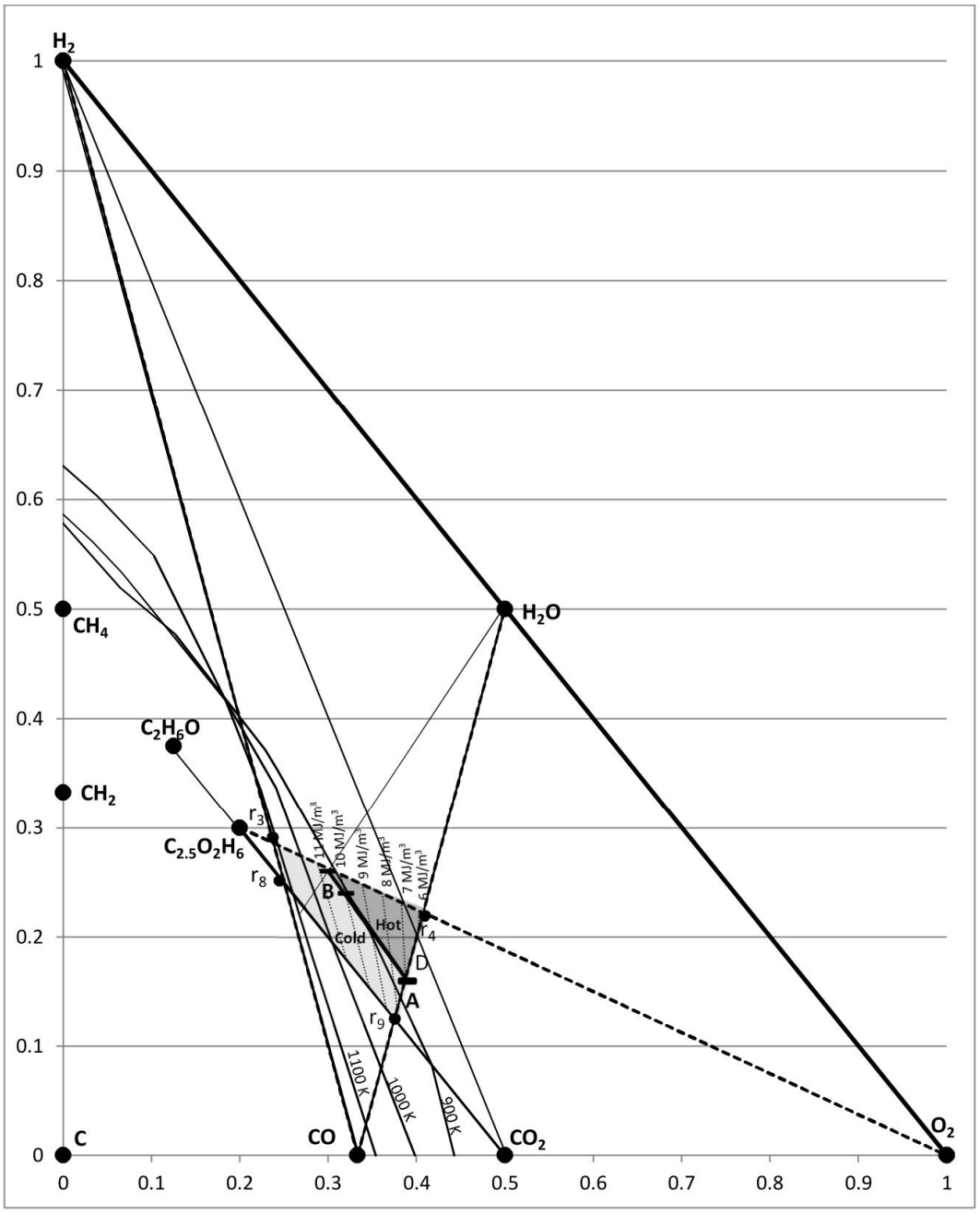


Figure 6.23: DME production using Feed 1 without a CO_2 recycle stream

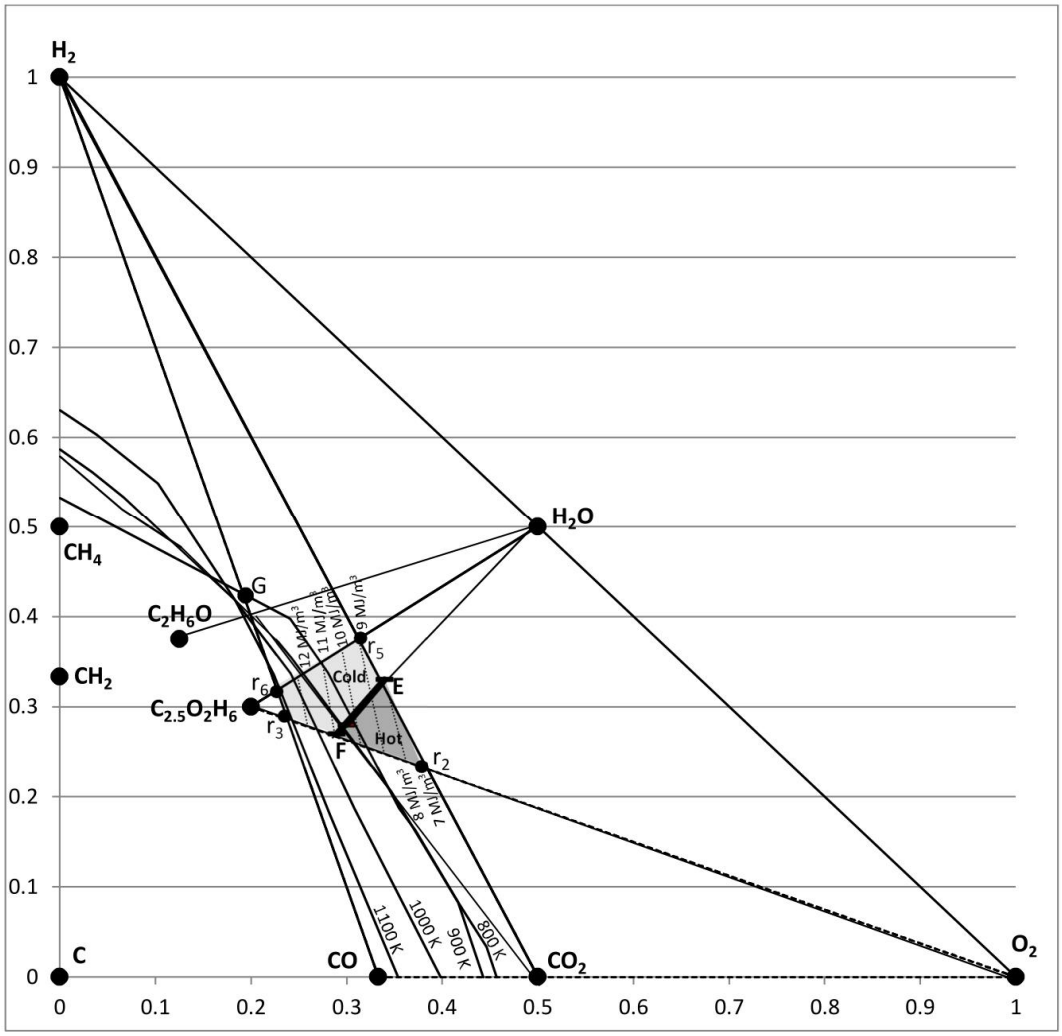


Figure 6.24: DME production using Feed 2

6.6 CO_2 Emission Free Processes

From the scenarios shown above, it can be seen that it is very difficult to eliminate CO_2 altogether from a process. Furthermore, if fuel is produced with CO_2 being minimized through production, one still needs to take into account emissions emitted once the fuel is used by consumers. In industry, certain chemicals are produced using CO_2 as a feedstock. These chemicals are not used as fuels, but merely used for cleaning purposes such as solvents, and other laboratory uses such as intermediates in chemical synthesis. If LFG is used with the objective of minimizing CO_2 whilst producing useful chemicals, it will give rise to a cleaner, more environmentally friendly chemical process.

6.6.1 Basic Flow Diagram

For Feed 1, two points on the TBL were used to develop a locus of which chemicals could be produced without producing CO_2. In order to produce the chemicals, CO_2 had to be introduced into the system. The points on the TBL used were as follows (as seen in Section 5.1 above):

$$A: \quad C_{2.5}O_2H_6 + 1.73\,CO_2 + 0.88\,O_2 \rightarrow 4.23\,CO + 3H_2O \qquad 0\ kJ/mol$$

$$B: \quad C_{2.5}O_2H_6 + 0.75\,O_2 \rightarrow 2.5\,CO + H_2O + 2H_2 \qquad 0\ kJ/mol$$

By combining the two equations and using Solver to resolve a value for the ratio α (similar to the calculation of calorific values – See Appendix C), a new equation was formed which represents one of the processes of producing one of the chemicals. If α is chosen to be 0.1, the equation will be as follows:

$$C_{2.5}O_2H_6 + 0.17\,CO_2 + 0.76\,O_2 \rightarrow 2.67\,CO + 1.20\,H_2O + 1.80\,H_2 \qquad 6.27$$

If H_2O is removed from the system, CO and H_2 can react to form the desired chemical without any production of CO_2 emissions. In this case the desired chemical is $CH_{1.44}O_{0.93}$. The process is represented in Figure 6.25 below.

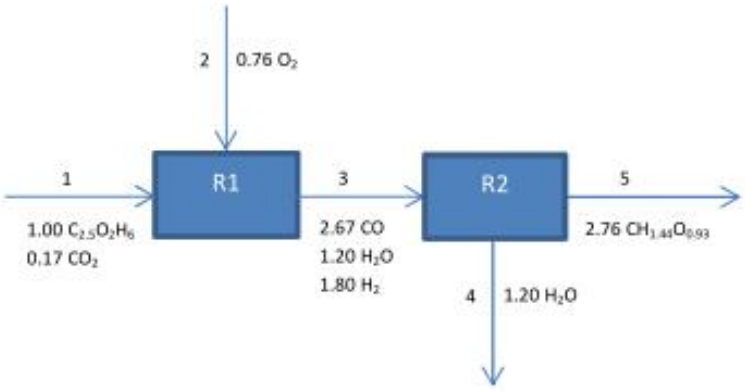


Figure 6.25: Production of chemicals with zero emissions – Feed 1

The process described in Figure 6.25 depicts a clean process, free of CO_2 emissions. The CO_2 produced is used as a feedstock together with LFG, hence

reducing the CO_2 emitted to the atmosphere from the landfill, as approximately 60% of landfill gas accounts for methane and 40% accounts for carbon dioxide.

A similar process was done for α = 0.5; 0.7 and 0.9 in order to obtain a range of different chemicals represented by the locus. The results can be seen in Table 6.1 below.

Table 6.1: Formation of zero emission locus

α	Equation	Chemical Product	Eq No.
0.5	$C_{2.5}O_2H_6 + 0.87\,CO_2 + 0.82\,O_2 \rightarrow 3.37\,CO + 2.00\,H_2O + 1.00\,H_2$	$CH_{0.80}O_{0.65}$	UU
0.7	$C_{2.5}O_2H_6 + 1.21\,CO_2 + 0.84\,O_2 \rightarrow 3.71\,CO + 2.40\,H_2O + 0.60\,H_2$	$CH_{0.48}O_{0.52}$	VV
0.9	$C_{2.5}O_2H_6 + 1.56\,CO_2 + 0.87\,O_2 \rightarrow 4.06\,CO + 2.80\,H_2O + 0.20\,H_2$	$CH_{0.16}O_{0.38}$	WW

The BE's were calculated for each product (refer to Appendix A for an illustration on calculating BE's). Once the BE's were calculated, it was plotted on the CHO diagram to represent a locus which is represented by line XY in Figure 6.28 below. This locus represents a range of chemicals which will use up, rather than produce CO_2 during production.

In the case of Feed 2, the TBL represented by line EF produces CO_2 as compared to using CO_2 as a reactant as seen with Feed 1. By using the water-gas shift reaction, the CO_2 can be removed from the system to produce a locus of syngas. Equations E and F represent the TBL for Feed 2 (see Section 5.1 above). The equations are as follows:

$$E: \quad C_{2.5}O_2H_6 + 1.90\,H_2O + 0.55\,O_2 \rightarrow 2.5\,CO_2 + 4.90\,H_2 \qquad 0\ kJ/mol$$

$$F: \quad C_{2.5}O_2H_6 + 0.68\,O_2 \rightarrow 1.64\,CO + 0.86\,CO_2 + 3\,H_2 \qquad 0\ kJ/mol$$

Line EF is taken as a straight line as the deviance between the points E and F is relatively small (approximately 0.0020), therefore by using point E, a process can be developed to produce a locus of syngas with zero CO_2 emissions. The process can be seen in Figure 6.26 below.

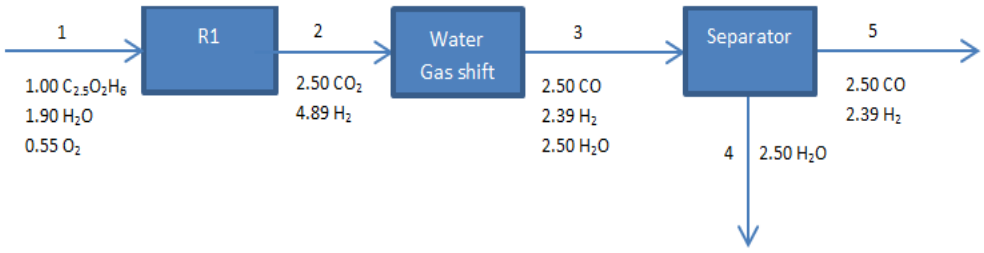


Figure 6.26: Production of synfuels with zero emissions – Feed 2

From Figure 6.26 it can be seen that LFG reacts with H_2O and O_2 to produce CO_2 and H_2. To eliminate the CO_2, the water-gas shift reaction is used and is represented by Equation 6.28 below. This reaction produces CO and H_2O.

$$2.50\,CO_2 + 2.50\,H_2 \rightarrow 2.50\,CO + 2.50\,H_2O \qquad 6.28$$

Syngas is the main product formed if the H_2O is removed from the process. If point F on the TBL line is used, the same amount of syngas is formed as line EF is a straight line.

In order to form a locus on which syngas can be produced, equation r_2 was used as this marks the end point of the hot side of the stoichiometric region. Equation r_2 is given as follows (Section 4.4.1):

$$r_2: C_{2.5}O_2H_6 + 1.5\,O_2 \rightarrow 3\,H_2 + 2.5\,CO_2 \qquad -464.4\,kJ/mol$$

When using reaction r_2 to form syngas from Feed 2, the mass balance is as shown in Figure 6.27 below.

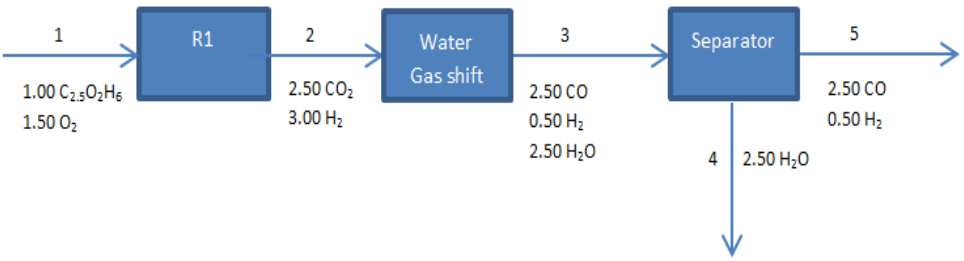


Figure 6.27: Production of synfuels with zero emissions – Feed 2 (r_2)

The mass balance shown in Figure 6.27 is similar to the one shown in Figure 6.26, except it gives a different ratio of CO:H_2. This enables one to operate a process along the locus ST (Figure 6.29) to produce ratios of CO:H_2 from 2.50:2.39 to 2.50:0.50 for the TBL (line EF) and r_2 respectively.

6.6.2 Chemical Generation depicted on the CHO diagram

Figure 6.28 represents the locus of chemicals that can be found with zero CO_2 emissions. The chemicals at this stage are unknown and therefore tests will need to be conducted to establish the chemicals produced.

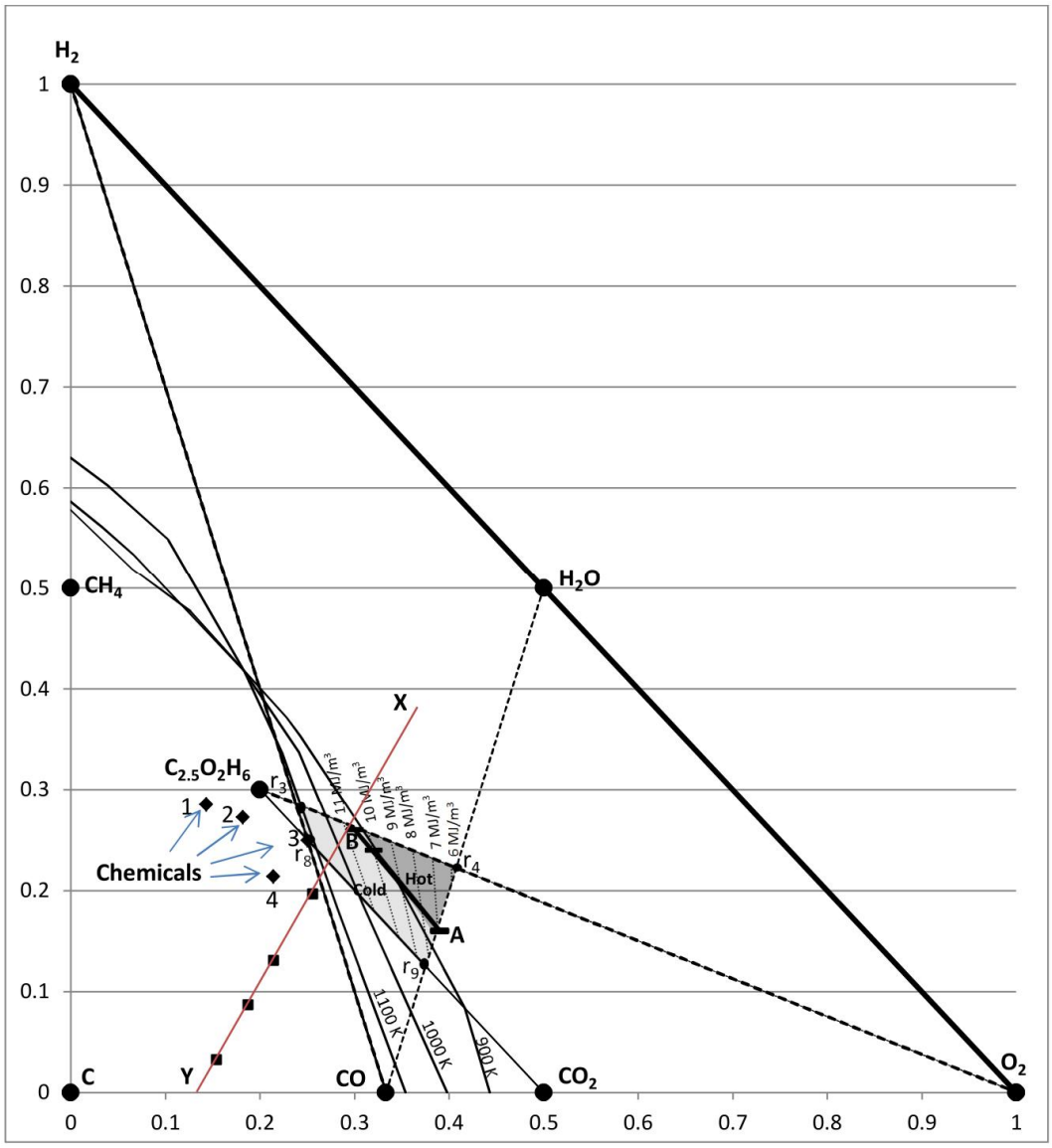


Figure 6.28: CHO diagram for Feed 1 – representing locus of chemicals

From Figure 6.28 it can be seen that LFG can be reacted with O_2 until it reaches the TBL at point B. At this point, syngas (H_2 and CO) and water is produced. If water is removed at point B, it will force the reaction towards point Y. Line XY, as described above represents all chemicals which use up CO_2 during their production, hence producing zero carbon emissions during the process. Anywhere on line XY, chemicals of this nature can be produced, depending on how much water is removed from the system. The more water removed from the system, the closer to Y the chemicals will exist whilst the less water removed from the system, the chemicals will emerge closer to X.

Chemicals produced to the left of the locus as in the case of chemicals 1, 2, 3 and 4, are said to export CO_2 during its production phase. These chemicals come in the form of ethyl acetate, methyl acetate, acetic acid and acetic anhydride respectively. Moving towards the locus from chemicals 1, 2, 3 and 4 will bring the process closer to the locus and closer to the point of zero emissions. Chemicals produced to the right of the locus import CO_2 during its formation, hence cleaner production. Due to this reason, chemicals to the right of the locus will require additional CO_2 than what LFG can supply depending on how close to the locus the chemical produced exists. A process such as this, producing chemicals which import CO_2, can be constructed near a plant which creates large amounts of CO_2 emissions as in the case of the petroleum and electricity generation industries, as it could use the emissions from these outside processes as a feedstock, thereby reducing overall emissions for both parties involved.

The same applies for Feed 2. As can be seen in Figure 6.25, the locus is represented by line ST. The TBL shown as line EF is taken as a straight line as the deviance between the points D and F is relatively small (approximately 0.002). As can be seen from Equation E above, the reaction which occurs at point E produces CO_2 and H_2. If the CO_2 is reacted according to the water-gas shift reaction shown by Equation 6.28, CO and H_2O are formed. When H_2O is removed from the system (arrow moving from E to S), it forces the system to point S. At point S, all CO_2 produced from Equation E is used up, therefore leading to zero CO_2 emissions. Due to line EF being a straight line, the same concept would apply to point F, and the system would be forced to point S. When Equation r_2 is considered, H_2 and CO_2 are again produced, but this time at point r_2. The CO_2 and H_2 are once again reacted according to the water-gas shift reaction to produce CO and H_2O. By removing H_2O from the system (arrow moving from r_2 to T), the system is forced to point T. At point T, all CO_2 produced from Equation r_2 is used up, therefore leading to zero CO_2 emissions. Line ST is representative of a locus of syngas. Anywhere on this line, syngas of different ratios of H_2:CO can be produced with zero CO_2 emissions. The shaded region EFL is the stoichiometric region and is the optimal region of operation as any reaction occurring in that region would be exothermic (represented by point H) and would require less

energy for the process to occur. Reactions to the left of the TBL will be endothermic reactions as this is the cold side (point C) and therefore would require an energy intensive process for the reactions to occur. Furthermore, any process occurring within the stoichiometric region can be forced to the locus ST and therefore would be able to produce syngas with zero emissions if H_2O is removed.

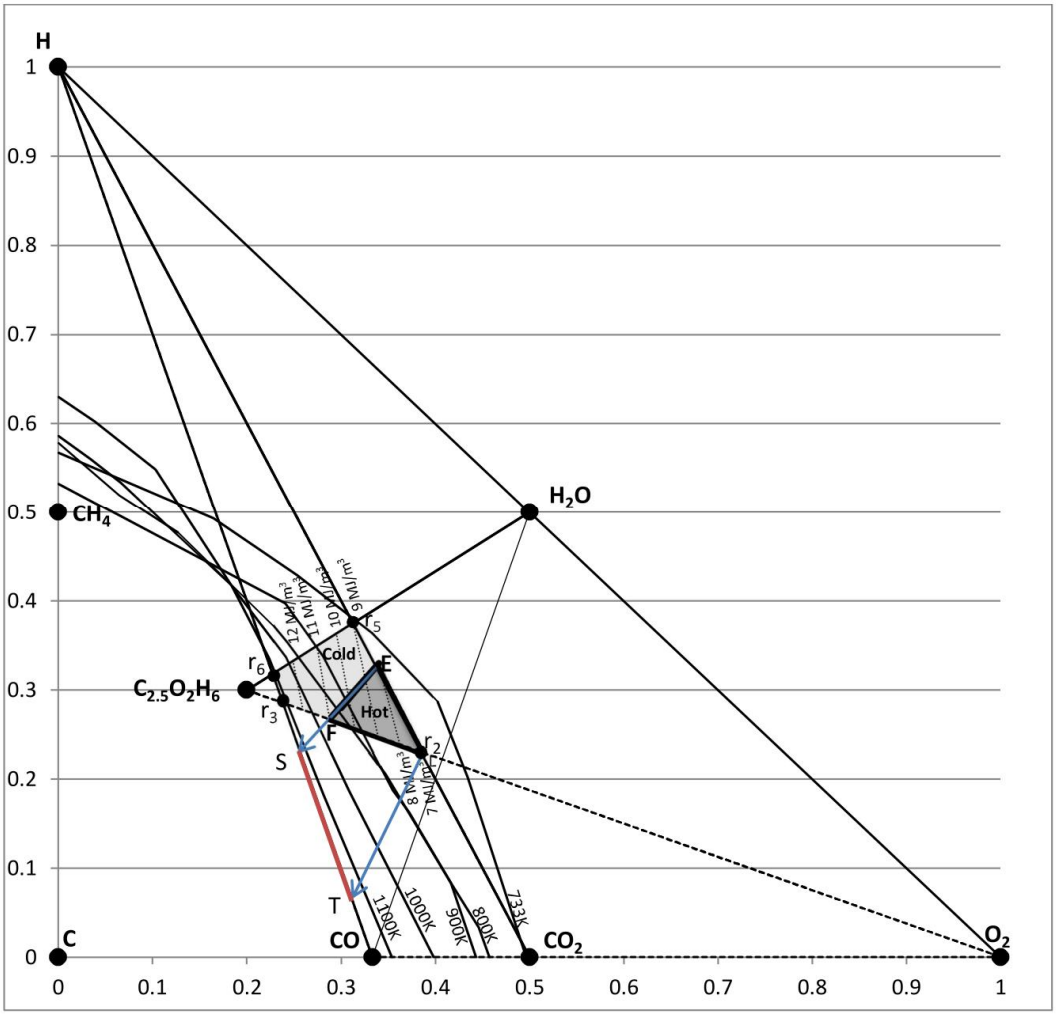


Figure 6.29: CHO diagram for Feed 2 – representing locus of syngas

The processes described above thus gives a region of operation which is exothermic, hence requiring less energy for the process to go to completion, no carbon deposition expected as the process can operate close the carbon boundary and a locus is established allowing an array of chemicals and syngas of different ratios to be produced, thus allowing for flexibility in operating conditions.

7 Conclusions

The processes outlined within this dissertation are a development of a graphical technique that allows various technologies to be developed with syngas production as an intermediate step. The graphical technique considers:

- A mass balance to determine the stoichiometric region for syngas production;
- The energy balance limits the stoichiometric region to a line which corresponds to autothermal operation;
- Carbon boundaries and corresponding temperatures are considered in order to identify further restrictions on the stoichiometric region; and
- Contours of HHV enable a systematic approach to identify regions to obtain high calorific value syngas.

Electricity generation, methane production for natural gas, synfuels, DME and CO_2 emission free processes were evaluated on the CHO diagram in order to assess the most desirable region for operation to take place as well as to consider the environmental impacts associated with each process. The conclusion for each scenario is given below.

Electricity

Electricity generation would be the easiest process to follow as the technology already exists for such a process and many projects are currently in place around the world which converts LFG into electricity. This process however only has a 35% conversion of energy into electricity if conventional technologies such as internal combustion engines are used and produces large amounts of CO_2 emissions. Electricity production is highly exothermic; hence no energy is required to drive the reaction to completion. The system can occur on the TBL where it is adiabatic by using Feed 1, however CO_2 is required in the feed stream and this is introduced by means of a recycle stream as seen in Figure 6.2. By using Feed 2 as seen in Figure 6.3, the initial reaction also occurs on the TBL. The calorific values for Feed 1 and 2 are 7 and 11MJ/m^3 respectively. Electricity can also be produced using an SOFC. The amount of CO_2 produced when dry

reforming is used is less than half the amount produced using an internal combustion engine. This SOFC process on its own occurs out of the stoichiometric region and is highly exothermic. By using Feed 2, the SOFC process begins on the TBL at point E which is adiabatic. At this point the calorific value is between 8 – 9MJ/m^3. Although this process yields the same amount of CO_2 as electricity generation through an internal combustion engine, the SOFC has an efficiency of approximately 70% as compared to an internal combustion engine. The SOFC process does not fall within the stoichiometric region and the carbon boundaries defined, however no carbon will deposit on the anodes if the gas is stripped from all impurities (Ye et al., 2010 and Lorente et al., 2012) and therefore hydrocarbons and landfill gas can be transformed into useful energy. It is important to note that the overall process for electricity production through an SOFC will still remain at the combustion point represented by point CE and therefore all electricity processes would yield the same amount of CO_2 emissions despite the technology used.

Electro-catalytic reduction of CO_2

Methane rich gas can be produced from CO_2 by reacting it with either H_2 or H_2O. Three processes were considered in this dissertation, namely the electro-catalytic reduction of CO_2 with H_2O (Figure 6.8), electro-catalytic reduction of CO_2 with H_2 (Figure 6.9) and the Sabatier reaction (Figure 6.10). All three processes aim to convert excess CO_2 into methane; therefore there are no CO_2 emissions. The Sabatier reaction may be expensive as a large amount of H_2 is required in the feed.

By using Feed 1, all three reactions occur out of the stoichiometric region in the exothermic region. These reactions may be carried out at low temperatures; however none of the reactions occur within the stoichiometric boundary and hence are not considered favourable.

By introducing Feed 2, the electro-catalytic reduction of CO_2 with H_2 occurs on the TBL. This process is adiabatic and has a calorific value between 8 – 9MJ/m^3.

By operating at 800K, no deposition of carbon would form. Although this option may be feasible, one needs to account for increased costs involved for catalysts and electrodes used in the process. The reaction also uses pure hydrogen and this further increases the cost as hydrogen first needs to be separated from the LFG through methane dry reforming as explained by Olah et al., 2009. Pure H_2 gas could also be purchased although there would be cost implications as H_2 is quite expensive.

Production of Synfuels

The production of synfuels was analysed using different processes. By using Feed 1 (Figure 6.13), the process is operated on the TBL and 41% of CO_2 is emitted to the atmosphere as compared to 59% of the desired product. The calorific value for this process is approximately 9.5MJ/m^3 and in order for no carbon deposition to occur, the system must operate at 900K.

Two scenarios are seen when Feed 2 is introduced (Figure 6.14 and 6.15). The system represented in Figure 6.14 occurs on the TBL with a calorific value of 11MJ/m^3 and the CO_2 emitted to the atmosphere is 24% compared to 39% of synfuel produced. The second scenario (Figure 6.15) does not occur on the TBL and is highly energy intensive. The CO_2 emitted is 25% as compared to 38% of synfuel.

Each scenario depicted indicates that an amount of energy will need to be inputted for the reaction to go to completion. The amount of energy required is unknown for now. Figure 6.18 however will be the most energy intensive process as the entire process does not occur on the TBL. Although both Figures 6.16 and 6.17 occur on the TBL at 900K, Figure 6.16 has a lower calorific value as compared to Figure 6.17; hence the conversion to useful fuels would not be as high as the scenario depicted in Figure 6.17. A case study would have to be done in order to analyse the amount of energy required for both processes to reach completion.

One would need to assess the benefits of greener production versus the costs of energy intensive processes.

Production of DME

The production of DME using Feed 1 and 2 was also analysed. Two processes exist for Feed 1 and are represented by Figure 6.19 and 6.20. Both reactions occur on the TBL, however the process represented in Figure 6.19 emits 41% CO_2 compared to 26% of the DME and the process seen in Figure 6.20 emits 40% CO_2 compared to 30% DME. Figure 6.19 has a calorific value between 6 – 7MJ/m^3 and Figure 6.20 between 10 and 11MJ/m^3.

A third scenario exists with Feed 2 which also occurs on the TBL and has a calorific value of 11MJ/m^3. The CO_2 emitted to the atmosphere is 39% as compared to 32% of the desired product.

Although DME is seen as an excellent fuel source due to its high cetane value and can be easily stored and transported, the processes represented for DME production above produce more emissions than the desired product and this is not seen as an attractive process from an environmental point of view. One would also have to consider the amount of energy inputted into the system, operating temperatures, whether there is a chance of carbon deposition, operating within the stoichiometric region and cost implications.

CO_2 Emission Free Processes

CO_2 emission free processes introduces' a concept where CO_2 produced through operations can be fed into a system as feedstock to produce useful chemicals and syngas, emitting zero or minimal CO_2 emissions. This concept enables a locus to be formed allowing a range of chemicals and syngas to be produced using different operating conditions.

When producing chemicals using Feed 1, chemicals to the left of the locus, in the case of chemicals 1, 2, 3 and 4, are said to export CO_2 during its production phase. Moving towards the locus will bring the process closer to the locus to form cleaner chemicals and closer to the point of zero emissions. Chemicals produced to the right of the locus import CO_2 during its formation, hence cleaner production. Due to this reason, chemicals to the right of the locus will require additional CO_2 than what LFG can supply depending on how close to the locus the chemical formed exists. Processes such as these can be constructed close to plants emitting high volumes of CO_2, thereby reducing overall emissions for both parties involved.

By using Feed 2, a range of syngas can be produced instead of chemicals. If the process occurs on the TBL, CO_2 is produced, however by using the water-gas shift reaction CO_2 is converted into CO and the excess H_2 forms syngas with the CO. Reaction r_2 is also used to create a locus ST on which a range of syngas can be produced. By using r_2, a stoichiometric region of operation is established which is exothermic and operation within this area allows for optimal process results.

The results for each process mentioned above is summarised in Table 7.1.

Table 7.1: Summary of Results

Scenarios		CO_2/ mol LFG	CH_4/ mol LFG	CH_2/ mol LFG	DME/ mol LFG	Chemicals / mol LFG	Syngas/ mol LFG
Combustion		2.50	-	-	-	-	-
Electro-catalytic reduction of CO_2[1]	Feed 2 - Using H_2	0	1..00	-	-	-	-
Synfuel	Feed 1	1.03	-	1.48	-	-	-

[1] This refers to Feed 2 only as results obtained with Feed 1 occurred out of the stoichiometric region and is therefore seen as unfavourable.

Scenarios		CO_2/ mol LFG	CH_4/ mol LFG	CH_2/ mol LFG	DME/ mol LFG	Chemicals / mol LFG	Syngas/ mol LFG
	Feed 2 - H_2O recycle	0.95	-	1.55	-	-	-
	Feed 2 - no recycle	0.40	-	0.60	-	-	-
DME	Feed 1 - CO_2 recycle	1.10	-	-	0.71	-	-
	Feed 1 - no recycle	1.00	-	-	0.75	-	-
	Feed 2	0.95	-	-	0.78	-	-
CO_2 Emission Free Processes	Feed 1 – Chemical production	<0.93 ≈0	-	-	-	α: 0.1 – 0.9 = 2.76 – 4.06	
	Feed 2 – syngas	0	-	-	-	-	$CO:H_2$ = 2.50:2.39-2.50:0.50

The amount of CO_2/ mol LFG shown in Table 7.1 is the amount that is emitted to the atmosphere and does not account for the overall generation of CO_2 within the system or the amount that is recycled. A comparison suggests that despite electricity generation being simpler, the process emits the highest amount of CO_2 and only 20 – 35 % or 70% of the initial LFG goes to useful electricity depending on the technology used (internal combustion engine versus SOFC respectively). The rest is lost as heat. The fuels producing processes (CH_2 and DME) utilise most of the LFG to form products and lower CO_2 emissions are achieved,

although extra processing is required and is not considered within this dissertation. The production of chemicals or syngas through zero CO_2 emission processes, produces zero or very little CO_2 as compared to the other processes and do not require energy intensive steps in order for the process to go to completion.

In order to choose the best process, energy balances would need to be done on each process and on each piece of equipment in order to determine the energy losses from the system and to determine how much energy is actually converted into useful sources of energy. Wasted heat from the process can be used to drive the turbines which generate electricity. Decisions should also be made on costs and long term benefits.

This work develops a systematic graphical technique that enables the study of possible conversion processes and flow sheets utilising LFG, although the effect of equilibrium has not been considered on the comparisons obtained. Furthermore, from this analysis it is shown that there are more possibilities of LFG usage for chemicals and fuel production in addition to traditional electricity generation.

REFERENCES

1. Ajhar, M., Travesset, M., Yüce, C. and Melin, T., 2010. *Siloxane Removal from landfill and digester gas – A technology overview.* Bioresource Technology Vol 101 pp 2913-2923
2. Battaerd, H. A. J. and Evans, D. G., 1979. *An Alternative Representation of Coal Composition Data.* Fuel, Vol 58, pp. 105 – 108.
3. Berger, S. and Mann, J., 2001. *Landfill gas Primer- An overview for environmental health professionals,* [Online]. Available at: http://www.atsdr.cdc.gov/hac/landfill/html/ intro.html. [Accessed on 06 June 2011], pp. 3-14.
4. Bove, R. and Lunghi, P., 2005. *Electric Power generation from landfill gas using traditional and innovative technologies.* Energy Conservation and Management Vol 47 pp 1391-1401
5. Broers, G.H.J. and Treijtel, B.W., 1965. *Carbon deposition boundaries and other constant parameter curves, in the triangle representation of C-H-O equilibria, with applications to fuel cells.* Adv. Energy Conv., Vol 5 (4). pp 365 – 382.
6. Brooks, K. P., Hu, J., Zhu, H., and Kee, R. J., 2006. *Methanation of carbon dioxide by hydrogen reduction using the Sabatier process in microchannel reactors.* Pacific Northwest National Laboratories, Richland, WA, USA, 99352, Vol 62. pp 1161 – 1170.
7. Centi, G. and Perathoner, S. 2009. *Opportunities and prospects in the chemical recycling of carbon dioxide to fuels.* Catalysis Today Vol 148. pp. 191-205.
8. Conestoga-Rovers and Associates (CRA), n.d. *Part 1: Understanding the Landfill gas Resource and Potential Applications*. Handbook for the Preparation of Landfill Gas to Energy Projects. [Online]. Available at: http://www.bvsde.paho.org/ bvsacd/cd51/preparation/part1.pdf. [Accessed on 21 March 2013].

9. Deed, C., Gronow, J., Rosevear, A., Braithwaite, P., Smith, R. and Stanley P., 2004. *Guidance on gas treatment technologies for landfill gas engines.* Environment Agency, Almondsbury, Briston, BS32 4UD, pp 1-67.
10. Desrosiers, R., 1979. *Thermodynamics of gas-char reactions.* T. B. Reed (Ed.), *A survey of biomass gasification.* Colorado: Solar Energy Research Institute.
11. Dey, G. R., Belapurkar, A. D. and Kishore, K., 2004. *Photo-catalytic reduction of carbon dioxide to methane using T_2O_2 as suspension in water.* Journal of Photochemistry and Photobiology A: Chemistry Vol 163 pp 503-508
12. Environ Holdings, 2012. *The Clean Development Mechanism (CDM) Project Cycle,* [Online]. Available at: *http://www.carbonventures.com/services/article.php?list=The%20Clean%20Development%20Mechanism%20(CDM)%20Project%20Cycleandid=4479andlink=The%20Clean%20Development%20Mechanism%20(CDM)%20Project%20Cycle.* [Accessed 14 May 2012].
13. Finocchio, E., Montanari, T., Garuti, G., Pistarino, C., Federici, F., Cugino, M. and Busca, G., 2009. *Purification of biogas from siloxanes by adsorption: on the regenerability of activated carbon sorbents.* Energy Fuels, Vol 23. pp. 4156-4159.
14. Greenman, J., Gálvez, A., Giusti, L. and Ieropoulos, I., 2009. *Electricity from Landfill Leachate using Microbial Fuel Cells: Comparison with a biological Aerated Filter.* Enzyme and Microbial Technology, Vol 44, pp. 112 – 119.
15. Gruber, G. and Princeton, N. J., n.d. *Equilibrium Considerations in the Methane Synthesis System.* FMC Corp, Vol 146, pp 118.
16. Gür, T. M., Wise, H., and Huggins, R. A., 1990. *Electrocatalytic Conversion of Carbon Dioxide to Methane and Oxygen with an Oxygen Ion-Conduction Electrolyte.* Department of Materials Science and Engineering, Stanford University, Stanford, California 94305, Vol 129, pp 216 – 224.

17. Haarstad, K., Bergersen, O., SØrheim, R. and Berg, B., 2003. *Sorted MSW landfill odour due to H_2S – sources and removal*. Margherita di Pula, S. (E.d), Proceedings Sardinia 2003, Ninth International Waste Management and Landfill Symposium. Cagliari, Italy.
18. Haga, K., Adachi, S., Shiratori, Y., Itoh, K. and Sasaki, K., 2008. *Poisoning of SOFC anodes by various fuel impurities.* Solid State Ionics Vol 179. pp. 1427-1431.
19. Hongguang, W. 2006. *Biomass energy development welcoming bright prospects*. [Online]. Available at: http://en.ce.cn/Insight/200703/02/t20070302_10560407.shtml [accessed on 9th September 2009].
20. Interwaste Environmental Solutions, 2010. *Interwaste product information sheet: Landfill Gas Operation*, [Online]. Available at: http://www.interwaste.co.za/contents__files/gas.1.2010.pdf. [Accessed 02 August 2011]
21. Iyumi, Y., 2010. *Recent advances in the photo catalytic conversion of carbon dioxide to fuels with water and/or hydrogen using solar energy and beyond.* Coordination Chemistry Reviews, Vol 257, pp 171 – 186.
22. Kauchali, S., 2012. *Analysis of Biomass Gasification Processes.* Gasification Technology and Research Group, School of Chemical and Metallurgical Engineering, University of the Witwatersrand, Johannesburg.
23. Kee, R.J., Zhu, H. and Goodwin, D.G., 2004. *Solid – Oxide Fuel Cells (SOFC) with hydrocarbon and hydrocarbon derived fuels.* California Institute of Technology and Colorado School of Mines, USA, pp 1 – 45.
24. Kennema, M. O., 2014. *Analysis of Reactions in Carbon Deposition in Dry Reforming of Methane over an Unsupported Ni Catalyst.* A Thesis presented to the University of Guelph, Masters of Science in Chemistry. Pp 1 – 87.
25. Koch, T., 2001. *Landfill Gas Extraction and Utilization in China potential technology*, [Online]. Available at:

http://www.erec.org/fileadmin/erec_docs/Projcet_Documents /RES_in_China/Kochbxl.pdf. [Accessed on 21 May 2011].

26. Last, S., 2009. *Landfill Gas Opportunities and Hazards.* [Online] IPPTS Associates. Available at: http://www.landfill-gas.com. [Accessed on 11 August 2011].
27. Last, S., 2009. *Landfill gas Opportunities and Hazards: Six articles about landfill gas.* IPPTS Associates, [Online]. Available at: www.landfill-gas.com. [Accessed 18 September 2011].
28. Lee, S., Xu, Q., Booth, M., Townsend, T. G., Chadik, P. and Bitton, G., 2006. *Reduced sulphur compounds in gas from construction and demolition debris landfills.* Waste Management Vol 26. pp. 526-533.
29. Li, X., Grace, J. R., Watkinson, A. P., Jim, C. J. and Ergüdenler, A., 2001. *Equilibrium modelling of gasification: A free energy minimisation approach and its application to a circulating fluidized bed coal gasifier.* Fuel, Vol 80, pp195 – 207.
30. Li, X.T., Grace, J.R., Lim, C.J., Watkinson, A.P., Chen, H.P. and Kim J.R., 2004. *Biomass Gasification in a circulating Fluidised Bed.* Biomass and Bioenergy, Vol 26, pp. 171 – 193.
31. Lisk, D. J., 1991. *Environmental effects of Landfills.* The Science of the Total Environment, Vol 100, pp 415 – 468.
32. Lorente, E., Millan, M. and Brandon, N.P., 2012. *Use of Gasification Syngas in SOFC: Impact of real Tar on Anode Materials.* International Journal of Hydrogen Energy, Vol 37, pp. 7271- 7278.
33. Lyndon B., 2008. *Electocatalytic Reduction of Carbon Dioxide to Methane.* Johnson Space Centre, [Online]. Available at: http://www.techbriefs.com/component/content /article/3449, [Accessed 28 July 2011].
34. Malik, V. A., Lerna, S. L. and MacLean, D. L., 1987. *Electricity, methane and liquid carbon dioxide production from landfill gas.* Gas Separation and Purification Vol 1 pp 77-83
35. Minh, N.Q., 2004. *Solid Oxide Fuel Cell Technology – Features and Applications.* Solid State Ionics, Vol 174, pp. 271 – 277.

36. Olah, G.A., Goeppert, A. and Prakash, G. K. S., 2009. *Chemical Recycling of Carbon Dioxide to Methanol and Dimethyl Ether: From Greenhouse Gas to renewable, Environmentally Carbon Neutral Fuel and Synthetic Hydrocarbon,* American Chemical Society, Vol 74, No. 2.
37. Panza, D. and Belgiorno, V., 2010. *Hydrogen sulphide removal from landfill gas.* Process Safety and Environmental Protection Vol 88. pp. 420-424.
38. Pilarczyk, E., Henning, K. D., Knoblauch, K. and Bergbau-Forschung GmbH, 1987. *Natural Gas from Landfill Gases.* Resources and Conservation, Vol 14, pp 283-294.
39. Prins, M. J., Ptasinski, K. J. and Janssen, F. J. J. G., 2003. *Thermodynamics of gas-char reactions: first and second law analysis.* Chemical Engineering Science, Vol 58, pp 1003 – 1011.
40. Reinhart, D. R., Townsend, T., 2002. *Control of odours from Constricted and Demolition Debris Landfills.* Project proposal. University of Central Florida.
41. Roberts, A., Brooks, R., Shipway, P., Gilchrist, R. 2014. *Reducing Energy Losses from Automotive Engine Lubricants by Thermal Isolation of the Engine Mass.* SAE Technical Paper 2014-01-0672.
42. Robson, G., 2004. *The history and development of bioethanol as an alternative fuel,* Biotechnology (Enterprise).
43. Schultz, K., Bogart, L., Besenbruch, G., Brown, L., Buckingham. R., Campbell, M., Russ, B. and Wong, B., n.d. *Hydrogen and Synthetic hydrocarbon fuels – A Natural Synergy*. General Atomics. [Online]. Available at: http://bioage.typepad.com /greencarcongress/docs/HydrogenSynfuel.pdf. [Accessed on 21 March 2013].
44. Stearns, R. P., Wright, T. D., and Stirrat, B. A., 1984. *Landfill Gas Recovery and Utilization at Industry Hills, California.* Waste Management and Research, Vol 2, pp 153 – 161.
45. Strachan, L.J., Wright M., Pass, J., Couth, B. and Broomfield, M., 2005. *Realising Landfill Gas Potential for Climate Change and renewable*

energy goals, [Online] Landfill conservancies. Available at: http://**landfill**conservancies.com/docs/strachan_paper_ **landfill**_ 2005.pdf [Accessed 22 May 2011]

46. Swanepoel, D. H. 2009. *Capacity Expansion Management of Landfill Gas Extraction Projects.* BEng final year project, Dept. of Industrial and Systems Engineering, University of Pretoria, South Africa.
47. Tay, D. H. S., Ng, D. K. S., Kheireddine, H. and El-Halwagi. M. M., 2011. *Synthesis of an Integrated Biorefinery via the C-H-O ternary diagram.* Clean Techn Environ Policy, Vol 13, pp 567-579.
48. Theeboom, E. and Nontangane, M., 2010. *Landfill Gas Flux Emissions Modelling and Air Quality – An overview using the recent Coastal Park Landfill Air Quality Assessment as a case study.* 2010 NACA conference, Polokwane.
49. Themelis, N. J. and Ulloa, P. A., 2006. *Methane generation in Landfill.* Renewable Energy Vol 32 pp 1243-1257
50. U.S. EPA LMOP. *LFG Energy Project Development Handbook*, [Online]. Available at: http://epa.gov/lmop/publications-tools/handbook.html. [Accessed 23 March 2011]
51. Uhrig, R. E., Schultz, K. R. and Bogart, S. L., 2007. *Implementing the "Hydrogen Economy" with Synfuel.* The Bent of Tau Beta Pi. [Online]. Available at: http://www.tbp.org/pubs/Features/Su07Uhrig.pdf. [Accessed on 21 March 2013].
52. United Nations Framework Convention on Climate Change, 2012. *Clean Development Mechanism (CDM)*, [Online]. Available at: *http://unfccc.int/kyoto_protocol/ mechanisms/clean_development_mechanism/items/2718.php* [Accessed 14 May 2012]
53. Urban, W., Lohmann, H. and Gomez, J.I.S., 2009. *Catalytically upgraded landfill gas as a cost-effective alternative for fuel cells.* Journal of Power Sources Vol 193. pp. 359-366.

54. Wei, J., 1979. *A Stoichiometric Analysis of Coal Gasification*. Industrial and Engineering Chemistry Process Design and Development, Vol 3, pp 554-558.
55. Weyant, J. P., Hill, J., Manne, A. S. andRichels, R., 1999. *The Cost of the Kyoto Protocol*. The Energy Journal (Special Issue).
56. WSP, 2009. *Background information document: Environmental Impact Assessment Process for the Proposed landfill Gas Utilisation Plant on the exiting Marie Louise Landfill Site on Dobsonville Road in Roodepoort, Gauteng*, [Online]. Available at: http://www.google.co.za/url?url=http://www.privateprojects.co.za/Global/DocumentUpload/DownloadDocument.aspx%3FdocumentID%3D32andrct=jandsa=Uandei=1G-ETr3xKue50QXetJkBandved=0CA4QFjAAandq=Background+information+document:+Environmental+Impact+Assessment+Process+for+the+Proposed+landfill+Gas+Utilisation+Plant+on+the+exiting+Marie+Louise+Landfill+Site+on+Dobsonville+Road+in+Roodepoort,+Gautengandusg=AFQjCNF2kd38mdImcRvWoXAEGA4porMUmA [Accessed 02 August 2011]
57. XE, 2005. *The World's Favourite Currency Site*, [Online]. Available at: *http://www.xe.com/ucc/convert/?Amount=1andFrom=ZARandTo=USD.* [Accessed 14 May 2012].
58. Xebec Adsorption Inc., 2007. *Treatment solutions for Landfill Gas Fuel Applications*, [Online]. Available at: http://www.xebecinc.com/pdf/e_white_paper.pdf. [Accessed on 05 April 2012].
59. Yasyerli, S., Filizgok, S., Arbag, H., Yasyerli, N., Dogu, G., 2011. *Ru incorporated Ni-MCM-41 mesoporous catalysts for dry reforming of methane: Effects of Mg addition, feed composition and temperature.* International Journal of Hydrogen Energy, Vol 36, pp. 4863-4874.
60. Ye, X., Wang, S.R., Zhou, J., Zeng, F.R., Nie, H.W. and Wen T.L., 2010. *Assessment of the Performance of Ni-yttria-stabilized Zirconia Anodes in*

Anode-supported Solid Oxide Fuel Cells operating on H_2 – CO Syngas Fuels. Journal of Power Sources, Vol 195, pp. 7264 – 7267.

61. Yotaro, O., Masahiro, Y., Tsutomu, S., Osamu, I., Takashi, O. and Norio, I., 2006. *New Direct Synthesis Technology for DME (Dimethyl Ether) and Its Application Technology.* JFE Technical Report No. 8. pp. 34 – 40.

Appendix A – Representation of CHO Diagrams

Bond Equivalent (BE) percentages are represented by molar percentages by multiplying the mole fraction of the main constituents C, O_2 and H_2 by their valent electrons 4, 2 and 1 respectively as shown by Li et al., 2001 and, Prins, 2003. The following equations are used to represent C, O_2 and H_2 as BE percentages:

$$C = \frac{4x_C}{4x_C + x_{H_2} + 2x_{O_2}} \quad \text{A1}$$

$$O = \frac{2x_{O_2}}{4x_C + x_{H_2} + +2x_{O_2}} \quad \text{A2}$$

$$H = \frac{x_{H_2}}{4x_C + x_{H_2} + +2x_{O_2}} \quad \text{A3}$$

In the case of elemental C, O_2 and H_2, the BE percentages are as follows:

$$C = \frac{4x_C}{4x_C + x_{H_2} + 2x_{O_2}} = \frac{4\times1}{(4\times1)+(1\times0)+(2\times0)} = \frac{4}{4} = 1$$

$$O = \frac{2x_{O_2}}{4x_C + x_{H_2} + +2x_{O_2}} = \frac{2\times1}{(4\times0)+(1\times0)+(2\times1)} = \frac{2}{2} = 1$$

$$H = \frac{x_{H_2}}{4x_C + x_{H_2} + +2x_{O_2}} = \frac{1\times1}{(4\times0)+(1\times1)+(2\times0)} = \frac{1}{1} = 1$$

The three elements are all found to be 1, hence the points C, O_2 and H_2 are found at the corners of the CHO diagram as seen below.

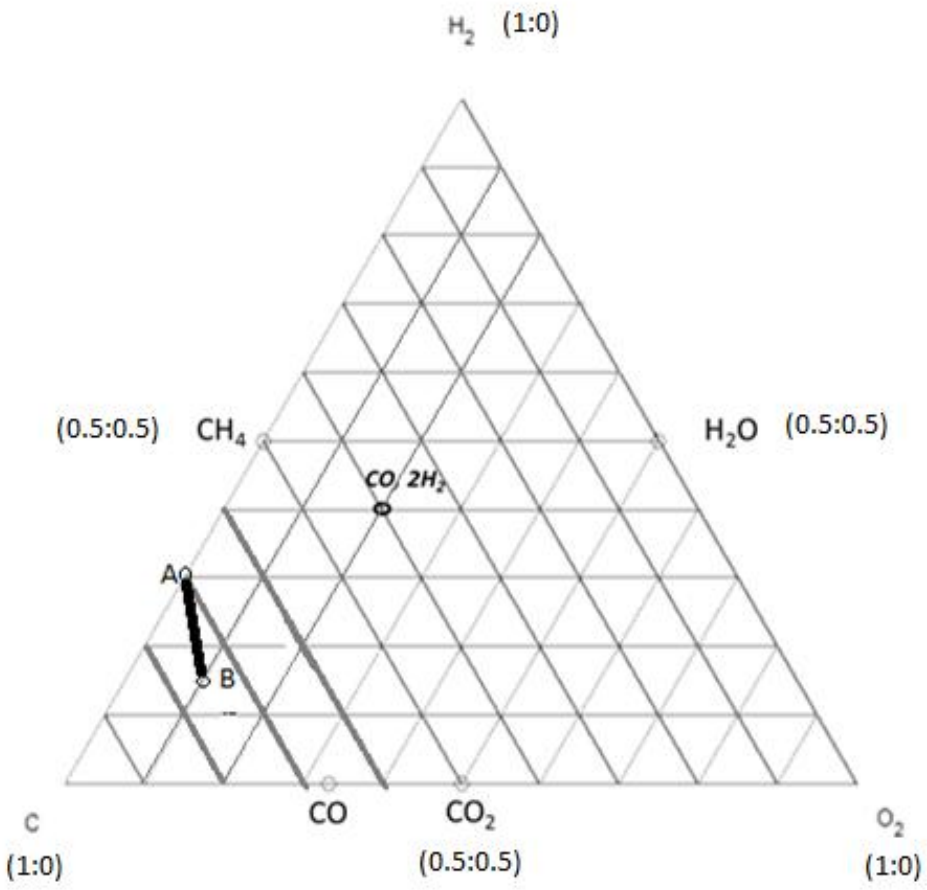


Figure A1: CHO Diagram

In order to plot a chemical compound and determine the reaction, the BE percentages of each component in the compound must be found. For example, CH_4 is represented by:

$$C = \frac{4x_C}{4x_C + x_{H_2} + 2x_{O_2}} = \frac{4\times1}{(4\times1)+(1\times4)+(2\times0)} = \frac{4}{(4+4)} = \frac{1}{2}\text{; and}$$

$$H = \frac{x_{H_2}}{4x_C + x_{H_2} + +2x_{O_2}} = \frac{1\times4}{(4\times1)+(1\times4)+(2\times0)} = \frac{4}{(4+4)} = \frac{1}{2},$$

which then places CH_4 at a point midway between H-C. Similarly, H_2O and CO_2 are found midway between H-O and C-O.

Mixtures can also be represented using the same technique, such as point B which contains 69% C, 5% H_2 and 26% O_2 by mass. In order to plot this mixture on the CHO diagram, the mass percentages must be converted to mole percent. The information given below was used to calculate the mole percentages of each component. Table A1 shows molar masses for components C, H and O.

$$Moles = \frac{Mass}{Molar\ Mass} \quad \text{A4}$$

Table A1: Molar Masses

Component	Molar Mass (g/mol)
C	12
H	1
O	16

Using the information above, the molar fractions were calculated as follows:

$$Mole_C = \frac{0.69}{12} = 0.06$$

$$Mole_O = \frac{0.26}{16} = 0.02$$

$$Mole_H = \frac{0.05}{1} = 0.05$$

Therefore the chemical formula of the mixture can be represented as $C_{0.06}O_{0.02}H_{0.05}$. From this formula, the BE percentages can be calculated and plotted to represent Point B as can be seen in Figure A2 below.

$$C = \frac{4x_C}{4x_C + x_{H_2} + 2x_{O_2}} = \frac{4 \times 0.06}{(4 \times 0.06) + (1 \times 0.05) + (2 \times 0.02)} = \frac{0.24}{0.33} = 0.73$$

$$O = \frac{2x_{O_2}}{4x_C + x_{H_2} + +2x_{O_2}} = \frac{2\times0.02}{(4\times0.06)+(1\times0.05)+(2\times0.02)} = \frac{0.04}{0.33} = 0.12$$

$$H = \frac{x_{H_2}}{4x_C + x_{H_2} + +2x_{O_2}} = \frac{1\times0.05}{(4\times0.06)+(1\times0.05)+(2\times0.02)} = \frac{0.05}{0.33} = 0.15$$

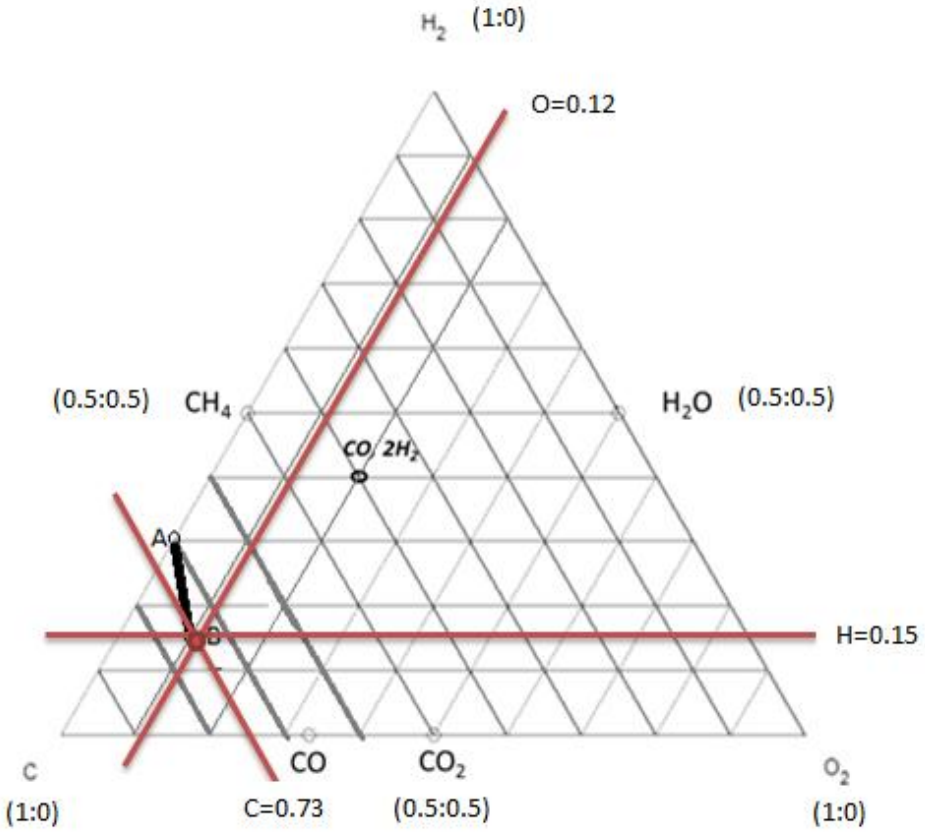


Figure A2: Representing mixtures

Appendix B – Determination of the Thermally Balanced Line

The Thermally Balanced Line (TBL) is representative of the product temperature equating to the inlet temperature (Wei, 1979) of a given process, and this occurs when exothermic reactions are balanced out by endothermic reactions. When this happens, heat is not lost or added to the system; hence the system operates under adiabatic conditions.

In order to determine the TBL, the exothermic reactions found within the system will need to be balanced by the endothermic reactions. There are seven reactions that make up the systems found within the report and can be found below:

$$r_2: C_{2.5}O_2H_6 + 1.5\,O_2 \rightarrow 3\,H_2 + 2.5\,CO_2 \quad \text{B1}$$

$$r_3: C_{2.5}O_2H_6 + 0.25\,O_2 \rightarrow 3\,H_2 + 2.5\,CO \quad \text{B2}$$

$$r_4: C_{2.5}O_2H_6 + 1.75\,O_2 \rightarrow 2.5\,CO + 3\,H_2O \quad \text{B3}$$

$$r_5: C_{2.5}O_2H_6 + 3\,H_2O \rightarrow 6\,H_2 + 2.5\,CO_2 \quad \text{B4}$$

$$r_6: C_{2.5}O_2H_6 + 0.5\,H_2O \rightarrow 3.5\,H_2 + 2.5\,CO \quad \text{B5}$$

$$r_8: C_{2.5}O_2H_6 + 0.5\,CO_2 \rightarrow 3\,H_2 + 3\,CO \quad \text{B6}$$

$$r_9: C_{2.5}O_2H_6 + 3.5\,CO_2 \rightarrow 3\,H_2O + 6\,CO \quad \text{B7}$$

The reactions above need to be categorized as endothermic or exothermic reaction. In order to establish this, higher heating values (HHV) at 650 K of the equations that follow were used to determine the enthalpies of the reactions given above (B1 – B7).

$$r_a: C + \tfrac{1}{2}O_2 \rightarrow CO \quad \text{(-110.4 kJ/mol)} \quad \text{B8}$$

$$r_b: C + O_2 \rightarrow CO_2 \quad \text{(-394.1 kJ/mol)} \quad \text{B9}$$

$$r_c: C + H_2O \rightarrow CO + H_2 \quad \text{(135.0 kJ/mol)} \quad \text{B10}$$

$$r_d: C + 2H_2O \rightarrow CO_2 + 2H_2 \quad \text{(96.6 kJ/mol)} \quad \text{B11}$$

$$r_e: 3C + 2H_2O \rightarrow 2CO + CH_4 \quad \text{(185.6 kJ/mol)} \quad \text{B12}$$

$$r_f: 2C + 2H_2O \rightarrow CO_2 + CH_4 \quad \text{(12.2 kJ/mol)} \quad \text{B13}$$

Using the above equations (B8 – B13), the enthalpy of formation of CO, CO_2, H_2O and CH_4 at 650 K can be determined as the enthalpy of formation of elements are equal to zero. Hence the following enthalpies can be found in Table B1.

Table B1: Enthalpies of Formation

Components	Enthalpy of Formation (kJ/mol)
C	0
O_2	0
H_2	0
CO	-110.4
CO_2	-394.1
H_2O	-245.4
CH_4	-84.5

It is important to note that no HHV exists for LFG hence the enthalpy for LFG was calculated using CH_4 and CO_2 in the ratio 60:40 and can be seen below.

$$\Delta H_{C_{2.5}O_2H_6} = 0.6\Delta H_{CH_4} + 0.4\Delta H_{CO_2}$$

$$= (0.6x(-84.5)) + (0.4x(-394.1))$$

$$= -208.34\ kJ/mol$$

Furthermore, the balanced equation for a 60:40 ratio of CH_4 to CO_2 is:

$$2.5 \times (0.6CH_4 + 0.4CO_2) = C_{2.5}O_2H_6$$

$$\therefore\ 1.5CH_4 + CO_2 = C_{2.5}O_2H_6$$

Once all enthalpies of formations are determined, the enthalpy for each reaction was calculated as follows:

$r_2: C_{2.5}O_2H_6 + 1.5\ O_2 \rightarrow 3\ H_2 + 2.5\ CO_2$

$\Delta H_{r_2} = (3\Delta H_{H_2} + 2.5\Delta H_{CO_2}) - (\Delta H_{C_{2.5}O_2H_6} + 1.5\Delta H_{O_2})$

$\Delta H_{r_2} = (3\Delta H_{H_2} + 2.5\Delta H_{CO_2}) - (1.5\Delta H_{CH_4} + \Delta H_{CO_2} + 1.5\Delta H_{O_2})$

$= (0 + (2.5(-394.1))) - ((1.5(-84.5)) + (-394.1) + 0)$

$= -464.4\ kJ/mol$

Similarly, the other equations were found to be:

r_3: 244.9 kJ/mol

r_4: -491.4 kJ/mol

r_5: 271.8 kJ/mol

r_6: 367.6 kJ/mol

r_8: 386.7 kJ/mol

r_9: 501.6 kJ/mol

Using these enthalpies, a table was drawn up for all the reactions used for Feed 1. The components are shown at the top of the table and the stoichiometric values are shown within the table.

Table B2: Balanced Reactions

	$C_{2.5}O_2H_6$	O_2	H_2	CO	H_2O	CO_2	ΔH (KJ/mol)
r_3	1	0.25	3	2.5	-	-	244.9
r_4	1	1.75	-	2.5	3	-	-491.4
r_8	1	-	3	3	-	0.5	386.7
r_9	1	-	-	6	3	3.5	501.6

Using the ΔH from Table B2 the enthalpy ratios were determined for each exothermic reaction with each endothermic reaction. For Feed 1, only r_4 was found to be an exothermic reaction, whilst r_3, r_8 and r_9 were found to be endothermic reactions. The enthalpy ratios can be found in Table B3 below.

Table B3: Enthalpy Ratios

Enthalpy Ratios	0.79	0.98	0.50
Exothermic Reactions	r_4	r_4	r_4
Endothermic Reactions	r_8	r_9	r_3

Once the ratios were obtained, the necessary equations were multiplied by the ratio to achieve an end result of zero enthalpy once the equations are added. This can be seen in the table that follows.

Table B4: Balanced Reactions – Point A on the TBL

	$C_{2.5}O_2H_6$	O_2	H_2	CO	H_2O	CO_2	ΔH (KJ/mol)
r_4	1	1.8	-	2.5	3	-	-491.35
r_9	1	0	0	5.9	2.9	3.4	491.35
A	2	1.8	0	8.4	5.9	3.4	0

When divided by 2, equation A reads:

A: $C_{2.5}O_2H_6 + 1.73\,CO_2 + 0.88\,O_2 \rightarrow 4.23\,CO + 3H_2O$

This makes up one point on the TBL.

A similar process was carried out for the second and third points on the TBL. This is tabulated below.

Table B5: Balanced Reactions – Point B on the TBL

	$C_{2.5}O_2H_6$	O_2	H_2	CO	H_2O	CO_2	ΔH (KJ/mol)
r_3	1	0.3	3	2.5	-	-	244.85
r_4	0.5	0.9	0	1.2	1.5	0	-244.85
B	1.5	1.1	3	3.7	1.5	0	0

When divided by 1.5, equation B reads:

B: $C_{2.5}O_2H_6 + 0.75\,O_2 \rightarrow 2.5\,CO + H_2O + 2H_2$

This makes up the second point on the TBL.

The third point is calculated as shown in Table B6.

Table B6: Balanced Reactions – Point C

	$C_{2.5}O_2H_6$	O_2	H_2	CO	H_2O	CO_2	ΔH (KJ/mol)
r_8	1	-	3	3	-	0.5	386.7
r_4	0.8	1.4	0	2	2.4	0	-386.7
C	1.8	1.4	3	5	2.4	0.5	0

When divided by 1.8, equation C reads:

C: $C_{2.5}O_2H_6 + 0.28\,CO_2 + 0.77\,O_2 \rightarrow 2.78\,CO + 1.32\,H_2O + 1.68H_2$

Point C however lies so close to line AB that the deviance from line AB is 0.0021 and is considered to be insignificant. For this reason, the TBL is given as line AB and not as a region ABC.

A similar case was done for Feed 2. The TBL for Feeds 2 is tabulated below in Table B7. The TBL for Feed 2 also has 3 points with the middle point D significantly close to the end points. The deviance from line EF is 0.0020 and therefore it is assumed that point D lies on line EF. Hence the TBL for Feed 2 is given as line EF.

Table B7: Equations representing the Thermally Balanced Line for Feed 2

Feed 2	
D:	$C_{2.5}O_2H_6 + 0.28\,H_2O + 0.66\,O_2 \rightarrow 1.40\,CO + 1.10\,CO_2 + 3.28\,H_2$
E:	$C_{2.5}O_2H_6 + 1.90\,H_2O + 0.55\,O_2 \rightarrow 2.5\,CO_2 + 4.89\,H_2$
F:	$C_{2.5}O_2H_6 + 0.68\,O_2 \rightarrow 1.64\,CO + 0.86\,CO_2 + 3\,H_2$

Feed 3 does not have a thermally balanced line; instead it has 3 individual points which represent the endothermic reactions by r_3, r_6 and r_8. No exothermic reactions or TBL exists for this process. The Equations for these points are represented in B8 below.

Table B8: Endothermic reactions for Feed 3

Feed 3	
r_3:	$C_{2.5}O_2H_6 + 0.25\,O_2 \rightarrow 3\,H_2 + 2.5\,CO$
r_6:	$C_{2.5}O_2H_6 + 0.5\,H_2O \rightarrow 3.5\,H_2 + 2.5\,CO$
r_8:	$C_{2.5}O_2H_6 + 0.5\,CO_2 \rightarrow 3\,H_2 + 3\,CO$

Appendix C – Calculating Calorific Values

Calorific value contours are useful when choosing a targeted calorific value and determining the reaction stream requirements. The higher the calorific value, the more energy can be drawn from the process, hence it makes sense to operate at higher calorific values rather than lower value.

The contours of the calorific values found in the report are based on the method of Li et al., 2004. High heating values (HHV's) for each reaction was initially assumed and this was used to calculate the values of α and β for each reaction. The main Equations used are shown below:

$$HHV_1 = \alpha \times r_x + (1 - \alpha) \times r_y \quad \text{C1}$$

$$HHV_2 = \beta \times r_x + (1 - \beta) \times r_z \quad \text{C2}$$

$$\therefore \alpha = \frac{(HHV_1 - r_y)}{(r_x - r_y)} \quad \text{C3}$$

Similarly

$$\therefore \beta = \frac{(HHV_2 - r_z)}{(r_x - r_z)} \quad \text{C4}$$

The seven reactions shown below make up the systems found within the report:

$$r_2: C_{2.5}O_2H_6 + 1.5\,O_2 \rightarrow 3\,H_2 + 2.5\,CO_2 \quad \text{C5}$$

$$r_3: C_{2.5}O_2H_6 + 0.25\,O_2 \rightarrow 3\,H_2 + 2.5\,CO \quad \text{C6}$$

$$r_4: C_{2.5}O_2H_6 + 1.75\,O_2 \rightarrow 2.5\,CO + 3\,H_2O \quad \text{C7}$$

$$r_5: C_{2.5}O_2H_6 + 3\,H_2O \rightarrow 6\,H_2 + 2.5\,CO_2 \quad \text{C8}$$

$$r_6: C_{2.5}O_2H_6 + 0.5\,H_2O \rightarrow 3.5\,H_2 + 2.5\,CO \quad \text{C9}$$

$$r_8: C_{2.5}O_2H_6 + 0.5\,CO_2 \rightarrow 3\,H_2 + 3\,CO \quad \text{C10}$$

$$r_9: C_{2.5}O_2H_6 + 3.5\,CO_2 \rightarrow 3\,H_2O + 6\,CO \qquad \text{C11}$$

Percentages of the products found in each reaction was then determined using the coefficients of the products and this is shown below in Table C1.

Table C1: Percentage of Products

	Products	Total	H_2	CO_2	CO	H_2O
r_2	$3\,H_2 + 2.5\,CO_2$	5.5	54.5	45.5		
r_3	$3\,H_2 + 2.5\,CO$	5.5	54.5		45.5	
r_4	$2.5\,CO + 3\,H_2O$	5.5			45.5	54.5
r_5	$6\,H_2 + 2.5\,CO_2$	8.5	70.6	29.4		
r_6	$3.5\,H_2 + 2.5\,CO$	6	58.3		41.7	
r_8	$3\,H_2 + 3\,CO$	6	50		50	
r_9	$3\,H_2O + 6\,CO$	9			66.7	33.3

According to Li et al., 2004, the equation for HHV at standard temperature and pressure (101.3 kPa and 273K) is given as:

$$HHV = (12.75\,[H_2] + 12.63\,[CO] + 39.82\,[CH_4] + 63.43\,[C_2H_4]\ldots)/100; \qquad \text{C12}$$

where each component represents the product formed from the reaction. The species contents are given in mol%, and their heats of combustion in MJ/m^3. Using Equation C12 and the percentages obtained in Table C1, the HHV for each reaction (r_2 to r_9) was then found for each Feed group and this is tabulated below.

Table C2: HHV in MJ/m^3 for product gases according to Li et al., 2004

Reaction	Feed 1	Feed 2	Feed 3
r_2	-	6.95	-
r_3	12.70	12.70	12.70

Reaction	Feed 1	Feed 2	Feed 3
$\mathbf{r_4}$	5.74	-	-
$\mathbf{r_5}$	-	9	-
$\mathbf{r_6}$	-	12.70	12.70
$\mathbf{r_8}$	12.69	-	12.69
$\mathbf{r_9}$	8.42	-	-

The HHV values found in Table C2 represents, as its name suggests, the highest heating value obtained for that given reaction. Hence for r_2, Feed 2, the highest calorific value obtained is 7MJ/m^3.

Once this is done, the equations were tabulated as was done in Appendix B, and the Solver Function in Excel was used to solve for α by setting the HHV value to a set number. This is represented by the highlighted figures. A portion of the calculation can be seen below.

Table C3: Calculating α

	Reactants				Products			
	$C_{2.5}O_2H_6$	O_2	CO_2		H_2	CO	H_2O	***HHV*** (MJ/m^3)
$\mathbf{r_3}$	1	0.25	-		3	2.50	-	12.70
$\mathbf{r_4}$	1	1.75	-		-	2.50	3	5.74
α=0.38								
$\mathbf{r_f}$	1	1.17	0		1.16	2.5	1.84	8.42

Once Solver found a value for α, the row containing r_f was calculated using Equation C1. Similarly β was found using r_4 and r_9. The results are tabulated below.

Table C4: Calculating β

	Reactants			Products			
	$C_{2.5}O_2H_6$	O_2	CO_2	H_2	CO	H_2O	***HHV*** (MJ/m^3)
r_4	1	1.75	-	-	2.5	3	5.74
r_9	1	-	3.50	-	6	3	8.42
β=0.38							
r_f	1	0	3.50	-	6	3	8.42

When r_9 is used to calculate β, the HHV cannot go above 8.42MJ/m^3 as this is at the edge of equations r_4 and r_9 (see Table C2, maximum limit for r_9 is 8.42MJ/m^3). Therefore r_8 was used to complete the remainder of the calculations and find the outstanding calorific values. Table C5 tabulates the calorific values found for each α and β value.

Table C5: Calculating α and β for Feed 1

		Reactants			Products			
		$C_{2.5}O_2H_6$	O_2	CO_2	H_2	CO	H_2O	***HHV*** (MJ/m^3)
α1	r_3-r_4	1	1.26	-	0.97	2.50	2.03	8
β1	r_4-r_9	1	0.27	2.95	0	5.45	3.00	8
α2	r_3-r_4	1	1.48	-	0.54	2.50	2.46	7
β2	r_4-r_9	1	0.93	1.64	0	4.14	3.00	7
α3	r_3-r_4	1	1.69	-	0.11	2.50	2.89	6
β3	r_4-r_9	1	1.58	0.34	0	2.84	3.00	6
α4	r_3-r_4	1	1.17	-	1.16	2.50	1.84	8.42
β4	r_4-r_9	1	0.00	3.50	0	6.00	3.00	8.42
α5	r_3-r_4	1	1.05	0	1.41	2.50	1.59	9
β5	r_8-r_9	1	0.00	3.09	0.41	5.59	2.59	9
α6	r_3-r_4	1	0.83	0	1.84	2.50	1.16	10
β6	r_8-r_9	1	0.00	2.39	1.11	4.90	1.89	10
α7	r_3-r_4	1	0.62	0	2.27	2.50	0.73	11

		Reactants				Products			
β7	r_8-r_9	1	0.00	1.69		1.81	4.19	1.19	11

From Table C5, BE percentages were found for C, O and H and this was plotted to achieve the calorific values for Feed 1. The BE percentages are shown below in Table C6.

Table C6: BE percentages for Calorific Values for Feed 1

	H	C	O
α1	0.24	0.40	0.36
β1	0.13	0.49	0.38
α2	0.23	0.39	0.38
β2	0.16	0.45	0.39
α3	0.22	0.37	0.40
β3	0.21	0.39	0.40
α5	0.25	0.41	0.34
β5	0.13	0.50	0.37
α6	0.26	0.43	0.31
β6	0.15	0.50	0.35
α7	0.27	0.45	0.29
β7	0.18	0.50	0.32

The BE percentages tabulated in Table C6 was then used to plot the calorific value contours for Feed 1 on the CHO diagram which is represented by Figure C1 below.

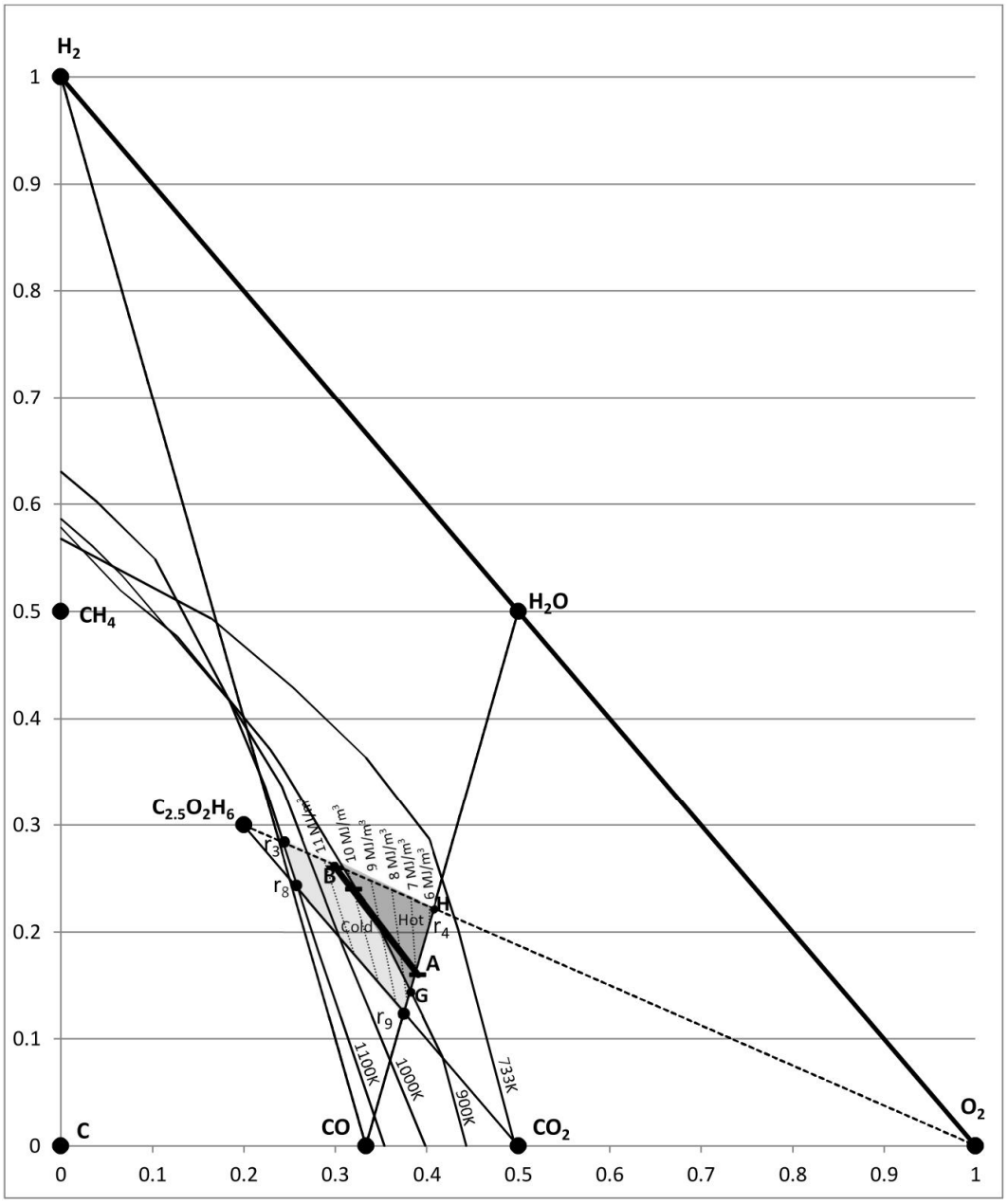


Figure C1: Representing Calorific Value Contours on the CHO Diagram for Feed 1.

A similar procedure was used to determine calorific value contours for Feed 2. Values representing α and β are found in Table C7.

Table C7: Calculating α and β for Feed 2

		Reactants				Products			
		$C_{2.5}O_2H_6$	O_2	H_2O		H_2	CO	CO_2	***HHV*** (MJ/m^3)
α1	r_3-r_2	1	1.49	0		3	0.02	2.48	7
β1	r_2-r_5	1	1.47	0.07		3.07	0	2.50	7
α2	r_3-r_2	1	1.27	0		3	0.46	2.04	8
β2	r_2-r_5	1	0.73	1.53		4.53	0	2.50	8
α3	r_3-r_2	1	1.05	0		3	0.89	1.61	9
β3	r_2-r_5	1	0	3		6	0	2.50	9
α4	r_3-r_2	1	0.84	0		3	1.33	1.17	10
β4	r_5-r_6	1	0	2.32		5.32	0.68	1.82	10
α5	r_3-r_2	1	0.62	0		3	1.76	0.74	11
β5	r_5-r_6	1	0	1.65		4.65	1.35	1.15	11
α6	r_3-r_2	1	0.40	0		3.	2.20	0.30	12
β6	r_5-r_6	1	0	0.97		3.97	2.03	0.47	12

From Table C7, BE percentages were found for C, O and H and this was plotted to achieve the calorific values for Feed 2. The BE percentages are shown below in Table C8.

Table C8: BE percentages for Calorific Values for Feed 2

	H	C	O
α1	0.23	0.39	0.38
β1	0.23	0.38	0.38
α2	0.24	0.40	0.36
β2	0.31	0.34	0.34
α3	0.25	0.41	0.34
β3	0.38	0.31	0.31
α4	0.26	0.43	0.31
β4	0.36	0.34	0.30

	H	C	O
α5	0.27	0.44	0.29
β5	0.35	0.38	0.27
α6	0.28	0.46	0.26
β6	0.33	0.42	0.25

The BE percentages tabulated in Table C8 was then used to plot the calorific value contours for Feed 2 on the CHO diagram which is represented by Figure C2 below.

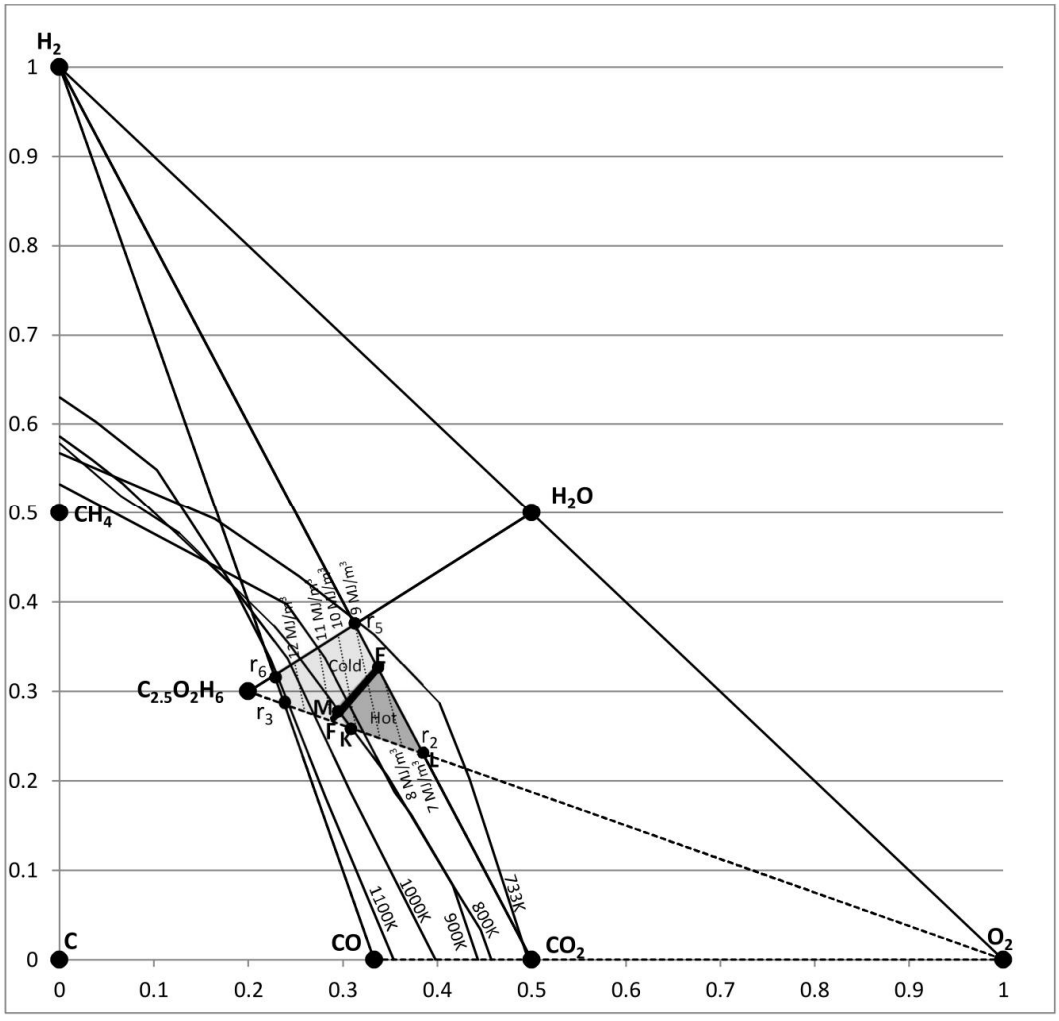


Figure C2: Representing Calorific Value Contours on the CHO Diagram for Feed 2.